

# **HYBRID DIRECT METHANOL FUEL CELLS**

A Thesis  
Presented to  
The Academic Faculty

by

Krishna Sathyamurthy Joseph

In Partial Fulfillment  
of the Requirements for the Degree  
Master of Science in the  
School of Chemical and Biomolecular Engineering

Georgia Institute of Technology  
AUGUST 2012

**COPYRIGHT 2012 BY KRISHNA SATHYAMURTHY JOSEPH**

# HYBRID DIRECT METHANOL FUEL CELLS

Approved by:

Dr. Paul A Kohl, Advisor  
School of Chemical and Biomolecular Engineering  
*Georgia Institute of Technology*

Dr. Carson Meredith  
School of Chemical and Biomolecular Engineering  
*Georgia Institute of Technology*

Dr. Matthew Realff  
School of Chemical and Biomolecular Engineering  
*Georgia Institute of Technology*

Date Approved: May 4, 2012

To my family and friends

## ACKNOWLEDGEMENTS

I wish to express my heartfelt gratitude to my thesis advisor Dr. Paul Kohl for his support, guidance and patient advice in my research. I would also like to thank Dr. Murat Unlu and Dr. Junfeng Zhou for all the assistance and insightful comments offered during the course of my research work here. I am thankful to all the other members of the Kohl group for their continued support and motivation which made my stay here a very pleasant and enjoyable experience.

I am also grateful to my committee members, Dr. Carson Meredith and Dr. Matthew Realff for taking the time to read my thesis and also to attend my thesis defense.

I am especially indebted to my parents, grandmothers, aunt, family and Bhavya for providing me with motivation, unconditional support and encouragement and for having been there every step of the way without which this would not be possible. I would also like to thank my undergraduate advisors Dr. K.R. Murali and Dr. N. Palaniswamy for their counsel and invaluable advice. I would like to make a special mention of all my friends who have been so wonderfully understanding and supportive all along.

# TABLE OF CONTENTS

	Page
ACKNOWLEDGEMENTS	iv
LIST OF TABLES	viii
LIST OF FIGURES	ix
LIST OF SYMBOLS	xiii
LIST OF ABBREVIATIONS	xv
SUMMARY	xvii
<u>CHAPTER</u>	
1 INTRODUCTION	1
1.1 Background	1
1.2 History of Fuel Cells	2
1.3 Proton Exchange Membrane Fuel Cells	5
1.4 Alkaline Fuel Cells	11
1.5 Hybrid Fuel Cells	20
1.5.1 Principle of Operation	26
1.5.1.1 Anode Hybrid Direct Methanol Fuel Cells	26
1.5.1.2 Cathode Hybrid Direct Methanol Fuel Cells	29
2 EXPERIMENTAL SECTION	32
2.1 Materials	32
2.2 Experimental	33
2.2.1 Thin Film Method	34
2.2.2 Ionomer Impregnation Method	35

2.2.3 MEA Assembly	36
3 ANODE HYBRID DIRECT METHANOL FUEL CELLS	37
3.1 Objective	37
3.2 Performance of Anode Hybrid Direct Methanol Fuel Cells	38
3.2.1 Impact of the Operating Conditions	38
3.2.1.1 Temperature	38
3.2.1.2 Methanol Concentration	40
3.2.1.3 Methanol Flow Rate	41
3.2.1.4 Oxygen Flow Rate	42
3.2.1.5 Air Flow Rate	44
3.2.2 Steady State Operation	45
3.2.3 Impact of Fabrication Protocol	46
3.2.4 Impact of the Ion Exchange Capacity of the Ionomer	50
3.2.5 Impact of the Ionomer Content	52
3.2.6 Impact of the Different Ionomers	54
3.2.7 Impact of the Ionomer Molecular Weight	56
3.3 Initial Voltage Drop	58
3.3.1 Initial Voltage Drop in Anode Hybrid Fuel Cells	64
3.3.2 Cationic Head Groups for Anode Hybrid Fuel Cells	67
3.4 Summary	71
4 CATHODE HYBRID DIRECT METHANOL FUEL CELLS	73
4.1 Objective	73
4.2 Performance of Cathode Hybrid Direct Methanol Fuel Cells	74
4.2.1 Impact of the Operating Conditions	74
4.2.1.1 Temperature	74

4.2.1.2 Methanol Concentration	75
4.2.1.3 Methanol Flow Rate	76
4.2.1.4 Oxygen Flow Rate	77
4.2.1.5 Air Flow Rate	78
4.2.2 Steady State Operation	80
4.2.3 Impact of Fabrication Protocol	81
4.2.4 Impact of the Ionomer Content	83
4.2.5 Impact of the Different Ionomers	84
4.2.6 Impact of the Ionomer Molecular Weight	86
4.2.7 Impact of Different Cationic Groups	87
4.2.8 Impact of the Non-Platinum Cathode Catalyst	89
4.3 Summary	93
5 CONCLUSIONS	94
REFERENCES	96

## LIST OF TABLES

	Page
Table 1.1: Comparison chart of different types of fuel cells	4
Table 1.2: Summary of different studies on alkaline fuel cells with methanol	19
Table 3.1: Properties of Ionomer I used in the anode hybrid fuel cell	38
Table 3.2: Optimized operating conditions for anode hybrid direct methanol fuel cells	44
Table 3.3: Properties of the ionomer with different IEC	51
Table 3.4: Properties of the ionomers with different backbone	55
Table 3.5: Properties of Ionomer II with different molecular weights	57
Table 3.6: Properties of Ionomer I with the ammonium and quinuclidine cationic groups	68
Table 4.1: Properties of the ionomer used for fabrication of AEM electrode	74
Table 4.2: Optimized operating conditions for cathode hybrid fuel cells	80
Table 4.3: Properties of Ionomer II with different molecular weight	86
Table 4.4: Properties of ionomers used for the non platinum electrode preparation	91

## LIST OF FIGURES

	Page
Figure 1.1: Schematic of a fuel cell	2
Figure 1.2: A schematic of the Grove gas voltaic battery	3
Figure 1.3: Proton exchange membrane fuel cell	5
Figure 1.4: Structure of Nafion	7
Figure 1.5: Specific gravimetric and volumetric energy density of selected fuels in comparison with batteries.	7
Figure 1.6: Alkaline fuel cell	12
Figure 1.7: Publications on alkaline fuel cells in recent years	14
Figure 1.8: Ion and water transport in AEMFC	15
Figure 1.9: Hybrid fuel cells: (a) AEM anode and PEM cathode and (b) PEM anode and AEM cathode	21
Figure 1.10: Schematic of hybrid fuel cell configurations: (a) high pH cathode and low pH anode (CHFC), (b) high pH anode and low pH cathode (AHFC)	25
Figure 1.11: Schematic of anode hybrid direct methanol fuel cell with AEM anode and PEM cathode	28
Figure 1.12: Schematic of cathode hybrid direct methanol fuel cell with PEM anode and AEM cathode	31
Figure 2.1: Schematic of Ionomer I	33
Figure 2.2: Schematic of Ionomer II	33
Figure 2.3: Schematic of Ionomer III	33
Figure 3.1: Polarization and power density curves of anode hybrid fuel cell operated at different temperatures: 55 °C (broken lines), 40 °C (lines), 25 °C (double dotted lines), with 2M MeOH at 5 ml/min on the anode and 50 sccm O <sub>2</sub> at the cathode	39

- Figure 3.2: Open circuit voltage (stars) and peak power density (circles) of fuel cell operated with different MeOH concentrations: 1M, 2M, 4M operated with 50 sccm O<sub>2</sub> at the cathode at 55 °C 41
- Figure 3.3: Power density (triangles) and open circuit voltage (squares) of fuel cell operated with different MeOH (2M) flow rates: 3, 5, 8 ml/min operated with 50 sccm O<sub>2</sub> at the cathode at 55 °C 42
- Figure 3.4: Polarization and power density curves of anode hybrid fuel cell operated with different oxygen flow rates at the cathode: 50 sccm (broken lines), 30 sccm (lines), 10 sccm (double dotted lines), and 2M MeOH at 5ml/min on the anode at 55 °C 43
- Figure 3.5: Power density (crosses) and open circuit voltage (rhombuses) of fuel cell operated with different air flow rates: 50, 100, and 150 sccm operated 2M MeOH at the anode at 55 °C 45
- Figure 3.6: Steady state performance of the fuel cell held at constant potential of 250 mV with 2M MeOH, flow rate 5 ml/min and O<sub>2</sub> flow rate 50 sccm supplied at atmospheric pressure at 55 °C 46
- Figure 3.7: Three phase boundary at catalyst surface 47
- Figure 3.8: Polarization and power density curves for the anode hybrid fuel cell operated with thin film anode (dotted lines), ionomer impregnated anode (lines) with 2M MeOH supplied at a flow rate of 5 ml/min and O<sub>2</sub> supplied to the cathode at 50 sccm (atmospheric pressure) at 55 °C 48
- Figure 3.9: Proposed structures of electrodes prepared by: (a) Thin Film method and (b) Ionomer impregnation method 49
- Figure 3.10: Polarization and power density curves of anode hybrid fuel cell operated with different IEC ionomers at the anode: 1.21 (broken lines), 1.55 (lines), 0.92 (dotted lines) meq/g 2M MeOH at 5 ml/min on the anode and 50 sccm O<sub>2</sub> on the cathode at 55 °C 51
- Figure 3.11: Polarization and power density curves of anode hybrid fuel cells with different ionomer contents : 15, 25, 40 % with 2M MeOH at 5 ml/min and 50 sccm O<sub>2</sub> at 55 °C 53
- Figure 3.12: Electrode structure of the electrodes with different ionomer distributions in the catalyst layer (a) Low ionomer content (b) High ionomer content (c) Optimum ionomer content 54
- Figure 3.13: Polarization and power density curves of anode hybrid fuel cell operated with different ionomers at the anode with 2M MeOH at 5 ml/min on the anode and 50 sccm O<sub>2</sub> on the cathode at 55 °C 56

- Figure 3.14: Polarization (open symbols) and power density (solid symbols) for the anode hybrid fuel cell with different molecular weight ionomers: 11.2 k, 11.8 k, 40.5 k operated with 2M MeOH at a flow rate of 5 ml/min and oxygen flow rate 50 sccm 58
- Figure 3.15: Proposed double layer structure for negatively charged electrode with specifically adsorbed anion 59
- Figure 3.16: Effect of concentration of tetra-alkyl ammonium hydroxide on the rate of reduction of chromate at - 0.75 V vs SCE at 25 °C 61
- Figure 3.17: Potential profile of double layer interface with different electrolytes for methanol oxidation on platinum electrode at potentials negative of potential of zero charge 63
- Figure 3.18: Polarization curve of fuel cell (dotted line), anode polarization curve (line) for anode hybrid direct methanol fuel cell operated with 2M MeOH at 5 ml/min on anode and O<sub>2</sub> and H<sub>2</sub> respectively at cathode 50 sccm at 55 °C 65
- Figure 3.19: Structure of (a) Ionomer I backbone, and the attached cationic groups: (b) Ammonium (c) Quinuclidine 68
- Figure 3.20: Polarization and power density curve of ammonium (dotted lines), quinuclidine (lines) ionomers for anode hybrid direct methanol fuel cell operated with 2M MeOH at 5 ml/min and O<sub>2</sub> at 50 sccm at 55 °C 69
- Figure 3.21: Steady state performance of the fuel cell with Ionomer I-5 held at constant potential of 250 mV 70
- Figure 4.1: Polarization and power density curves of cathode hybrid fuel cell operated at different temperatures: 55 °C (broken lines), 40 °C (lines), 25 °C (double dotted lines), with 2M MeOH at 5 ml/min on the anode and 50 sccm O<sub>2</sub> at the cathode 75
- Figure 4.2: Open circuit voltage (squares) and peak power density (triangles) of fuel cell operated with different MeOH concentrations: 1M, 2M, 4M operated with 50 sccm O<sub>2</sub> at the cathode at 55 °C 76
- Figure 4.3: Power density (circles) and open circuit voltage (stars) of fuel cell operated with different methanol (2M) flow rates: 3, 5, 8 ml/min operated with 50 sccm O<sub>2</sub> at the cathode at 55 °C 77
- Figure 4.4: Polarization and power density curves of cathode hybrid fuel cell operated with different oxygen flow rates at the cathode: 50 sccm (broken lines), 30 sccm (lines), 10 sccm (double dotted lines), and 2M MeOH at 5 ml/min on the anode at 55 °C 78

Figure 4.5: Polarization and power density curves of cathode hybrid fuel cell operated with different air flow rates at the cathode: 50 sccm (lines), 100 sccm (squares) and 2M MeOH at 5 ml/min on the anode at 55 °C 79

Figure 4.6: Steady state performance of the fuel cell held at constant potential of 250 mV with 2M MeOH, flow rate 5 ml/min and O<sub>2</sub> flow rate 50 sccm supplied at atmospheric pressure at 55 °C 81

Figure 4.7: Polarization and power density curves for the cathode hybrid fuel cell operated with thin film cathode (dotted lines), ionomer impregnated cathode (lines) with 2M MeOH supplied at a flow rate of 5 ml/min and O<sub>2</sub> supplied to the cathode at 50 sccm (atmospheric pressure) at 55 °C 82

Figure 4.8: Polarization and power density curves of cathode hybrid fuel cells with different ionomer contents: 15, 25, 40 % with 2M MeOH at 5 ml/min and 50 sccm O<sub>2</sub> at 55 °C 84

Figure 4.9: Polarization and power density curves of cathode hybrid fuel cell operated with different ionomers: Ionomer I, II, III at the cathode with 2M MeOH at 5 ml/min on the anode and 50 sccm O<sub>2</sub> on the cathode at 55 °C 85

Figure 4.10: Polarization (open symbols) and power density (solid symbols) curves for cathode hybrid fuel cells with different molecular weight ionomers: (a) 11.2 k (b) 11.8k (c) 25.8 k and (d) 40.5 k operated with 2M MeOH and 50 sccm O<sub>2</sub> at 55 °C 87

Figure 4.11: Structure of (a) Ionomer backbone, and the attached cationic groups: (b) Ammonium (c) Quinuclidine 88

Figure 4.12: Polarization and power density curves for cathode hybrid fuel cells with Ionomer I different cationic groups: quinuclidine (lines), ammonium (dotted lines) operated with 2M MeOH and 50 sccm O<sub>2</sub> at 55 °C 89

Figure 4.13: Polarization and power density curves of cathode hybrid fuel cells fabricated with Acta non platinum Catalyst with two different ionomers Ionomer I (lines), Ionomer II (dotted lines) operated with 2M MeOH and 50 sccm O<sub>2</sub> at 55 °C 91

Figure 4.14: Steady state polarization curves with Ionomer I (line) and II (dotted line) for non platinum catalyst based cathode hybrid fuel cell operated with 2M MeOH at 5 ml/min and 50 sccm O<sub>2</sub> at 55 °C 92

## LIST OF SYMBOLS

$\alpha$	Symmetry factor
$a_{CH_3OH,a}$	Activity of methanol at anode
$a_{H^+}^{PEM}$	Activity of $H^+$ ions in PEM
$a_{OH^-}^{AEM}$	Activity of $OH^-$ ions in AEM
$a_{H_2O,a}$	Activity of $H_2O$ at anode
$a_{H_2O,c}$	Activity of $H_2O$ at cathode
$E_0$	Standard electrode potential
$E_A^0$	Standard anode potential
$E_C^0$	Standard cathode potential
$E_j$	Junction potential
$F$	Faradays constant
$\Delta G$	Reversible free energy
$k^0$	Apparent rate constant
$k_t^0$	True rate constant
$K_w$	Water dissociation constant
$\Delta pH$	pH difference
$\varphi^{AEM}$	Absolute AEM phase potential
$\varphi_m$	Absolute electrode potential
$\varphi^{PEM}$	Absolute PEM phase potential
$\varphi_s$	Absolute solution potential
$\varphi_2$	Potential at OHP with respect to the bulk solution
$P$	Total pressure

$P_{CO_2,a}$	Pressure of CO <sub>2</sub> at anode
$P_{O_2,c}$	Pressure of O <sub>2</sub> at cathode
$R$	Universal gas constant
$T$	Temperature
$z$	Charge magnitude of ions in electrolyte

## LIST OF ABBREVIATIONS

AEM	Anion exchange membrane
AEI	Anion exchange ionomer
AEMFC	Anion exchange membrane fuel cell
AFC	Alkaline fuel cell
AHFC	Anode hybrid fuel cell
CHFC	Cathode hybrid fuel cell
DMF	Dimethyl formamide
DMFC	Direct methanol fuel cell
GDL	Gas diffusion layer
IEC	Ion exchange capacity
IHP	Inner Helmholtz plane
IPA	Iso propyl alcohol
MEA	Membrane electrode assembly
OCV	Open circuit voltage
OHP	Outer Helmholtz plane
ORR	Oxygen reduction reaction
PEM	Proton exchange membrane
PEMFC	Proton exchange membrane fuel cell
PTFE	Poly tetrafluoroethylene
PTMAOH	Poly diallyl dimethyl ammonium hydroxide
PZFC	Potential of zero free charge
SCE	Saturated calomel electrode

SHE

Saturated hydrogen electrode

TMAOH

Tetra methyl ammonium hydroxide

## SUMMARY

Proton exchange membrane fuel cells have been widely studied for the direct electrochemical conversion of fuels into power. Methanol based fuel cells have come to the forefront because of several advantages including easier storage and handling, direct conversion to power without the necessity for reforming the fuel. The proton exchange membrane fuel cell has several disadvantages including the low methanol oxidation kinetics, methanol crossover and the use of expensive platinum based catalysts. This has resulted in low performance for these fuel cells.

Alkaline anion exchange membrane fuel cells (AEMFC) are receiving increased attention owing to their advantages over the proton exchange membrane fuel cell (PEMFC). The main advantages include operation at higher pH which allows the use of non-noble metal catalysts such as Ag, and Ni, enhanced methanol and oxygen reduction rates, and minimizing the problem of methanol crossover and cathode flooding. The main limiting parameter for this type of fuel cell is the lack of alkaline anion exchange membranes with high conductivity, stability, low crossover and good transport properties.

The drawbacks associated with the alkaline and the proton exchange membrane fuel cells has led us to choose a new hybrid system that utilizes the advantages of both a PEMFC and AEMFC for operation with methanol. Two configurations: one with a high pH anode and low pH cathode (anode hybrid fuel cell (AHFC)), and another with a high pH cathode and a low pH anode (cathode hybrid fuel cell (CHFC)) have been studied in this work. The use of methanol as a fuel for these hybrid fuel cells was demonstrated and the principle of operation of these fuel cells is also explained.

The two different hybrid cell configurations were used in order to study the electrode fabrication on fuel cell performance. Further, the ionomer properties such as the ion exchange capacity and molecular weight were optimized for the best performance. A

comparison of the different ionomers with similar properties is carried out in order to obtain the best possible ionomer for the fuel cell. Ionomers with alternate cationic groups have also been investigated.

An initial voltage drop was observed at low current density in the high pH anode which may be due to the specific adsorption and formation of a diffuse double layer at the electrode surface by the quaternary ammonium head groups. Alternate ionomer cationic head groups were investigated. The impact of these groups on the voltage drop and fuel cell performance is also studied.

Finally, the performance of the cathode hybrid fuel cells with non platinum cathode catalysts was also demonstrated.

# **CHAPTER 1**

## **INTRODUCTION**

### **1.1 Background**

Fuel cells are electrochemical devices that are designed to convert chemical energy into electrical energy. Fuel cells are a variant of galvanic cells that consists of two electrodes, a positive electrode (anode) which produces electrons by oxidizing the fuel and the negative electrode (cathode) which reduces the oxidizing agent. The electrodes are in contact with an electrolytic solution which assists in the transport of the ions. The fuel and the oxidizing agents are supplied at the individual electrodes. The continuous operation of the fuel cell requires the supply of these reactants to the electrodes and also the removal of the products and also the heat produced by the reaction. A schematic of the fuel cell is shown in Figure 1.1 [1].

Since fuel cells don't go through a heat cycle to produce work, the thermodynamic limitations of Carnot efficiency do not apply. Fuel cells offer improved efficiency, and an extremely quiet and continuous operation without maintenance since there are a very few moving parts, significant advantages over the conventional fossil fuel based power generation systems. Some fuel cells offer higher power densities compared to batteries. Extensive research has been carried out on different types of fuel cells for different applications ranging from transportation to portable applications. A brief insight into the history and the development of fuel cells is provided in the next section, to provide a prelude to the research that has been carried out in fuel cells to date.

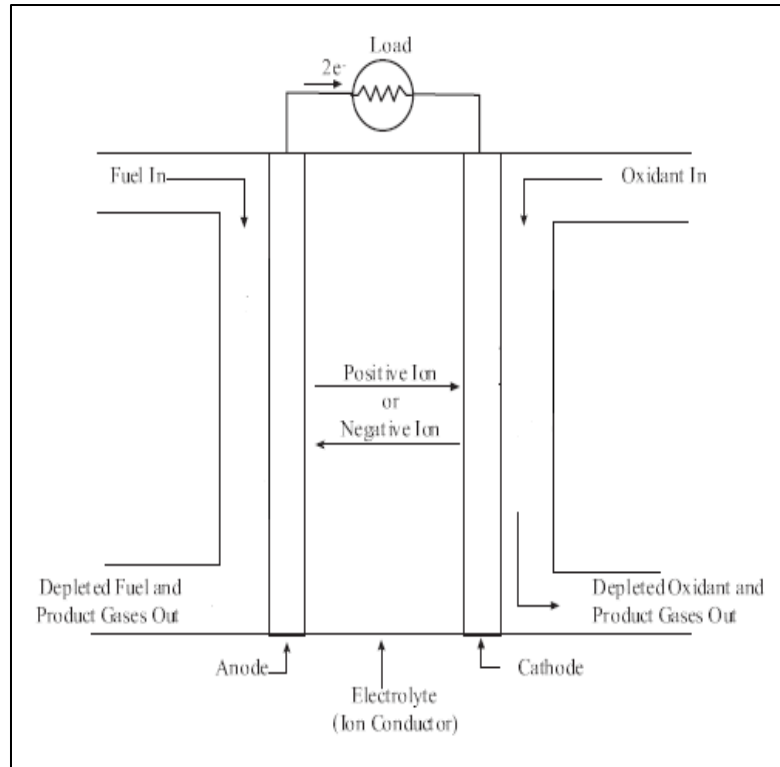


Figure 1.1: Schematic of a fuel cell

## 1.2 History of Fuel Cells

The first fuel cells were discovered by Sir William Robert Grove in the 1830s from his experiments on the electrolysis of water. The device consisted of two platinum electrodes dipped into a dilute sulfuric acid solution which resulted in the electrolysis of water into hydrogen and oxygen. He found that at electrodes where hydrogen and oxygen were liberated, a potential difference developed and when they were connected in an electrical circuit current flowed in between them. This device was called the gas voltaic battery and this was the earliest version of the fuel cell. A schematic of the cell is shown in Figure 1.2 [2].

Ludwig Mond and Carl Langer performed experiments using platinized platinum electrodes and a porous ceramic matrix to immobilize the sulfuric acid electrolyte. Hydrogen and oxygen were used to obtain reasonable currents of 2-3A. In 1894 Wilhelm Ostwald proposed devices for electrochemical oxidation of fuels without heat production and this formed the basis for the beginning and the advancement of fuel cell research.

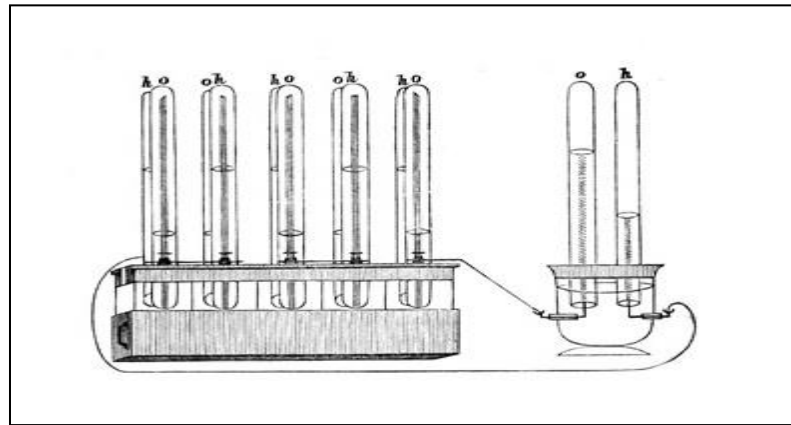


Figure 1.2: A schematic of the Grove gas voltaic battery

In 1932 Francis Thomas Bacon replaced the highly corrosive acidic solution which was used as electrolyte with alkaline solution, and it was called the alkaline fuel cell. This was complemented with the electrodes made from lithiated nickel which further enhanced the corrosion resistance. He demonstrated fuel cells producing power of 5 to 6 kW using high temperatures and pressures. The acidic and the alkaline based fuel cells were the main topics of research until the 1960s.

Research into the other type of fuel cells such as molten carbonate fuel cell, solid oxide fuel cell, and phosphoric acid fuel cell began with earnest in the 1960s. Fuel cells with methanol as fuel began to be used with the acidic electrolyte as it could not be used with alkaline electrolytes since the reaction product, carbon-dioxide formed carbonates

with the electrolyte resulting in performance loss. A comparison chart of different types of fuel cells along with their applications is listed below in Table 1.1.

Table 1.1: Comparison chart of different types of fuel cells [3]

Fuel Cell Type	Common Electrolyte	Operating Temperature	Typical Stack Size	Efficiency	Applications	Advantages	Disadvantages
Polymer Electrolyte Membrane (PEM)	Perfluoro sulfonic acid	50-100°C 122-212° typically 80°C	< 1kW-100kW	60% transportation 35% stationary	<ul style="list-style-type: none"> <li>• Backup power</li> <li>• Portable power</li> <li>• Distributed generation</li> <li>• Transportation</li> <li>• Specialty vehicles</li> </ul>	<ul style="list-style-type: none"> <li>• Solid electrolyte reduces corrosion &amp; electrolyte management problems</li> <li>• Low temperature</li> <li>• Quick start-up</li> </ul>	<ul style="list-style-type: none"> <li>• Expensive catalysts</li> <li>• Sensitive to fuel impurities</li> <li>• Low temperature waste heat</li> </ul>
Alkaline (AFC)	Aqueous solution of potassium hydroxide soaked in a matrix	90-100°C 194-212°F	10-100 kW	60%	<ul style="list-style-type: none"> <li>• Military</li> <li>• Space</li> </ul>	<ul style="list-style-type: none"> <li>• Cathode reaction faster in alkaline electrolyte, leads to high performance</li> <li>• Low cost components</li> </ul>	<ul style="list-style-type: none"> <li>• Sensitive to CO<sub>2</sub> in fuel and air</li> <li>• Electrolyte management</li> </ul>
Phosphoric Acid (PAFC)	Phosphoric acid soaked in a matrix	150-200°C 302-392°F	400 kW 100 kW module	40%	<ul style="list-style-type: none"> <li>• Distributed generation</li> </ul>	<ul style="list-style-type: none"> <li>• Higher temperature enables CHP</li> <li>• Increased tolerance to fuel impurities</li> </ul>	<ul style="list-style-type: none"> <li>• Pt catalyst</li> <li>• Long start up time</li> <li>• Low current and power</li> </ul>
Molten Carbonate (MCFC)	Solution of lithium, sodium, and/or potassium carbonates, soaked in a matrix	600-700°C 1112-1292°F	300 kW-3 MW 300 kW module	45-50%	<ul style="list-style-type: none"> <li>• Electric utility</li> <li>• Distributed generation</li> </ul>	<ul style="list-style-type: none"> <li>• High efficiency</li> <li>• Fuel flexibility</li> <li>• Can use a variety of catalysts</li> <li>• Suitable for CHP</li> </ul>	<ul style="list-style-type: none"> <li>• High temperature corrosion and breakdown of cell components</li> <li>• Long start up time</li> <li>• Low power density</li> </ul>
Solid Oxide (SOFC)	Yttria stabilized zirconia	700-1000°C 1202-1832°F	1 kW-2 MW	60%	<ul style="list-style-type: none"> <li>• Auxiliary power</li> <li>• Electric utility</li> <li>• Distributed generation</li> </ul>	<ul style="list-style-type: none"> <li>• High efficiency</li> <li>• Fuel flexibility</li> <li>• Can use a variety of catalysts</li> <li>• Solid electrolyte</li> <li>• Suitable for CHP &amp; CHHP</li> <li>• Hybrid/GT cycle</li> </ul>	<ul style="list-style-type: none"> <li>• High temperature corrosion and breakdown of cell components</li> <li>• High temperature operation requires long start up time and limits</li> </ul>

Despite the different variants available our main focus here would be the development of the proton exchange membrane and alkaline anion exchange membrane fuel cells based on methanol. The mechanisms of operation and the current problems in these devices are listed in order to provide some insight as to how this research would address these issues. Later a new generation of fuel cells called hybrid fuel cells that have been developed by combining these two will also be discussed.

### 1.3 Proton Exchange Membrane Fuel Cells

The PEMFCs consists of two electrodes where the oxidation and reduction reaction occurs. Platinum electrodes were traditionally used, and now recently platinum supported on carbon are preferred as catalysts. Hydrogen is the most commonly used fuel in these types of fuel cells providing the highest performance. The proton exchange fuel cell may be operated using liquid fuel such as methanol. A polymeric membrane acts as the electrolyte assisting in the transport of the  $H^+$  ions from the anode to the cathode. It prevents the leakage of electrons across it, and also prevents the reactants at the anode and cathode from mixing. The schematic representation of a PEMFC for operation with hydrogen and methanol is shown below in Figure 1.3 [4].

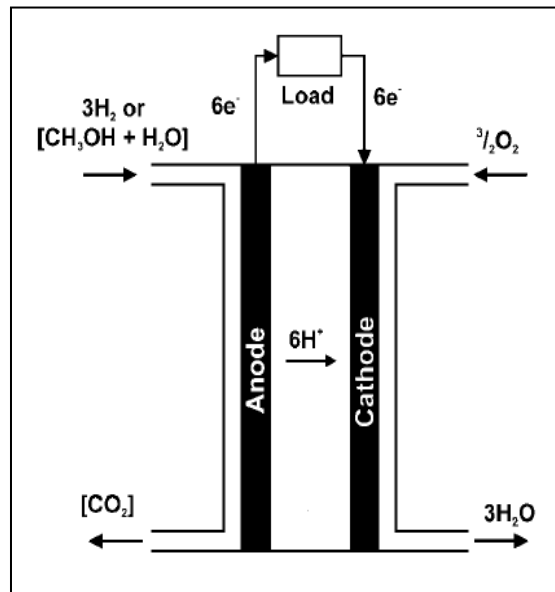
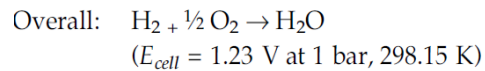
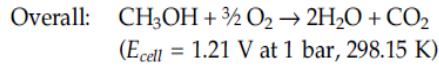
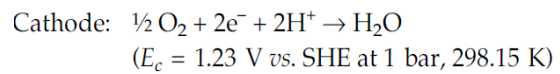
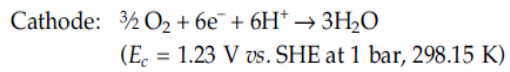
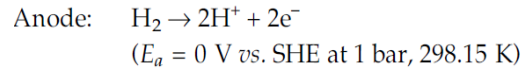
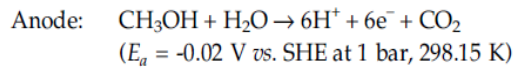


Figure 1.3: Proton exchange membrane fuel cell

The electrode reactions for PEM fuel cells operated with MeOH and  $H_2$  are given below



The solid polymer electrolyte fuel cell was first developed by General Electric for use on manned space vehicles. These cells consisted of solid polystyrene sulfonic acid membranes for the transport of protons or  $\text{H}^+$  ions. The other operations are similar to the acidic fuel cell with the liquid electrolyte. The development of the polymeric membrane Nafion® by DuPont in 1967 furthered the use of these types of fuel cells.

Nafion is a perfluorosulfonic acid membrane with a structure similar to teflon having ether linkages on its side chain, followed by a  $\text{CF}_2$  group before the sulfonic acid. The nafion based membranes had twice the conductivity of previously used membranes. The  $\text{CF}_2$  groups also provided stability in the anode and the cathode which contained a small portion of hydrogen peroxide produced as a by-product. The most dramatic effect of the use of the nafion was that the lifetime of these membranes was increased by 4 times compared to previously used membranes. The structure of nafion is depicted below in the Figure 1.4 [5].

Research on these fuel cells was ended after the Gemini space program and alkaline fuel cells were adopted for further programs. Scientific research on PEM started once again in the late 1980s. Currently, PEM fuel cells are among the most studied topics in fuel cells by various research groups around the world [6].

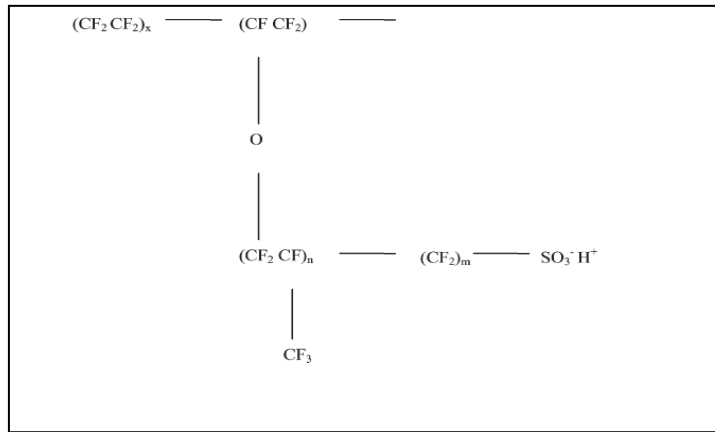


Figure 1.4: Structure of Nafion

Methanol is a fuel of interest in PEMFCs owing to its high volumetric energy density, efficiency, and ease of transportation and handling. The elimination of the bulky reformers that are required in hydrogen based systems to convert fuel to hydrogen is a further advantage of these types of fuel cells. A chart showing the energy density of different fuels comparing them with batteries is given in Figure 1.5 [7].

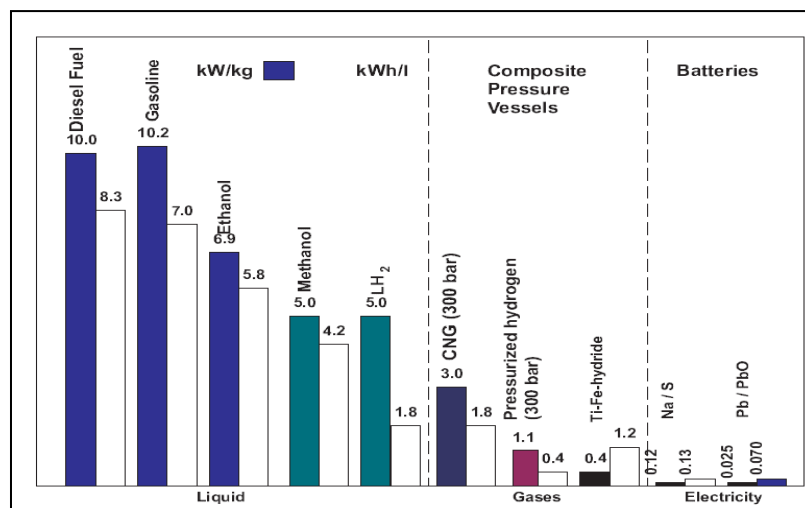


Figure 1.5: Specific gravimetric and volumetric energy density of selected fuels in comparison with batteries

The major reason that these fuel cells have come to the forefront is owing to advancements in portable electronics which have created a need for a new higher energy density, low-cost and long-lasting energy source. The portable electronic devices include: note book computers, video cameras, still cameras, cellular phones and medical appliances that are being mass produced. Powering these devices is currently achieved by using storage batteries such as nickel-cadmium, nickel-hydride, and more recently lithium-ion batteries which lasts for several hours but once they are drained they need hours of recharging which is a severe drawback for these devices.

Methanol based fuel cells have gained attention because of their long uninterrupted functioning, an important advantage over batteries. After the fuel is exhausted they can be immediately recharged by changing the fuel cartridge. The fact that direct methanol fuel cells (DMFC) are approaching reasonable power densities combined with their design simplicity makes them a very attractive for portable power systems and remote power applications. These electronic devices also need very low power of a few milli-watts or a few watts at the most. Fuel cells designed for small applications have been termed mini fuel cells or micro fuel cell with the former term being preferred [2]. DMFCs with power densities as high as  $0.5 \text{ W/cm}^2$  at elevated temperatures ( $130 \text{ }^\circ\text{C}$ ) with dry air as the oxidant have been demonstrated [8].

DMFCs have not achieved their full potential owing to several inherent problems. Most scientific research has been carried out in order to address these short comings. The main drawbacks today with these systems are related to the methanol oxidation rate at the anode where the reaction proceeds at three or four order of magnitudes slower than the electro-oxidation of hydrogen. This is because the methanol oxidation reaction involves a six electron transfer reaction as compared to the two electron transfer in a hydrogen based fuel cell. A high catalyst loading is essential for the reaction to provide considerable power which in turn increases the overall cost of the cell.

The main efforts in the reduction of platinum loading in fuel cells are concerned with the cathode. Currently, the oxygen reduction reaction (ORR) at the cathode is carried out with platinum based catalysts. The use of non-noble metal catalysts for ORR has been demonstrated. These catalysts include organic transition metal complexes of iron, and cobalt with tetra-methyl phenyl porphyrins. The oxygen reduction activity for such metals are lower compared to that of Pt and the stability of these metal ions are in question as they were found to dissolve irreversibly in the acidic environment that exists during fuel cell operation. However at the moment, better fabrication protocols to enhance the catalyst utilization, and a reduction in the overall catalyst usage seems to be the alternative at hand while the search for a suitable non-noble metal catalyst continues.

The main drawback in the methanol based systems is a phenomenon called the methanol crossover across the proton exchange membrane. Methanol is transported across the membrane due to diffusion, owing to a concentration gradient across the membrane and also due to the electro-osmotic drag along with the  $H^+$  ions. Nafion membrane allows methanol transport, which upon reaching the cathode is oxidized to  $CO_2$  and  $H_2O$ . This competing oxidation reaction results in a mixed potential at the cathode, a reduction in the open circuit potential, and also a significant reduction in the coulombic efficiency. Further the cathode reaction sites are used for methanol oxidation resulting in a decrease in the overall cathode catalyst utilization. This problem is further aggravated at higher temperature where there is an increase in the diffusion coefficient and also an increase in the swelling of the polymer membrane allowing for an increase in the methanol crossover [9]. The cost of nafion membranes 750 US  $\$/m^2$  is also a factor that adds to the overall cost of a fuel cell and hence a stumbling block that needs to be overcome [10].

The crossover problem can be tackled by developing alternative proton exchange membrane that is more selective to proton transport than to methanol. Several classes of polymers including sulfonated poly (ether ether ketone) and poly (ether sulfone) [11],

poly vinylidene fluoride and many others have also been considered as a replacement for Nafion. Cross-linking of the polymers has also been tried however their conductivity is still not comparable to nafion despite higher methanol permeability resistance [12,13].

Increasing the thickness of the polymer membrane is another method of reducing crossover. However, this has the disadvantage of increasing the overall ohmic resistance of the cell and hence results in reduced performance. Another means of reducing the crossover is to reduce the methanol concentration utilized at the cathode hence reducing the concentration gradient across the membrane. Dilution of the methanol solution leads to reduced crossover but this leads to a reduction in energy content and it might also lead to transport limitations at the anode at higher current densities [14]. Increasing the cathode reactant pressure or flow rate is another means of reducing the methanol crossover however this results in a parasitic power loss and is not desirable [15]. Finally the use of non-noble metal cathodes which have a high selectivity for oxygen reduction and a high tolerance towards methanol would be ideal, however as mentioned there has to be a significant improvement in catalyst activity for these catalysts to be used as a replacement for platinum.

Cathode flooding is another major drawback in direct methanol fuel cells. Water is produced at the cathode owing to the oxygen reduction reaction and with the transport of  $H^+$  ions it was found that roughly 2.5 molecules of water were also dragged along. The presence of a large amount of water results in flooding of the cathode and an overall reduction in the performance of methanol fuel cells. The excess water blocks the channels for oxygen transport resulting in a transport limitation for oxygen. The removal of the water from the cathode requires the use of high cathode flow rates which further contributes to the parasitic power consumption and further the loss of water from the anode needs to be compensated [16]. This makes the system very sensitive to the effect of relative humidity. For example, if the gas is saturated with water vapor some

condensation might take place within the pore and the gas is unable to pick up any moisture from within the pores, hence aggravating the existing problem of flooding.

Several methods have been utilized in order to overcome the effect of the cathode flooding the most important of which being the use of high cathode flow rates. The use of the micro-porous layer was believed to create a hydraulic pressure differential which led to the back diffusion of the water across the membrane and hence resulting in the cathode pores being free from water [17, 18]. The hydrophobicity of the backing layer also plays a crucial role in the removal of the water from the cathode through the pores [19]. Controlling the hydrophobicity results in the development of a capillary pressure that is favorable for the liquid transport away from the catalyst layer and hence is another way of reducing the cathode flooding [20]. The inclusion of hydrophobic materials such as PTFE decreases the porosity and hence might lead to a transport limitation for the oxygen at the cathode.

To summarize the main issues that are hindering the commercialization and successful operation of a direct methanol fuel cell include (i) high cost of catalyst and nafion membranes, (ii) methanol cross-over, and (iii) cathode flooding

Alkaline fuel cells may overcome these limitations. These fuel cells will be described in detail in the next section.

#### **1.4 Alkaline Fuel Cells**

Alkaline fuel cells were the first practical fuel cells to be used for the generation of electricity from hydrogen. The alkaline fuel cells were the first to be applied for trials in vehicular applications and these fuel cells were also an integral part of the space programs. Alkaline fuel cells were initially shown to produce high power densities and achieve high energy conversion efficiencies [21]. Non-noble metal catalysts such as

silver, and nickel could be used as electrodes, since the alkaline environment is not as strongly corrosive as in the acid fuel cells [22]. The alkaline fuel cells used by NASA provided a very high performance when pressurized to 60 psig and 80 °C. Power densities as high as 0.9 W/cm<sup>2</sup> were obtained. Despite this impressive performance, alkaline fuel cells are not very widely used and research on such fuel cells has been discontinued. The reasons for their discontinuation will be explained later but first the mechanism of operation of such fuel cells will be elucidated.

The alkaline fuel cells consist of two electrodes (Pt based) or with a non-noble metal cathode, and an electrolyte (liquid or polymer membrane) that can be used for the transport of the OH<sup>-</sup> ions. The direction of the transport is opposite to that in conventional PEMFC. Water is generated at the anode and is consumed as a reactant at the cathode unlike in PEM fuel cells where water is generated at the cathode. The schematic and the mechanism of alkaline fuel cells operated with methanol and hydrogen have been illustrated below in Figure 1.6.

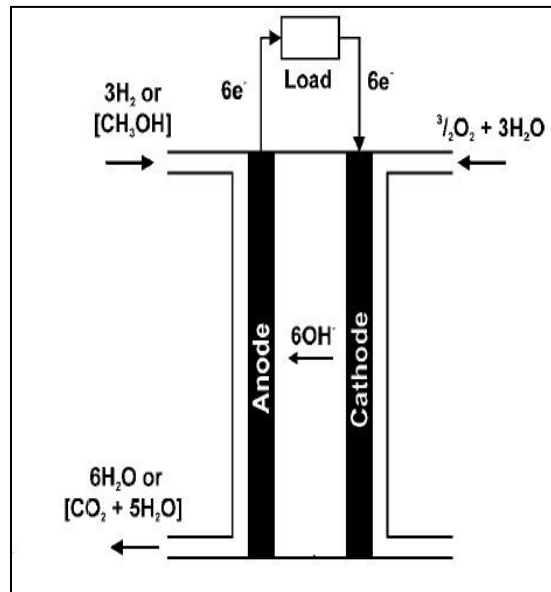
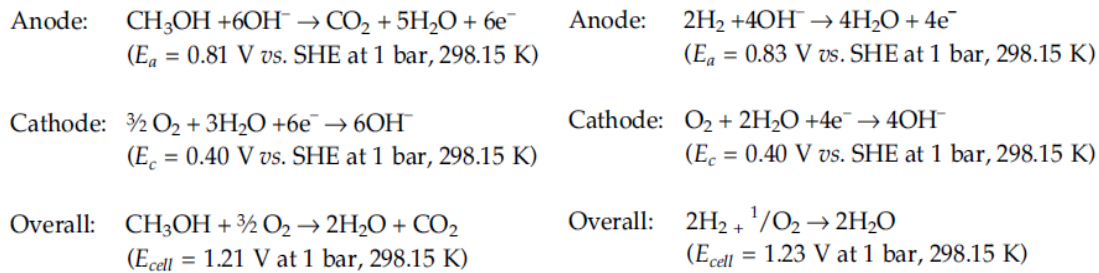


Figure 1.6: Alkaline fuel cell [4]



The alkaline fuel cells used previously consists of a highly alkaline electrolyte such as KOH. The alkaline electrolytes were the main reason for the discontinuation of AFCs as there is an issue of the degradation of the electrolyte with formation of a carbonate/bicarbonate in the liquid electrolyte in the presence of CO<sub>2</sub>. The formation of the carbonate in the electrolyte results in the increase in the electrolyte viscosity resulting in increased mass transport resistance and a loss in the ionic conductivity of the electrolyte. The reduced OH<sup>-</sup> transport further results in a reduced anodic reaction rate [23]. The cathodic reaction is also retarded owing to the decreased oxygen solubility. The carbonation of the electrolyte has restricted the use of these systems to cases where oxygen is used as the oxidant.

A further problem in DMFC is that the anode oxidation reaction involves the formation of carbon dioxide and the carbonation of the electrolyte cannot be avoided. Even though methanol based AFCs have been demonstrated the performance of these fuel cells gradually declined over time [24]. This has been responsible for the decrease in the interest in research on alkaline fuel cells.

Recently interest in these cells has been renewed especially with the use of alkaline anion exchange polymer membranes as electrolytes similar to those used in the proton exchange membrane fuel cells. The increase in interest is evident in the number of publications that have been made on this topic in recent years is shown in Figure 1.7 [25].

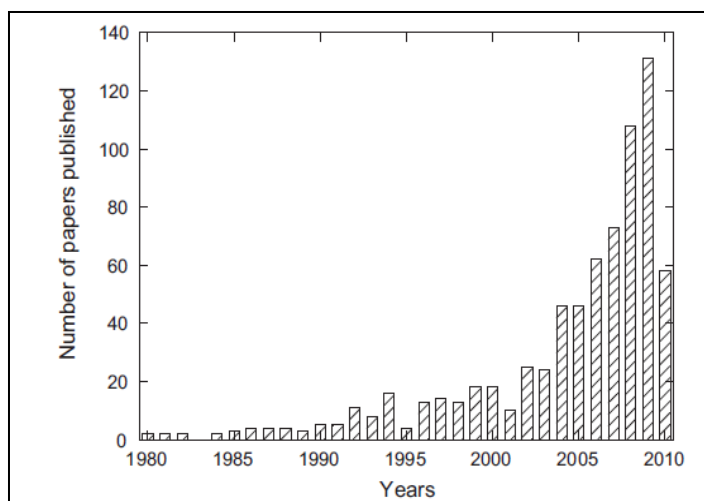


Figure 1.7: Publications on alkaline fuel cells in recent years

The use of an alkaline anion exchange membrane in direct methanol fuel cell was carried out with the commercially available Morgane® ADP membranes, that were mainly used for salt electro dialysis. These anion exchange membrane were used for the transport of the OH<sup>-</sup> ions in the fuel cell [26]. These fuel cells still used a fuel composed of methanol and NaOH, this was possibly to improve the ionic conductivity within the electrode. The liquid electrolyte helped the extension of the reaction zone within the catalyst; otherwise most of the reaction would be occurring in the catalyst membrane interface, due to the non-availability of soluble anion exchange ionomers. However this was the first such research to demonstrate the feasibility of AEM DMFCs.

AEM DMFCs have several important advantages over the conventional PEM fuel cells. They are listed below.

- Enhanced methanol oxidation kinetics in alkaline environment [27].
- Utilization of non-noble metal based catalyst such as nickel, and silver owing to the less corrosive alkaline environment [28-30].
  - Reduced cost.
  - Methanol tolerance of such catalysts would be an added advantage.

- Subdued peroxide radical initiated membrane degradation.
- Ion transport from cathode to the anode.
  - Reduced methanol crossover.
  - Cathode flooding averted as water transport due to electro-osmotic drag is from cathode to anode, and water is also a reactant in the oxygen reduction reaction.
  - Allows for the use of thinner low resistance membrane.

A schematic showing the direction of ion and water transport in AEMFC is given in Figure 1.8 [31].

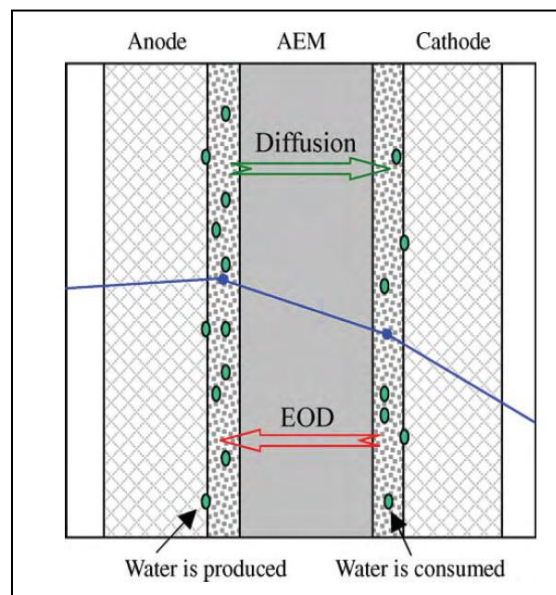


Figure 1.8: Ion and water transport in AEMFC

The most important advantage with the use of the alkaline AEMFC is that it does not involve the use of a liquid KOH electrolyte and hence the precipitation of the carbonate which was a concern in previous AFC is no longer a concern here. Thus the alkaline anion exchange membrane fuel cell encompasses the advantages of the AFC and addresses the issues of the PEM fuel cell.

The major focus of research in this field is on the development of AEM and the development of non-noble metal catalysts. The synthesis of AEMs is achieved by attachment of the functional groups to the polymer backbone and then performing a chloromethylation reaction on the polymer and then converting the chloromethyl groups into tetraalkylammonium cations. The quaternary ammonium which is covalently bonded to the polymer backbone attracts negatively charged OH<sup>-</sup> ions and help in their ionic transport [32]. Benzyl trimethyl ammonium cations are most commonly used because they have no β-hydrogens and thus do not undergo Hofmann elimination reactions. Phosphonium [33], and imidazolium [34] functional groups have also been used in AEMs.

Some studies have also been carried out using commercial membranes such as Tokuyama® [29], Fumasep® [32] in AEMDMFCs. Several other systems that have been investigated for the use as AEM a few of them are mentioned here namely: poly sulfone [35,36], poly(ether-imide), polybenzimidazole doped with KOH [37]. The performance with these membranes is not very high and the conductivity of these membranes is low which could be the factor that could limit the overall performance of such fuel cells. The mobility of the OH<sup>-</sup> ions is also lower owing to their larger size compared to H<sup>+</sup> ions [38].

Alkaline anion exchange membranes are still in their infancy and several improvements need to be made. An increase in conductivity, stability, and transport properties seem to be most desirable. In actual AEMDMFCs despite all the advantages the performance of these fuel cells are still very low compared to the conventional PEM based fuel cells. Fuel cells constructed with platinum electrodes gave a peak power density of 8.5 mWcm<sup>-2</sup> with methanol as the fuel and oxygen with 2.5 bar back pressure at 80°C using a radiation grafted poly (ethylene co-tetrafluoroethylene) (ETFE) [39].

Studies using alternative cathodes have also been pursued. Pd-Sn/C cathodes have been fabricated and tested in a passive DMFC with Pt/Ru anode and Tokuyama

membrane. The peak power density obtained was  $5.8 \text{ mW/cm}^2$  with 2M MeOH and the addition of 3M KOH [40].  $\text{MnO}_2/\text{C}$  based cathode was used in a fuel cell and a peak power of  $16 \text{ mW/cm}^2$  at  $60 \text{ }^\circ\text{C}$  was obtained with a membrane prepared by the radiation grafting of vinyl benzylchloride onto poly (tetrafluoroethylene-co-perfluoropropyl vinyl ether). The fuel consisted of 1M MeOH and 1M KOH [41].

A few studies also made use of the conventional Pt electrodes [26, 42]. Tokuyama membranes and Pt electrodes were used in order to obtain the highest performance obtained with air was  $12.5 \text{ mW/cm}^2$  with 7M MeOH and 1M KOH at room temperature. This result is encouraging because of the use of a highly concentrated fuel and also the use of atmospheric air as the oxidant to obtain reasonable performance. The main conclusion however called for the development of a soluble ionomer similar to Nafion which would enable enhanced catalyst utilization and better performance [43].

The effect of the operating parameters on AEMFC performance with Pt based electrodes with Tokuyama membrane provided a maximum performance of  $168 \text{ mW/cm}^2$  at  $90 \text{ }^\circ\text{C}$  with oxygen and a fuel composed of 2M KOH and 1M MeOH [44]. A fuel cell characterized with commercial Fumasep membrane using Pt electrodes provided power densities of  $0.32 \text{ mW/cm}^2$  at  $50 \text{ }^\circ\text{C}$  and MeOH concentration of up to 15 M were used in these experiments [32]. The data obtained from the different studies are summarized in Table 1.2.

A few observations could be made from the most recent studies. In summary the fuel cells with AEM membranes theoretically seem to be holding several advantages over PEM based fuel cells, however the performances of AEM fuel cells with Pt based electrodes are still very low. The conductivity of the membranes used in most of these studies is very low and this combined with the low mobility of the  $\text{OH}^-$  ions is another major problem.

Most of the fuel cell performances mentioned here involve the use of an alkaline electrolyte in the fuel and performances without these are very moderate. This indicates the necessity of a soluble ionomer similar to that of nafion in order to ensure improved catalyst utilization within the layers and not just the catalyst at the membrane-electrode interface. Further the addition of these liquid alkaline electrolytes in the catalyst layers again introduces the problem that was experienced with the conventional AFCs, carbonation and blockage of the catalyst layers slowly undermining the overall performance. Stability and long term operation of these fuel cells have not been reported up to date owing to this carbonation and such performances are short lived and decrease once the catalyst pores are blocked with these carbonates.

The problems that need to be sorted can be summed up as follows:

- High conductivity and stability membranes.
- Soluble ionomer for dispersion in the catalyst layer.
- High activity non-noble metal catalyst.

Research in the AEM fuel cells mostly focuses on these issues. In addressing the issues associated with these fuel cells research has branched out with the development of other variations that combine the advantages of both the PEM and the AEM together. These new variants called hybrid fuel cells are the latest breed of fuel cells. These fuel cells will be the major concern of the study here. The basics of these fuel cells are discussed in detail.

Table 1.2: Summary of different studies on alkaline fuel cells with methanol

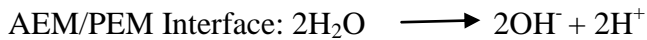
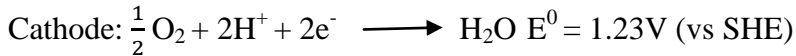
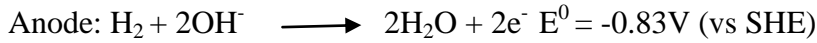
Anode	Cathode	Membrane	Fuel	Peak Power	Operating conditions
Pt on Ti mesh (1.79mg/cm <sup>2</sup> ) [26]	Pt (0.77mg/cm <sup>2</sup> ) (air)	Morgane ADP membrane	2M MeOH and 1M NaOH	17.8 mW/cm <sup>2</sup>	60 °C, Cathode - 1bar
Pt-Ru/C (4mg/cm <sup>2</sup> ) [39]	Pt/C (4mg/cm <sup>2</sup> ) (O <sub>2</sub> )	Radiation grafted ETFE	MeOH	8.5 mW/cm <sup>2</sup>	80 °C, 2 bar - anode, 2.5 bar- cathode
Pt-Ru/C (2mg/cm <sup>2</sup> ) [40]	Pd-Sn/C (1.46 mg/cm <sup>2</sup> )	Tokuyama membranes	3M MeOH and 1M KOH	5.8 mW/cm <sup>2</sup>	Passive DMFC
Pt-Ru/C (3mg/cm <sup>2</sup> ) [41]	MnO <sub>2</sub> /C (5.1mg/cm <sup>2</sup> ) (O <sub>2</sub> )	Radiation grafted membrane	1M MeOH and 1M KOH	16 mW/cm <sup>2</sup>	60 °C
Pt-Ru/C (4mg/cm <sup>2</sup> ) [43]	Pt/C (4mg/cm <sup>2</sup> )	Tokuyama A-010 membrane	7M MeOH and 1M KOH	12.5 mW/cm <sup>2</sup>	Room temperature, Air
Pt-Ru/C (8mg/cm <sup>2</sup> ) [44]	Pt/C (8mg/cm <sup>2</sup> )	Tokuyama A-006 membrane	2M KOH and 1M MeOH	168 mW/cm <sup>2</sup>	90 °C (O <sub>2</sub> - 1270 ml/min)

## 1.5 Hybrid Fuel Cells

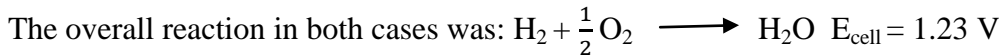
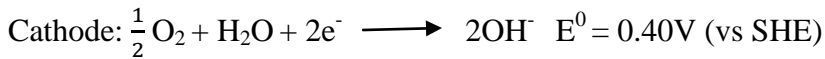
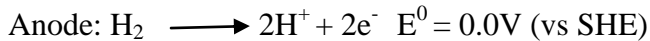
A recent advancement that has been made is the novel hybrid fuel cell design, where the advantages of the PEM and the AEM fuel cells have been combined. The design of the fuel cell is very simple with a high pH electrode (AEM), a low pH electrode (PEM) and a PEM membrane. This fuel cell is able to exploit the high conductivity of Nafion and also the high pH operation. This type of fuel cell can be used to understand the operating behavior at one electrode and also to optimize the ionomer for the fuel cell performance [45, 46].

The most initial design of the hybrid fuel cell was shown to consist of two half cells, with the AEM electrode assembled on an AEM membrane and a PEM electrode assembled on a PEM membrane. The two half cells were later pressed together to form the MEA. The theory of such membranes has also been elucidated. The two configurations are clearly represented in Figure 1.9.

Case (a):



Case (b):



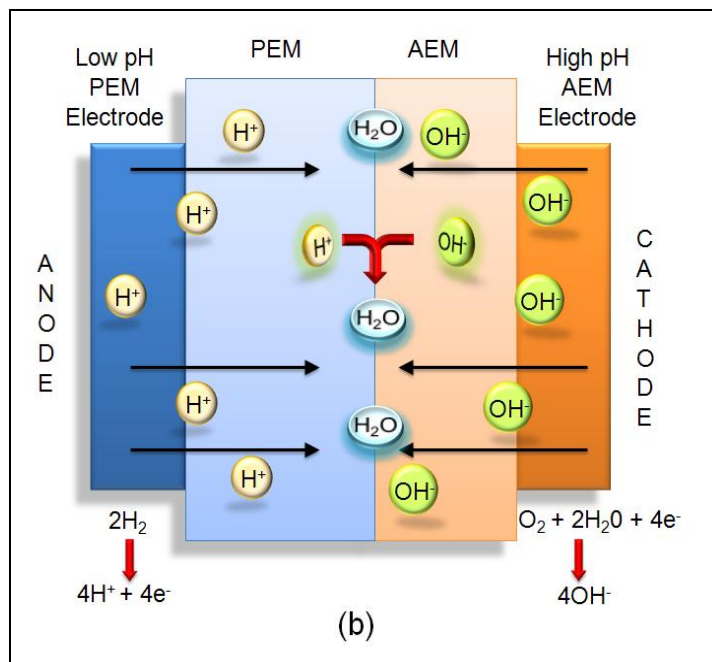
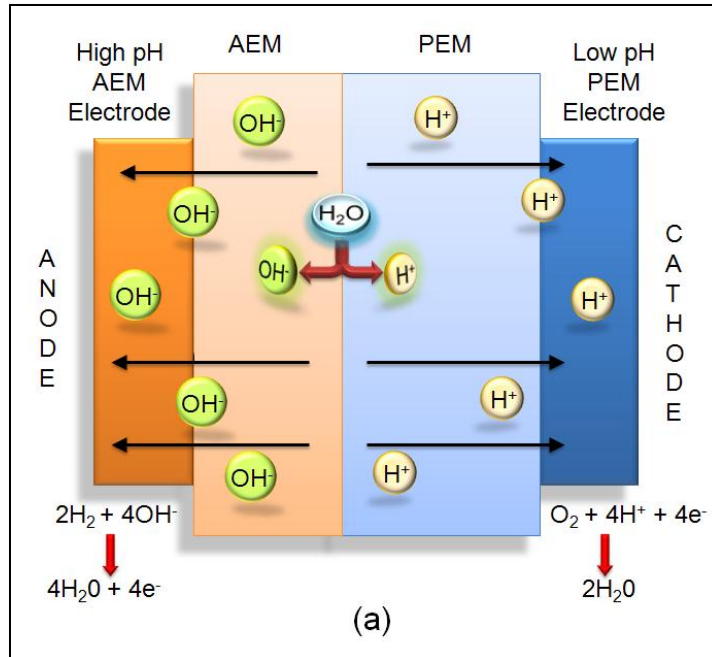


Figure 1.9: Hybrid fuel cells: (a) AEM anode and PEM cathode and (b) PEM anode and AEM cathode

One of the configurations involves the splitting of water at the PEM/AEM interface and the other configuration involves the production of the water at the interface by the reaction. The overall potential of the cell has been maintained at 1.23V in both these configurations.

The interfacial behavior of the PEM and AEM junction has been compared to that of a p-n junction semiconductor. The charge carriers in the PEM are the H<sup>+</sup> ions and that in the AEM are the OH<sup>-</sup> ions. At the PEM/AEM interface there is a recombination of the ions to form water. The immobile groups in the polymer consisting of the sulfonic acid group in PEM and the quaternary ammonium groups within the AEM generate a field. The field generated by the immobile groups counteracts the diffusion of the ions to the interface results in the generation of a potential difference at the junction given by [45]:

$$E_j = \varphi^{AEM} - \varphi^{PEM} = \frac{RT}{F} \ln( a_{H^+}^{PEM} a_{OH^-}^{AEM} ) - \frac{RT}{F} \ln (K_w)$$

Where  $E_j$  is the junction potential,  $\varphi^{AEM}$  is the potential of the AEM at the interface,  $\varphi^{PEM}$  is the potential of the PEM,  $K_w$  is the water dissociation constant at the interface,  $a_{H^+}^{PEM}$ ,  $a_{OH^-}^{AEM}$  are the activities of H<sup>+</sup> ions in the PEM and the OH<sup>-</sup> ions in the AEM respectively.

The dissociation of water at the bipolar membrane interface is also referred to as the electric field enhanced (EFE) water dissociation has been widely studied [47]. The theory of such water dissociation has been explained that when there are no other ions in the interface between the cation and anion exchange membranes, then the electrical charges are transported by the H<sup>+</sup> ions and OH<sup>-</sup> ions. The reversible free energy required for such operation in a bipolar membrane is given by the Nernst equation for two different solutions having different H<sup>+</sup> ion concentration as follows.

$$\Delta G = F * \Delta U = 2.3 R * T * \Delta pH$$

Where  $\Delta G$  is the reversible free energy and  $\Delta U$  is the potential difference,  $R$  is the gas constant,  $T$  is the temperature, and  $\Delta pH$  is the pH difference between the two phases of the bipolar membrane.

In case of a one normal (1N),  $H^+$  and  $OH^-$  containing solution phases separated by a bipolar membrane the difference in potential between the two phases, i.e.,  $\Delta U$  is 0.828 V at 25°C [48]. This difference in potential between the AEM and PEM interface is therefore responsible for the potential of the fuel cell remaining at 1.23 V.

In case (a) of Figure 1.9, the  $H^+$  ions and the  $OH^-$  ions migrate away from the interface with the creation of a depletion region at the interface. The depletion region leads to the water dissociation that occurs at the AEM/PEM junction and further the junction potentials shifts the potential towards the values expected from the thermodynamics. Therefore the potential holds out to be what is expected in a conventional AEM fuel cell. In Figure 1.9 case (b) the loss in the voltage at the cathode is compensated by junction potential which provides a positive bias resulting in a cell voltage of 1.23V.

In the bipolar membrane the potential drop is dependent upon the current density, the solution resistance, and also the individual membrane resistance. The potential drop may be higher or lower depending upon the factors mentioned above and also depends on the interphase between the membranes. The thickness of the interface between the two ion exchange groups should be kept below 5 nm; especially considering the fact that specific resistance of water is very high. If the distance between the AEM and PEM increases then water dissociation is limited [49]. This might explain the open circuit voltages for such cells differing from their expected values.

The high pH anode based fuel cells fails because of the limited water transport to the AEM/PEM interface, therefore a very small quantity gets dissociated and hence these

cells cannot support higher current densities. The main advantage in the design with the high pH cathode is that it results in the production of water at the membrane interface and is responsible for keeping the membrane hydrated. The main issue with the hydrogen based fuel cells and using a dry gas feed is that the membrane gets dehydrated resulting in decreased conductivity and performance. This issue is addressed in this fuel cell, however the main issue is that since two different membranes are used there is an increased ionic resistance due to the increased thickness.

This issue of increased ionic resistance was addressed by eliminating the AEM membrane and the use of just the Nafion based membranes in similar fuel cell configurations. Fuel cells with a high pH electrode, a low pH electrode and a Nafion membrane were developed. A schematic representation of a these fuel cell is shown in Figure 1.10 [46].

The configuration with the AEM cathode: case (a) in Figure 1.10 is designated as the Cathode Hybrid Fuel Cell (CHFC) where the recombination of the ions to water occurs at the PEM/AEM cathode interface. The configuration with the AEM anode: case (b) is designated as the Anode Hybrid Fuel Cell (AHFC) here the water dissociation occurs at the AEM anode/PEM interface. The overall theoretical operating potential of 1.23V was said to be obtained with this configuration. This has been explained similar to the previous hybrid configuration with the junction potential and the Nernst potential owing to pH shift in both electrodes tending to cancel each other out.

The hybrid configurations have been mainly used in order to analyze the effect of the variation of active surface area with the three phase boundary between the catalyst, ionomer and the reactants. Despite the predicted improved kinetics of the hydrogen oxidation and the oxygen reduction, the performance in these hybrid configurations is still low and these configurations were used to understand the individual performances at the AEM anode and cathode.

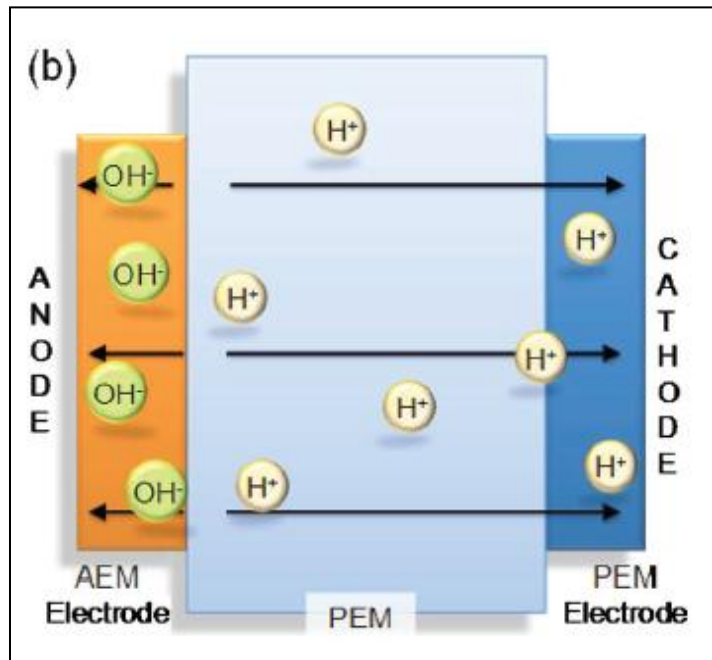
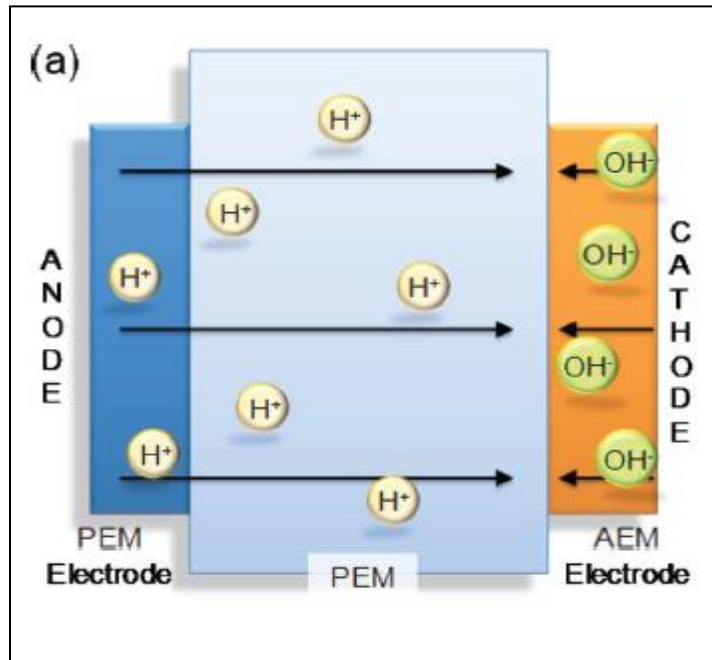


Figure 1.10: Schematic of hybrid fuel cell configurations: (a) high pH cathode and low pH anode (CHFC), (b) high pH anode and low pH cathode (AHFC)

The hybrid configurations were utilized to further understand and characterize anion exchange ionomer (AEI) in the CHFC configuration. The explanation being put forth is that in this configuration the PEM anode does not contribute to the overall impedance and hence the effect at the AEM cathode can be analyzed [50]. This configuration was further used to analyze the impact of the different electrode fabrication protocols using electrochemical impedance spectroscopy. It served as a diagnostic tool for understanding the source of electrode performance improvement. The peak power obtained with these fuel cells are  $315 \text{ mW/cm}^2$ . This performance is still lower compared to that of the conventional PEM based fuel cells. However these fuel cells have contributed greatly to the understanding of the AEM electrodes. The absence of a standard AEM membrane has brought these types of fuel cells to the forefront.

Research on these types of fuel cells have been mainly focused on hydrogen based systems. The realization that such systems could be as well applied to methanol based fuel cells and would be of great benefit in the characterization of ionomers and help in understanding and optimizing electrode properties that could be eventually useful in making these hybrid cells and also the anion exchange membrane fuel cells based on methanol for use in the low power application was the main motivation behind this study.

### **1.5.1 Principle of Operation**

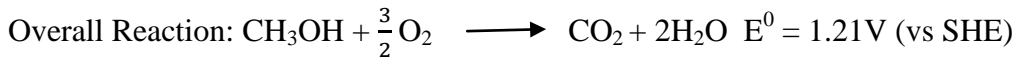
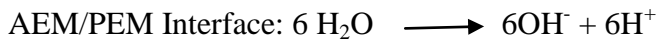
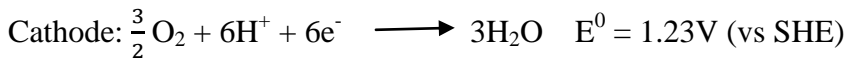
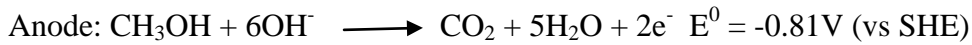
Two different types of hybrid fuel cells are considered as described previously. They are the (a) anode hybrid direct methanol fuel cells and (b) cathode hybrid direct methanol fuel cells. A brief principle of operation of both these fuel cells is given here.

#### 1.5.1.1 Anode Hybrid Direct Methanol Fuel Cells

The anode hybrid fuel cell operated with direct methanol comprises of a high pH anode where the oxidation of the methanol takes place under alkaline conditions and a

low pH electrode where the reduction of oxygen takes place under acidic conditions. A PEM membrane is used as the ion exchange electrolyte in this fuel cell. In this fuel cell the two junctions between the PEM electrode / PEM membrane, and the one at the AEM electrode/PEM membrane. The latter is very crucial in the overall performance of the fuel cell. The dissociation of the water takes place at this interface and this provides the AEM electrode with the OH<sup>-</sup> ions to maintain the alkaline conditions necessary for operation at the anode. This also provides the H<sup>+</sup> ions which are transported across the membrane and necessary for the oxidation reduction at the low pH anode. A schematic of the reaction mechanism is provided in Figure 1.11.

The reactions in the hybrid fuel cells are represented as follows:



Therefore the overall reaction of the anode hybrid direct methanol fuel cell resembles that of a conventional PEM based DMFC. It is interesting to note the overall potential of the cell has been maintained at 1.21V in this fuel cell. This can be explained owing to the junction potentials at the PEM/AEM interface.

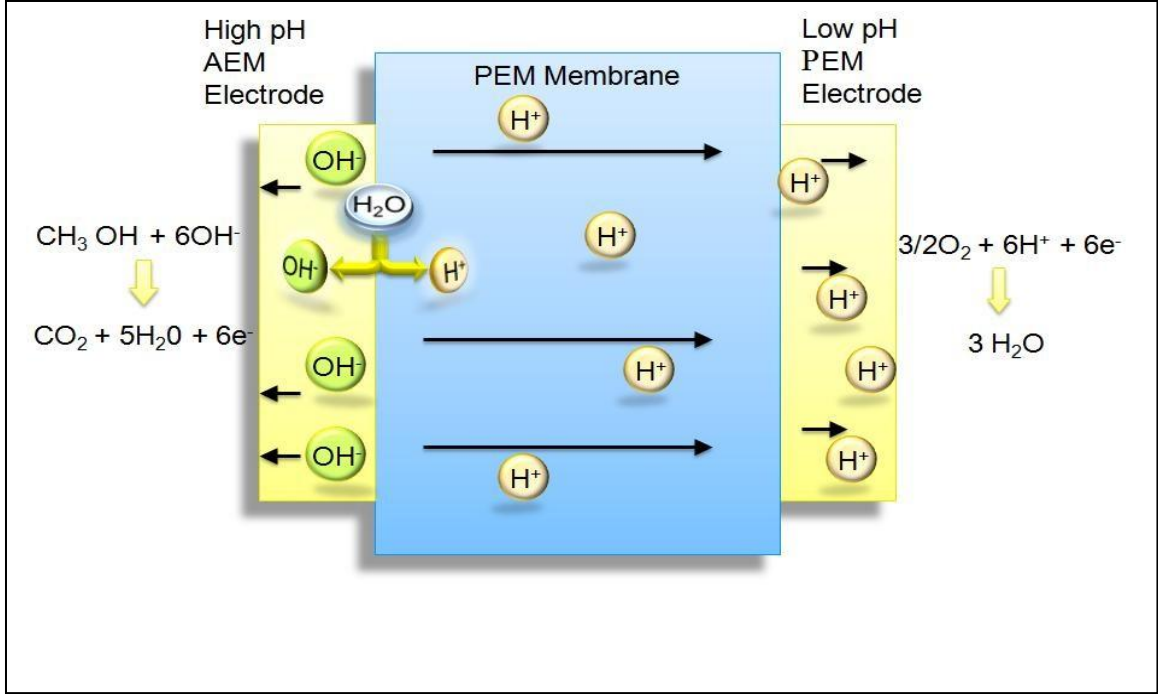


Figure 1.11: Schematic of anode hybrid direct methanol fuel cell with AEM anode and PEM cathode

The overall open circuit potential of a conventional direct methanol fuel cell is obtained from the Nernst equation[51]:

$$E = E_C^0 - E_A^0 + \frac{RT}{6F} \ln \left\{ \left[ \frac{a_{CH_3OH,a} a_{H_2O,a}}{a_{H_2O,c}^2} \right] [P_{CO_2,a}]^{-1} \left[ \frac{P_{O_2,c}}{P} \right]^{3/2} \right\} + \frac{RT}{F} \ln (a_{H^+}^{PEM} a_{OH^-}^{AEM}) + E_j$$

Where the  $E$  represents the potential of the fuel cell,  $E_C^0$  and  $E_A^0$  represents the standard potential for the anode and the cathode respectively.  $a_{CH_3OH,a}$  represents the activity of methanol at the anode.  $a_{H_2O,a}$ ,  $a_{H_2O,c}$ ,  $a_{H^+}^{PEM}$ ,  $a_{OH^-}^{AEM}$  are the activities of water at the anode and the cathode,  $H^+$  ions in the PEM and the  $OH^-$  ions in the AEM respectively.  $P_{CO_2,a}$  is the pressure of  $CO_2$  produced at the anode and  $P_{O_2,c}$  is the oxygen pressure supplied at the cathode,  $P$  is the total pressure.

The junction potential at the AEM /PEM interface introduces an additional term to the Nernst equation which is given by [45]

$$E_j = \varphi^{AEM} - \varphi^{PEM} = -\frac{RT}{F} \ln(a_{H^+}^{PEM} a_{OH^-}^{AEM}) + \frac{RT}{F} \ln(K_w)$$

The junction potential is said to balance the potential of the fuel cell at 1.21 V. The difference in the pH between the AEM and PEM results in potentials of up to 0.83V for unit activities of the H<sup>+</sup> and OH<sup>-</sup> ions. The activity terms in the Nernst equation and the junction potential cancel each other out. Thus the overall Nernst equation becomes:

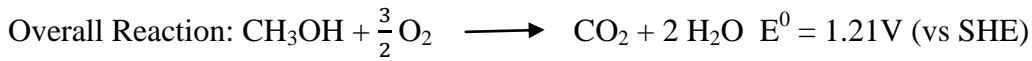
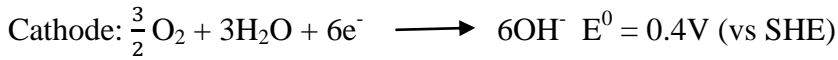
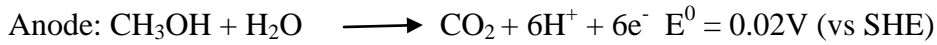
$$E = 1.21 + \frac{RT}{6F} \ln \left\{ \left[ \frac{a_{CH_3OH,a} a_{H_2O,a}}{a_{H_2O,c}^2} \right] [P_{CO_2,a}]^{-1} \left[ \frac{P_{O_2,c}}{P} \right]^{3/2} \right\}$$

#### 1.5.1.2 Cathode Hybrid Direct Methanol Fuel Cells

The cathode hybrid direct methanol fuel cell operates with an AEM cathode and a PEM anode. The AEM electrode is assembled onto a PEM half cell comprising of the PEM anode and the membrane. The oxygen reduction reaction in this configuration takes place under alkaline conditions. The critical part of this assembly is the junction between the AEM cathode/PEM membrane interface. At this junction the recombination of the H<sup>+</sup> and the OH<sup>-</sup> ions occurs and results in the formation of water. In the AEM cathode water is a reactant unlike in the PEM fuel cells. The water generated at the interface is utilized for the cathode reaction. In the general AEM fuel cells the water for the cathode reaction diffuses over from the anode side. Despite the belief that AEM cathode cannot be flooded since water is a reactant, it was shown that cathode flooding does occur [31]. The production of water at the interface therefore reduces the water gradient and hence lower

water diffusion across the membrane and reduced cathode flooding. This also allows for possible use of concentrated methanol solution at the anode with the water diffusing from the cathode being sufficient to supply the water necessary for the methanol oxidation reaction. This significantly improves the overall energy density of the system since methanol dilution is no longer necessary.

The reactions in the hybrid fuel cells are represented as follows:



The overall reactions of these fuel cells are similar to the conventional PEM fuel cells. The overall potential of the cell is again maintained at 1.21 V. This is explained due to the junction potential at the AEM/PEM interface. Similar to the case in the anode hybrid fuel cell the voltage loss is compensated by the AEM/PEM junction which constitutes a positive bias to the cell voltage. The operation of the cathode hybrid fuel cell is shown in Figure 1.12. The overall cell potential in this configuration is given by:

$$E = E_C^0 - E_A^0 + \frac{RT}{6F} \ln \left\{ \left[ \frac{a_{\text{CH}_3\text{OH},a} a_{\text{H}_2\text{O},a}}{a_{\text{H}_2\text{O},c}^2} \right] [P_{\text{CO}_2,a}]^{-1} \left[ \frac{P_{\text{O}_2,c}}{P} \right]^{3/2} \right\} - \frac{RT}{F} \ln (a_{\text{H}^+}^{\text{PEM}} a_{\text{OH}^-}^{\text{AEM}}) + E_j$$

Again considering the junction potential at the AEM/PEM interface, the activity terms of the Nernst and the junction potential gets cancelled out and the overall potential of the cell is given below.

$$E = 1.21 + \frac{RT}{6F} \ln \left\{ \left[ \frac{a_{CH_3OH,a} \cdot a_{H_2O,a}}{a_{H_2O,c}^2} \right] [P_{CO_2,a}]^{-1} \left[ \frac{P_{O_2,c}}{P} \right]^{3/2} \right\}$$

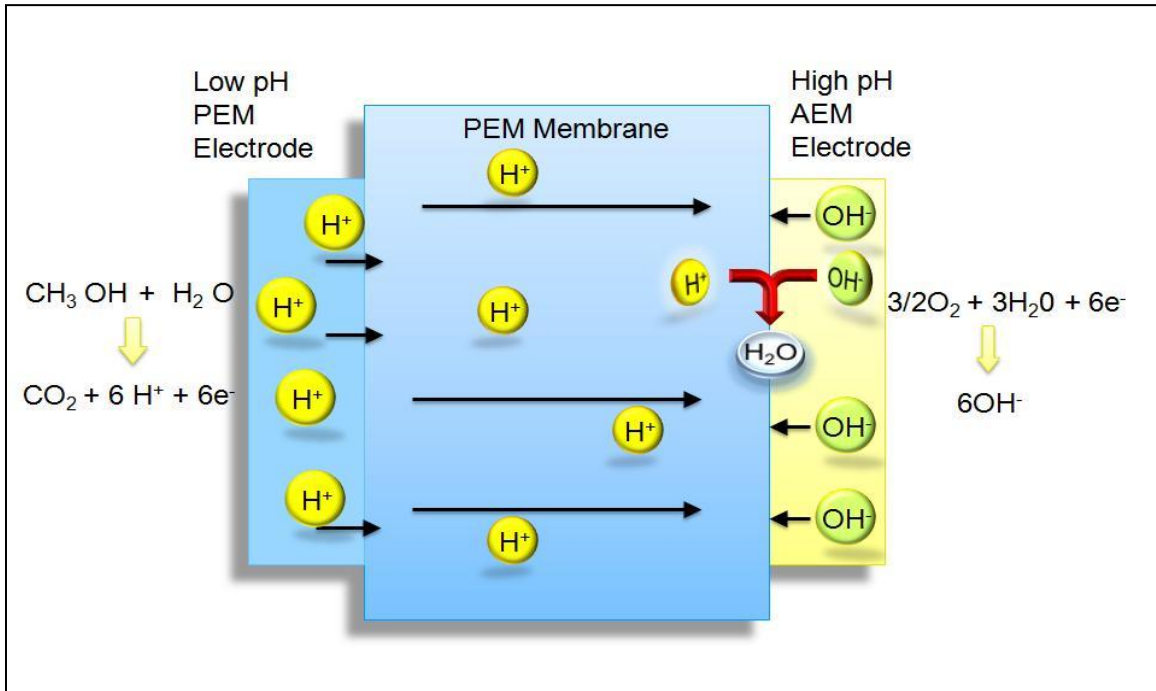


Figure 1.12: Schematic of cathode hybrid direct methanol fuel cell with PEM anode and AEM cathode

The principle of operation of these hybrid fuel cells having been discussed here. The following chapter deals with the materials and experimental procedures used in this study. The performance and optimization of the anode and cathode hybrid fuel cells operated with different ionomers and different operating conditions were discussed next. The impact of the different cationic groups in the ionomer and their effect on the hybrid fuel cell is also discussed.

## **CHAPTER 2**

### **EXPERIMENTAL SECTION**

#### **2.1 Materials**

The catalyst material used were : Pt/Ru (75 wt%) on C and Pt/C (40, 66.6 wt %) were obtained from Electrochem Inc. Nafion 117 membranes used in all experiments were obtained from Ion Power Inc. High purity solvents (99.9%) such as dimethyl formamide (DMF), isopropyl alcohol (IPA), methanol (MeOH) and sodium hydroxide crystals were obtained from VWR. Deionized water was used for all experiments. Hydrophilic gas diffusion layers (GDL) namely 2050 L from Toray industries were utilized in the fabrication of the anodes. The cathodes were fabricated with TGPH 90 also from Toray, which is a slightly more hydrophobic material reinforced with Teflon. The non platinum catalyst electrodes were obtained from Acta SpA.

Nafion ionomer 5 wt % in the solubilized form was used for the fabrication of the low pH electrodes. Several poly arylene ether sulfone based ionomer with different properties was used in the manufacture of the high pH electrode. Three different ionomer backbones were used in preparation of AEM electrodes. The ionomers have been named Ionomer I, II and III. The structure of Ionomer II and III are similar and the methods of preparation of these ionomers are slightly different. These three ionomers have been predominantly used in all studies here. These ionomers are shown in Figure 2.1-2.3. This ionomer was dissolved in dimethyl formamide (DMF) to obtain a 1 wt % ionomer solution.

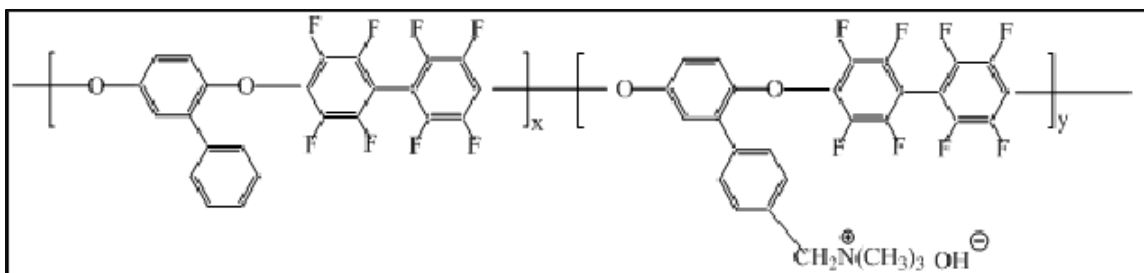


Figure 2.1: Schematic of Ionomer I

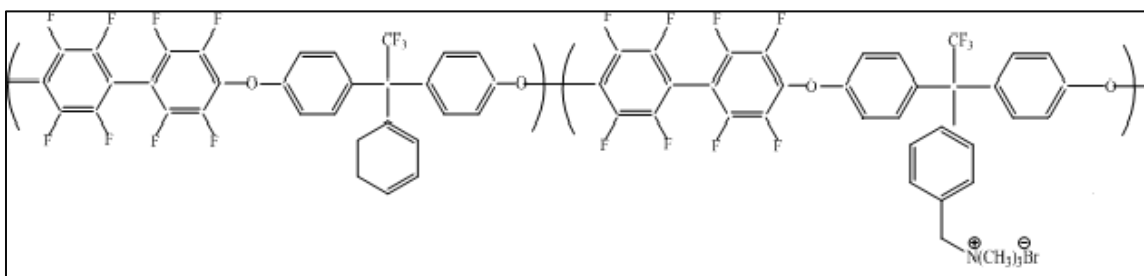


Figure 2.2: Schematic of Ionomer II

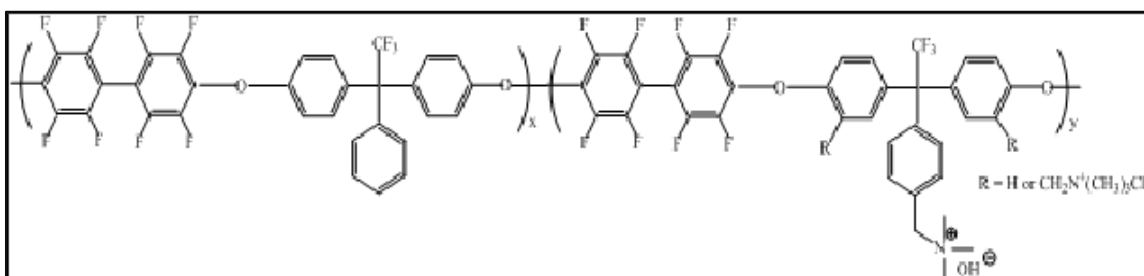


Figure 2.3: Schematic of Ionomer III

## 2.2 Experimental

Nafion 117 membrane was used as the polymer electrolyte. The nafion membranes were pretreated in by boiling in 3%  $\text{H}_2\text{O}_2$  and then followed by treatment with 1M  $\text{H}_2\text{SO}_4$  and then with  $\text{H}_2\text{O}$  both at 80 °C. It is rinsed with distilled water several times and stored in distilled water until it was used in the MEA fabrication. The electrodes for the hybrid fuel cell were fabricated by using different fabrication protocol.

The two main fabrication protocols that were employed include the thin film method and the ionomer impregnation method [52].

Irrespective of the fabrication protocol the following parameters remain the same throughout: A hydrophilic carbon paper Toray 2050L and Pt (50 wt %) / Ru (25 wt %) was always used as the GDL and catalysts for the anode. The anode catalyst loading was  $4 \text{ mg/cm}^2$ . A hydrophobic carbon paper Toray TGPH 90 and Pt/C (40 wt %) were used consistently for the cathode. The cathode catalyst loading was fixed at  $2 \text{ mg/cm}^2$ . Only the fabrication of the cathode has been illustrated, the anode could be prepared by following the same fabrication protocol and by just replacing the catalyst and the carbon paper. The preparation of the anode therefore has not been explained in detail.

### **2.2.1 Thin Film Method**

The electrodes in the thin film method were prepared by mixing the catalyst Pt/C (40 wt %) directly with the alkaline ionomer (1 wt % in DMF) solution so that the ionomer content is 10 wt % with respect to the catalyst. Finally DMF and ethanol mixture (3:2 by weight) were added in order to prepare the catalyst slurry. The prepared mixture was then sonicated for 30 minutes at room temperature. The mixture was then sprayed on to the hydrophobic GDL until the desired loading was achieved. A small amount of the ionomer (5 wt %) was sprayed on to the top surface of the catalyst layer to prevent the direct contact of the catalyst with the membrane. The electrodes were then dried at room temperature and were immersed in 0.1 M NaOH solution overnight in order to exchange the  $\text{Cl}^-$  to  $\text{OH}^-$  ions. Then they were soaked in distilled water overnight to remove the excess  $\text{OH}^-$  ions.

The preparation of the low pH cathodes were carried out using the Pt/C (40 wt %) and was mixed with Nafion (5 wt % in alcohol) solution so that it constituted 15 wt % with respect to the catalyst. Water and iso propyl alcohol (IPA) (1:3 by weight) was used

to prepare the catalyst slurry. The slurry was then sprayed on to the electrode surface of the Toray TGPH 90 carbon paper. The catalyst coated GDL was then dried at room temperature.

### **2.2.2 Ionomer Impregnation Method**

The electrodes were prepared by first spraying the catalyst ink without the ionomer followed by spraying the ionomer. The catalyst ink was prepared by mixing Pt/C (40 wt %) with DMF and Ethanol (3:2 by weight) and PTFE (5 wt % in H<sub>2</sub>O) solution amounting to 10 wt% of the catalyst. The ink was ultrasonically agitated for 30 minutes and sprayed directly onto the non-treated carbon paper (TGPH 90). The electrode was then heat treated in an inert atmosphere at 250 °C. The alkaline ionomer (1 wt % in DMF) solution was then sprayed on top of the catalyst surface so that it accounted for 15 wt % compared to the catalyst. The electrodes were then dried at room temperature exchanged in a procedure similar to that described before

The Pt (40 wt %) / C for the cathode was mixed with PTFE (5 wt % in H<sub>2</sub>O) solution amounting to 10 wt % of the catalyst. Water and iso propyl alcohol (IPA) (1:3 by weight) was further added to the slurry, which was sonicated for 30 minutes and was later sprayed on the hydrophobic carbon paper. The electrodes were heat treated at 250 °C. Nafion (5 wt % in alcohol) amounting to 15 wt % of the catalyst was then sprayed onto the electrode surface. The electrode was then dried at room temperature and ion exchanged in a procedure similar to that described with the thin film method.

### 2.2.3 MEA Assembly

The electrodes having been prepared, a nafion (5 wt % suspension by weight)/IPA mixture (1:2 by volume) was sprayed directly onto the surface of the low pH electrode immediately before assembly. A PEM half cell was formed by pressing this electrode onto the Nafion 117 membrane at 135 °C and 2 MPa gauge pressure for 5 minutes. The PEM half cell is assembled first and the AEM electrode is assembled onto the half cell later as follows. The high pH electrode was sprayed with 100  $\mu$ L of the same Nafion/IPA mixture used above. This was done to improve the adhesion between the electrode and the PEM membrane. The assembly was then pressed onto the PEM half cell at 50 °C and 2 MPa pressure for 5 minutes to form the MEA.

The MEA was then assembled into a fuel cell setup from Fuel Cell Technologies with a single serpentine pattern for the fuel and gas flows on poco graphite blocks. Methanol preheated to 55°C was pumped into the cell at the rate of 5ml/min using a peristaltic pump (Fisher Scientific). O<sub>2</sub> was introduced to the cathode counter current to the methanol flow at the rate which varied between 10-50 sccm in all tests at ambient pressure. In tests with air the flow rate was maintained between 50-150 sccm. The cell temperature was maintained at 55 °C for all tests. The MEA was equilibrated by discharging at a constant load of 450 mV for 10 hours for the earliest MEAs. It was desired that the fuel cell be tested under more rigorous conditions and to achieve the accelerated aging of the cell, therefore the MEAs fabricated in the later part of this work were operated at 250 mV for 10 hours before the electrochemical data were obtained. The polarization curves for the MEAs were obtained by using a Princeton PAR 2273 potentiostat to obtain all the voltammetric curves.

## CHAPTER 3

### ANODE HYBRID DIRECT METHANOL FUEL CELLS

#### 3.1 Objective

The objective of this work is improving DMFC performance through the use of the hybrid fuel cell configuration. Anode hybrid fuel cells with a high pH anode and a low pH cathode with a PEM membrane has been demonstrated with hydrogen, however the use of these fuel cells in the methanol based systems has not been studied. Therefore the main objective is to demonstrate and optimize the anode hybrid fuel cell for methanol. The principle of operation of these hybrid fuel cells with methanol was presented in the introduction section. The anode hybrid fuel cells were used here in order to analyze the ionomer performance in the fuel cell. The impact of the variation of the methanol concentrations, fuel and oxidant flow rates were also assessed in order to obtain the optimum operating conditions. The impacts of the electrode fabrication protocol, and ionomer on the catalyst utilization were understood. An optimization of these conditions for operation were sought in order to obtain the highest performance with these fuel cells. A comparative study of different ionomers was also carried out. Finally with all the optimized conditions the impact of the molecular weight of the ionomers on the performance of the fuel cell was analyzed. The initial voltage drop occurring in the anode hybrid fuel cells have been explained and this drop has been assigned to the AEM anode. An ionomer with a different cationic group has been utilized to try to remedy this initial voltage drop.

### 3.2 Performance of Anode Hybrid Direct Methanol Fuel Cell

The performance of the anode hybrid fuel cell is demonstrated by fabricating the electrodes by the thin film method. The fuel cell assembled with the high pH anode consists of an ionomer whose properties are described in Table 3.1.

Table 3.1: Properties of Ionomer I used in the anode hybrid fuel cell

Ionomer	IEC (meq/ g)	Water Uptake (%) ( 25°C)
Ionomer I-1	1.21	25

First the operating conditions of these fuel cells are optimized after which the other parameters are studied

#### 3.2.1 Impact of the Operating Conditions

##### 3.2.1.1 Temperature

The operation temperatures of fuel cells have been shown to play a very important role in PEM fuel cells [53,54]. An increase in the temperature usually results in an improved performance resulting from the enhanced methanol oxidation [27] and oxygen reduction kinetics. The performance of the hybrid fuel cells at three different temperatures of 25 °C, 40 °C and 55 °C was studied. The tests were performed with a 2M methanol solution supplied to the anode at 5 ml/min and oxygen supplied to the anode at 50 sccm.

The overall performance in the fuel cell increased with the increase in the temperature. An improvement in the performance in the activation and the ohmic region

was observed. This is resultant from the enhanced kinetics at both the electrodes and increase in reactant diffusion rates with temperature. The increased temperature also probably assists in enhanced water removal from the cathode catalyst layer by evaporation allowing for better oxygen transport. It also results in increased methanol permeation from the anode to cathode resulting in an increased crossover current.

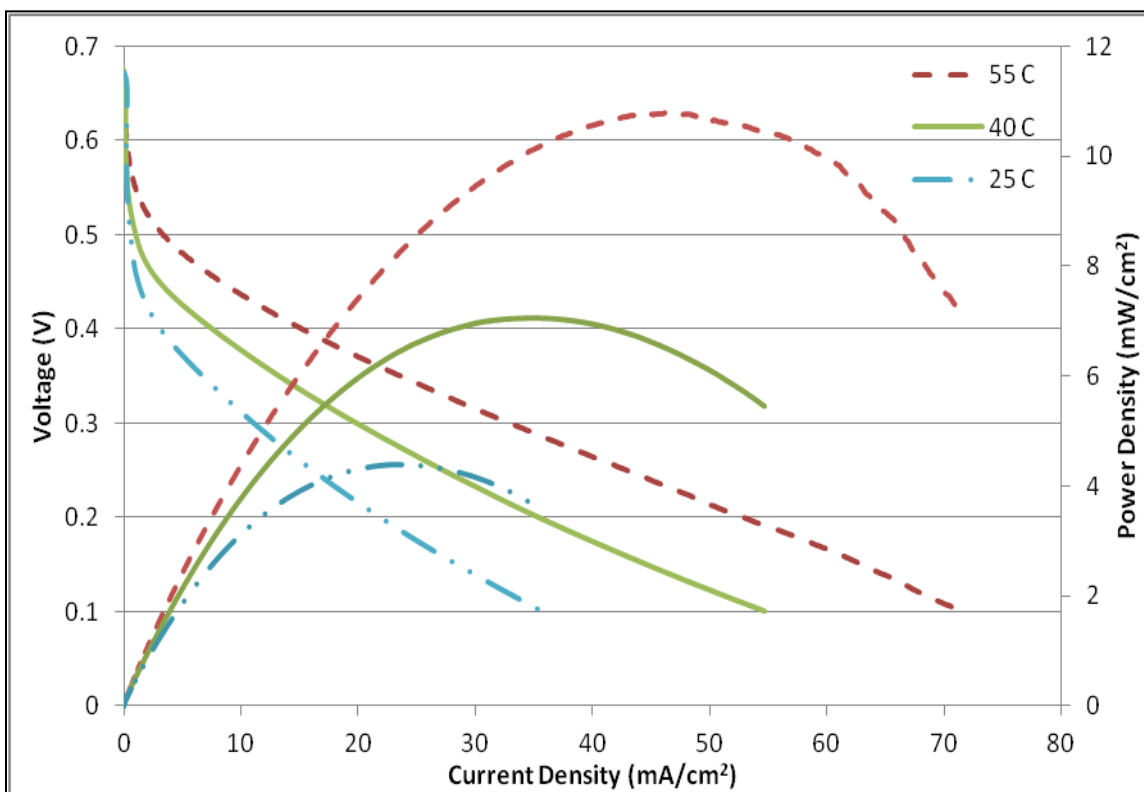


Figure 3.1: Polarization and power density curves of anode hybrid fuel cell operated at different temperatures: 55 °C (broken lines), 40 °C (lines), 25 °C (double dotted lines), with 2M MeOH at 5 ml/min on the anode and 50 sccm O<sub>2</sub> at the cathode

The crossover effect is evident from the open circuit potentials at the different temperatures. Despite the increased cross over the improved kinetics account for a better performance. The combined positive effect seems to outweigh the negative effect and increasing the temperature resulting in an overall improved performance. Temperatures

beyond 55 °C are not used since the AEM ionomers used in this study start deteriorating at 65 °C.

### 3.2.1.2 Methanol Concentration

The impact of the methanol concentration on the performance was studied with three different methanol concentrations 1M, 2M and 4M methanol. The performance with higher methanol concentrations i.e. 2M and 4M methanol are 10.76 and 9.18 mW/cm<sup>2</sup> respectively. The main drawback with the conventional PEM based fuel cells is that operation with higher methanol concentrations results in methanol crossover, and a mixed potential at the cathode owing to the methanol oxidation reaction happening along with the oxygen reduction reaction. The electro-osmotic drag of the protons also results in methanol being dragged along with the protons.

In the anode hybrid fuel cell movement of the OH<sup>-</sup> ions produced at the electrode/membrane interface is opposite to the direction of methanol transport. H<sup>+</sup> ions are produced at the AEM/PEM interface and the electroosmotic drag of methanol along with these ions are reduced compared to conventional fuel cells wherein H<sup>+</sup> ions are produced from within the catalyst layer and drag along methanol during their transport. The application of the AEM ionomer on the electrode surface might provide another diffusion barrier to the methanol and probably result in lower methanol transport when compared to the conventional PEM based fuel cells. However still there is a decrease in the performance due to methanol diffusion from the anode to the cathode.

The encouraging fact here is that the overall performance of the fuel cell does not significantly decrease with the increase in the methanol concentration. The performance of the 1M and 4M MeOH are very similar at higher current densities.

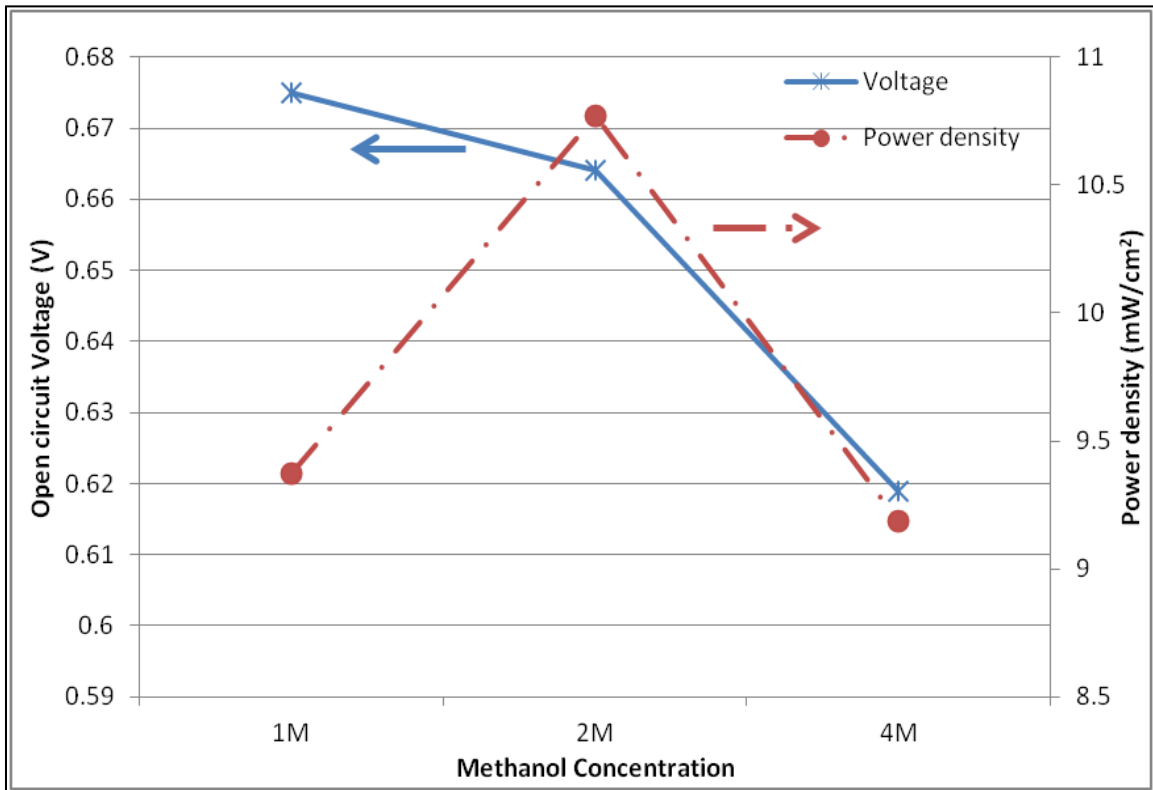


Figure 3.2: Open circuit voltage (stars) and peak power density (circles) of fuel cell operated with different MeOH concentrations: 1M, 2M, 4M operated with 50 sccm O<sub>2</sub> at the cathode at 55 °C.

### 3.2.1.3 Methanol Flow Rate

The impact of the flow rate of the methanol is next studied with increasing methanol flow rate. Initially the performance of the fuel cell increases with the increase of the flow rate. This is due to the increased rate of transport of the methanol to the reaction sites with the increased convection resulting in the cell being able to support higher currents. The increased convection also provides for the increased rate of removal of CO<sub>2</sub> from within the catalyst layer. A peak performance of 10.75 mW/cm<sup>2</sup> is obtained with the flow rate of 5 ml/min. Once the methanol flow rate increases beyond a particular point the performance starts to decline, owing to the greater increase in the methanol

crossover from the anode to the cathode. This is due to the stoichiometric excess of methanol being supplied and only a fraction undergoes anodic oxidation with most unreacted methanol crossing over to the cathode side resulting in a mixed potential at the cathode. This is evident from the decrease in the OCV of the cell observed with the increasing flow rate. The performance of the fuel cell with different methanol flow rates is illustrated below in Figure 3.3.

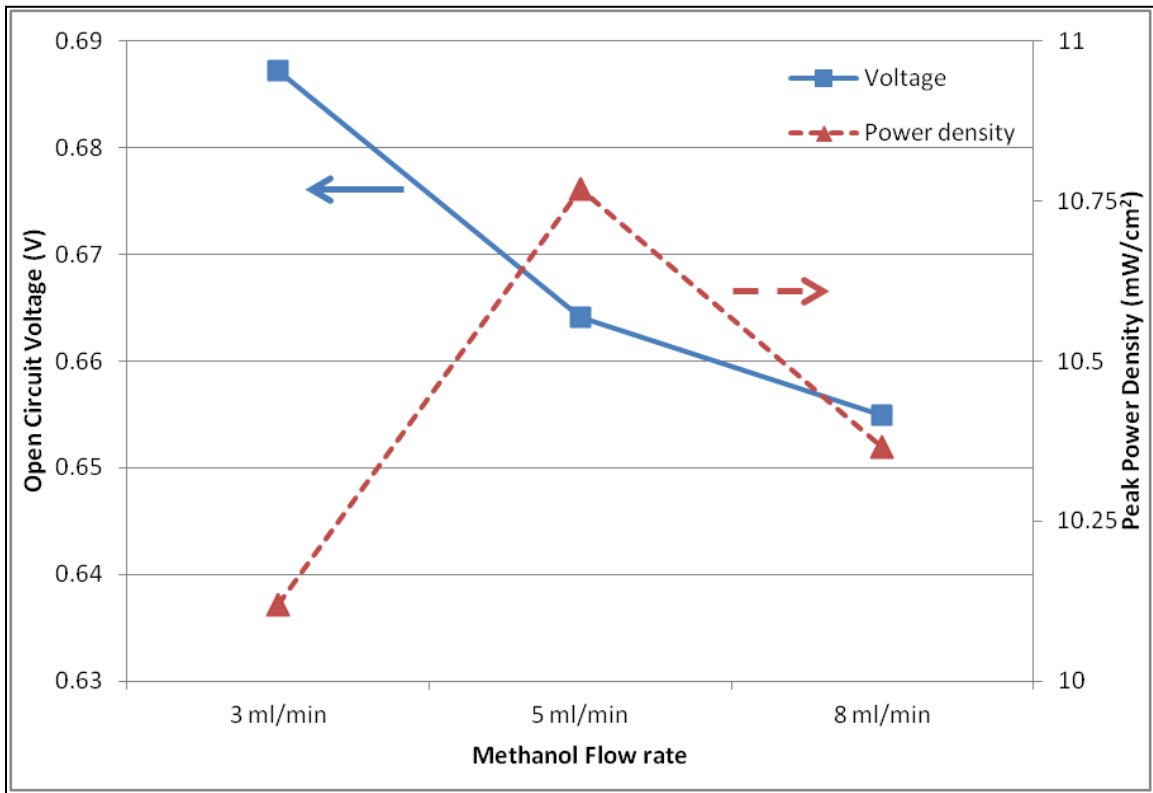


Figure 3.3: Power density (triangles) and open circuit voltage (squares) of fuel cell operated with different methanol (2M) flow rates: 3, 5, 8 ml/min operated with 50 sccm O<sub>2</sub> at the cathode at 55 °C

#### 3.2.1.4 Oxygen Flow Rate

The impact of the oxygen flow rate on the performance is also studied here. The tests were carried out by varying the flow rate of oxygen while the conditions at the anode are 2M MeOH at 5 ml/min and maintaining the cell temperature at 55°C. The cell

performance increases with the increase in the oxygen flow rate. This is illustrated in Figure 3.4.

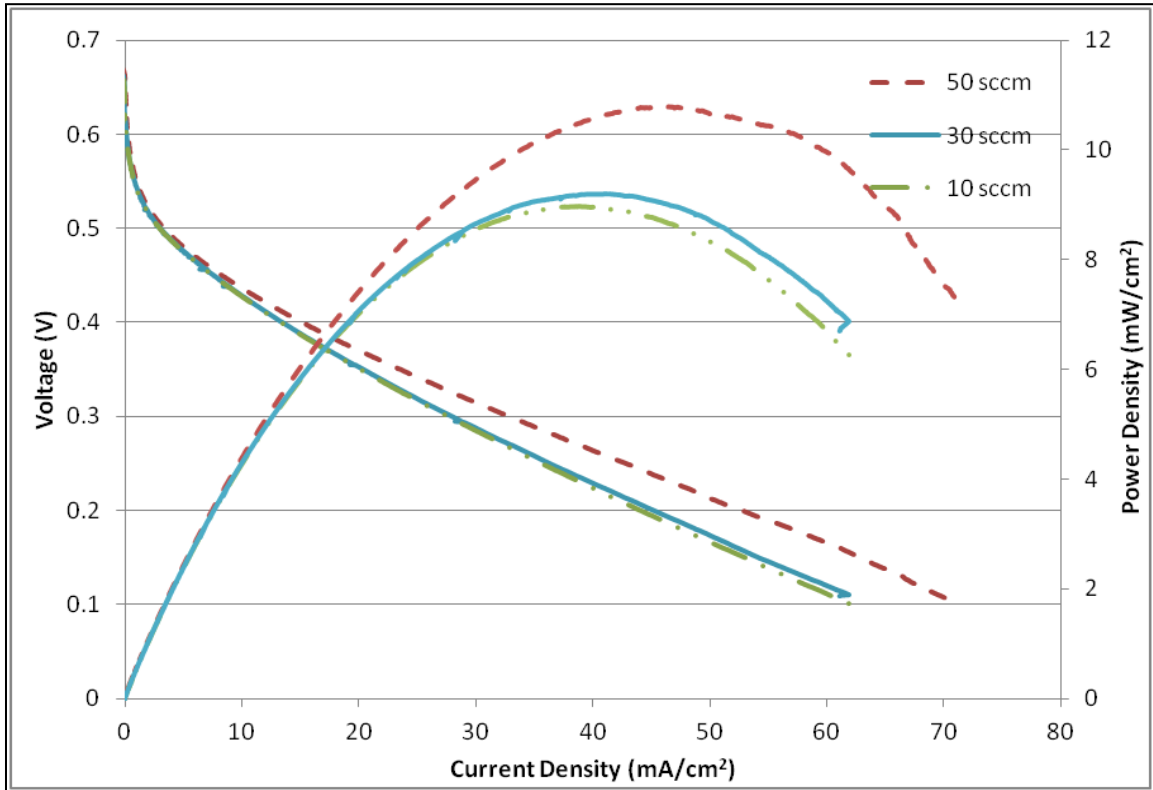


Figure 3.4: Polarization and power density curves of anode hybrid fuel cell operated with different oxygen flow rates at the cathode: 50 sccm (broken lines), 30 sccm (lines), 10 sccm (double dotted lines), and 2M MeOH at 5ml/min on the anode at 55°C.

The oxygen flow rate has an effect at higher current densities since it helps in the removal of the water that is formed in the gas diffusion layer channels and helps increase the overall catalyst utilization due to better transport. Increasing the flow rate helps improve the open circuit voltage of the cell this is believed to be the effect of the physical removal of the methanol that crosses over from the anode and some also believe that it is responsible for the enhanced methanol oxidation rate at the cathode [54]. The increase in flow rate increases the backpressure and hence reduces methanol diffusion from the

anode. The maximum performance was obtained with 50 sccm. Increasing the cathode flow rate further does not improve the overall performance of this is an indication that the cell performance is limited by the AEM anode.

### 3.2.1.5 Air Flow Rate

The flow rate of air to the cathode was also varied and the performance of the fuel cell was studied with 2M methanol being supplied to the anode at 5 ml/min. The decline in performance with air compared to the oxygen based systems is mainly the result of the reduction in the oxygen partial pressure. Higher flow rates of air are utilized and an improvement in the performance was observed. This is the result of the greater availability of the oxygen at the reaction sites, further the increased flow rate helps in removal of the water within the catalyst layers and also in the physical removal of the methanol crossing over from the anode.

Increasing the air flow rate results in the increase in the OCV, similar to that observed in the cell with oxygen supplied to the cathode. However increasing the flow rate beyond 100 sccm decreases the performance since it results in the dry out of the ionomer in the catalyst layer. The performance of the hybrid cells with different flow rates are indicated in Figure 3.5.

The ideal operating conditions for the fuel cell can be summarized as follows:

Table 3.2: Optimized operating conditions for anode hybrid direct methanol fuel cells

Parameter	Operating condition
Temperature	55 °C
Methanol Concentration	2 M
Methanol Flow Rate	5 ml/min
Oxygen Flow Rate	50 sccm
Air Flow Rate	100 sccm

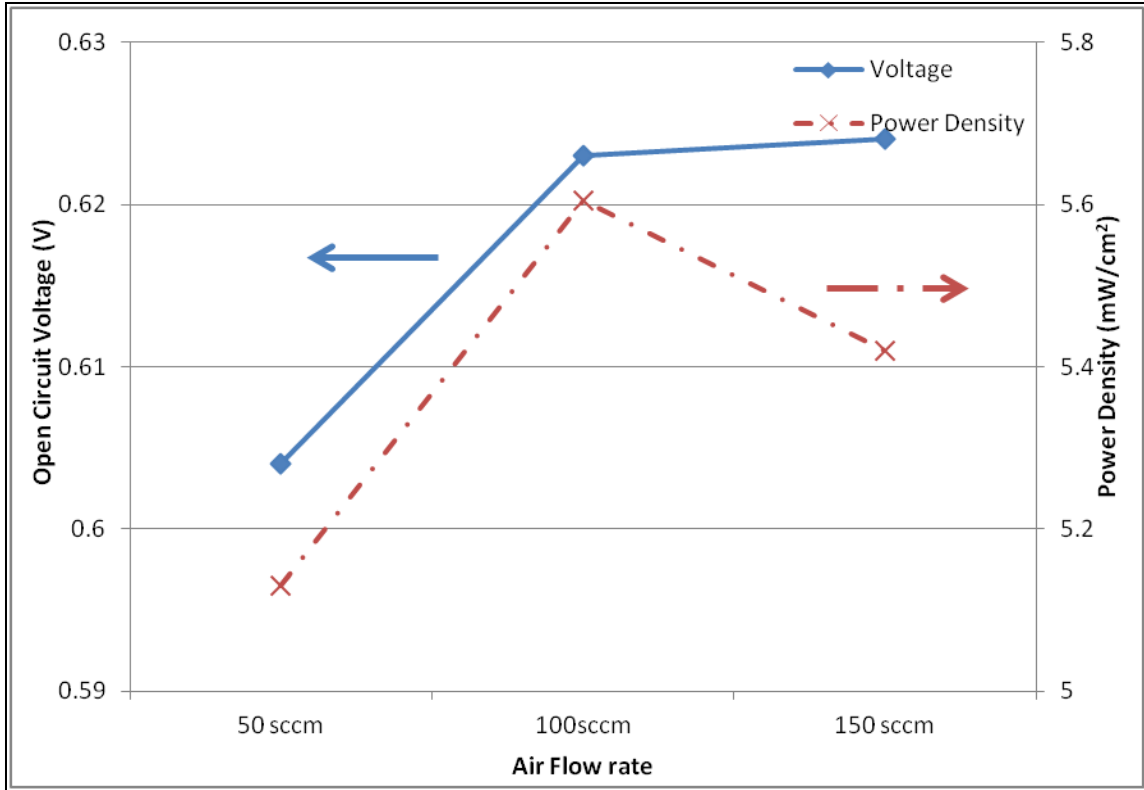


Figure 3.5: Power density (crosses) and open circuit voltage (rhombuses) of fuel cell operated with different air flow rates: 50, 100, and 150 sccm operated 2M MeOH at the anode at 55 °C

### 3.2.2 Steady State Operation

The main drawback with conventional AEM systems is that the steady state performance of such cells is poor and performance drops with continuous operation. The steady state performance of the semi hybrid fuel cells at 250 mV is shown in Figure 3.6. The performance of the fuel cell is quite stable for approximately 10 hours with 2 M Methanol. This test was performed after continuous testing of the fuel cell for 4 days where in it was continuously operated and subjected to several experiments. This provides ample evidence that this system is very stable and can operate over long periods of time.

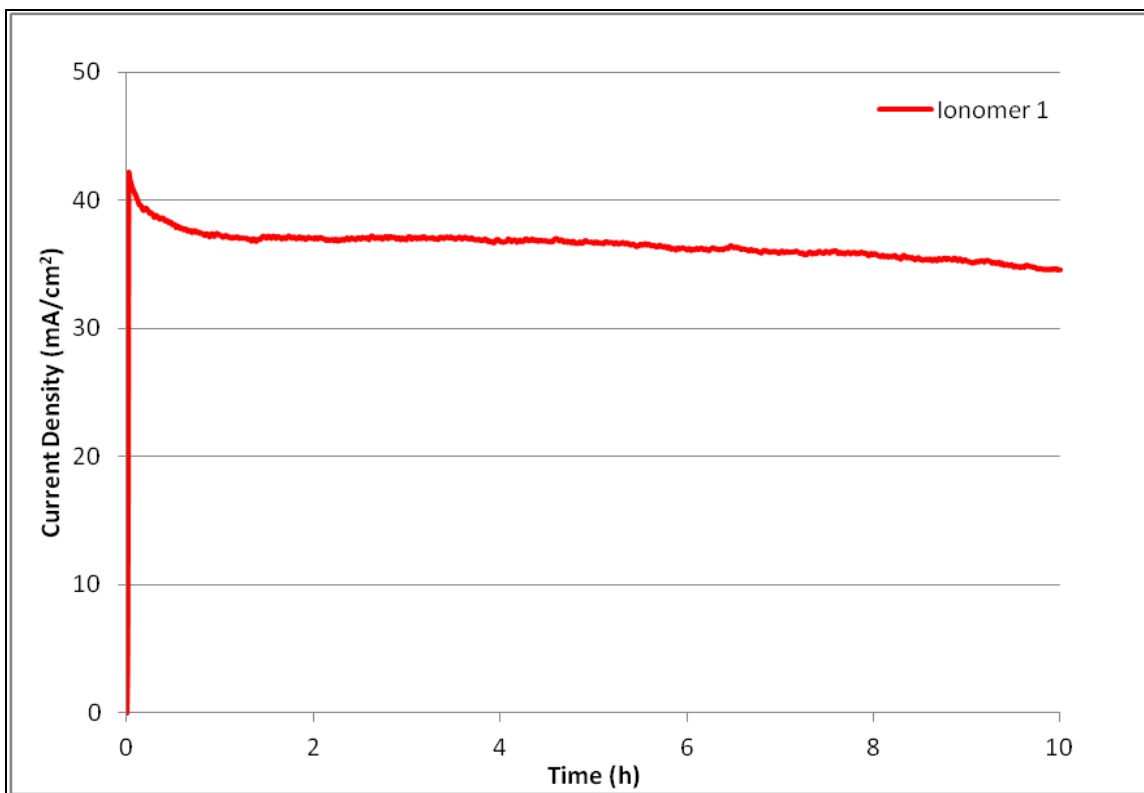


Figure 3.6: Steady state performance of the fuel cell held at constant potential of 250 mV with 2M MeOH, flow rate 5 ml/min and O<sub>2</sub> flow rate 50 sccm supplied at atmospheric pressure at 55 °C

### 3.2.3 Impact of Fabrication Protocol

An effective electrode balances the three transport process which include (i) transport of the ions, (ii) transport of the electrons, and (iii) transport of the reactants and products to and from the reaction sites respectively [55].

A balance between all the transport properties needs to be achieved in order for the fuel cell to function effectively. The three phase interface between the catalyst, the ionomer and the reactants are really important and is shown in Figure 3.7. Therefore this interface needs to be tailored in order to achieve optimum performance in fuel cells. The

three phase interface is tailored by modifying the fabrication protocols. Two different fabrication protocols are employed here.

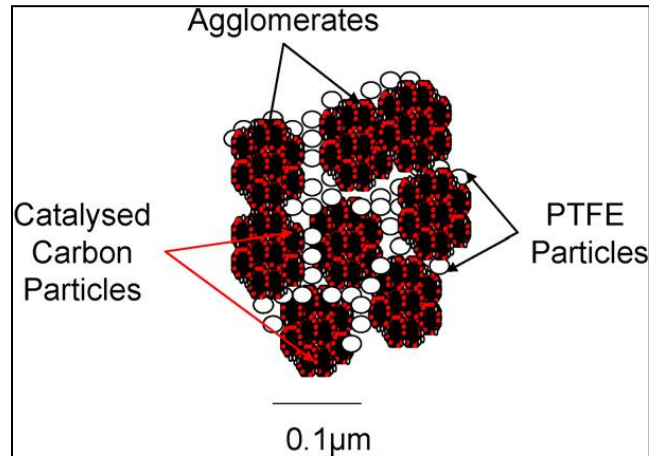


Figure 3.7: Three phase boundary at catalyst surface [56]

The two MEAs were fabricated with identical PEM half cells with the electrodes fabricated by the ionomer impregnation method. This was done to ensure a fair comparison as the only variation between the two MEAs is the anodes. The anodes were fabricated by the thin film method and ionomer impregnation method. The properties of the ionomer used were indicated in Table 3.1 and the performances of the two MEAs are shown in Figure 3.8.

The overall performance of this fuel cell with 2M Methanol without the use of an alkaline electrolyte is  $18.5 \text{ mW/cm}^2$  at  $55 \text{ }^\circ\text{C}$  as shown in Figure 3.8. The performance with the thin film method is  $10.76 \text{ mW/cm}^2$ . This performance is still very low however this is comparable to the performance obtained alkaline anion exchange membrane fuel cells without the use of an alkaline electrolyte ( $8.5 \text{ mW/cm}^2$ ). This result with the complete AEMFC was again obtained with pressurization and also at higher temperature of  $80 \text{ }^\circ\text{C}$  [39]. Higher values have been obtained but these involve the use of an alkaline

electrolyte which results in high power densities but this is short lived as the carbonation of the electrode again degrades the performance.

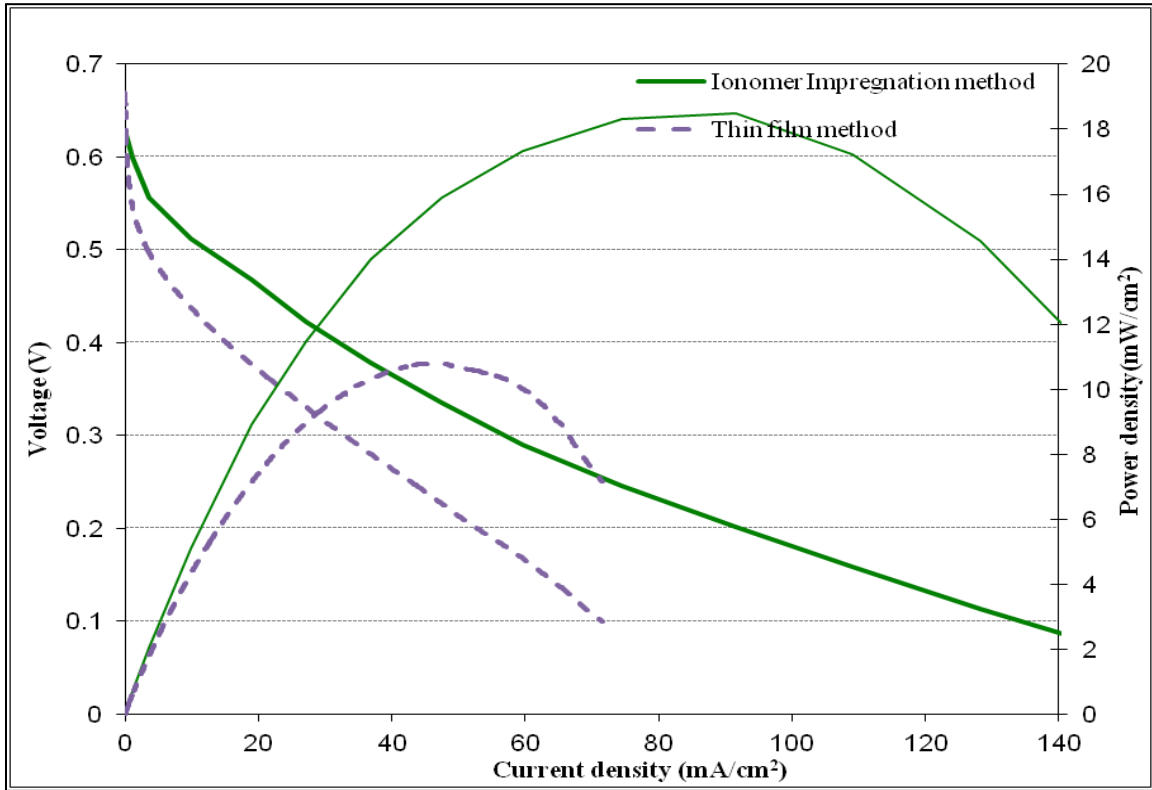


Figure 3.8: Polarization and power density curves for the anode hybrid fuel cell operated with thin film anode (dotted lines), ionomer impregnated anode (lines) with 2M MeOH supplied at a flow rate of 5 ml/min and O<sub>2</sub> supplied to the cathode at 50 sccm (atmospheric pressure) at 55 °C

This difference in the performance along with the variation in the fabrication protocol might be explained with the help of the schematic structure of the electrodes in Figure 3.9 [52]. The two protocols used here involve the use of different materials as binder for the catalyst. The thin film method involves the use of a PTFE, a hydrophobic material as binder whereas in the ionomer impregnation the ionomer itself acts as binder. The variation in the performance in the two fabrication protocols might result from the water absorption properties of the binders used.

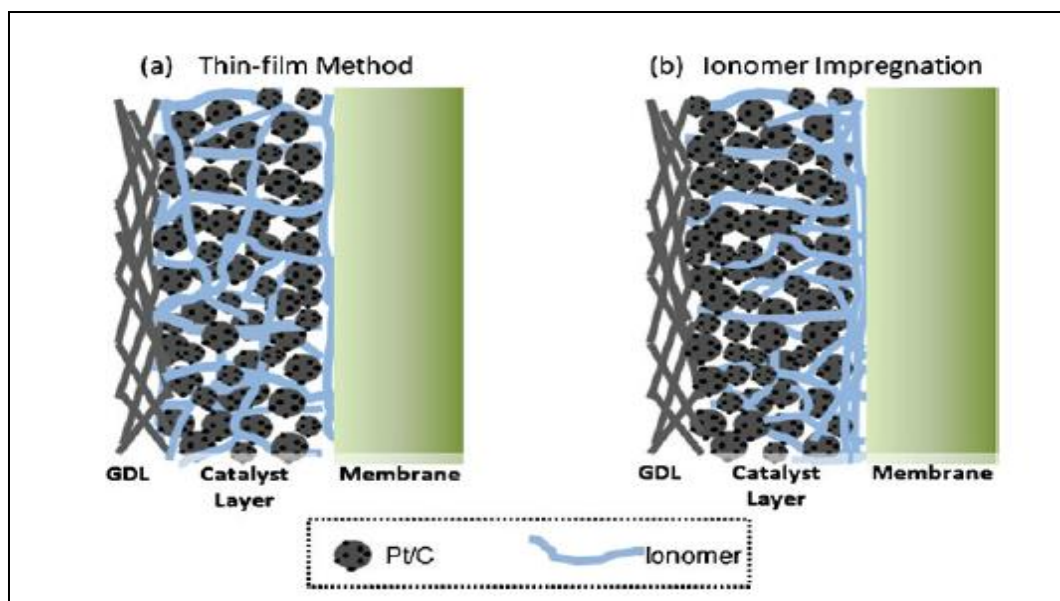


Figure 3.9: Proposed structures of electrodes prepared by: (a) Thin Film method and (b) Ionomer impregnation method

The thin film method uses the ionomer as the binder and therefore it has good ionic conductivity since the ionomer is uniformly distributed within the catalysts layers. The excessive water uptake in the ionomers have been shown to block the transport of the material to the catalyst sites and further the produced  $\text{CO}_2$  cannot also be removed from within the catalysts layers, resulting in reduced catalyst utilization.

When the hydrophobic material is used as a binder and the ionomer is sprayed from the top only a small portion of the ionomer penetrates through the catalyst layer. The overall ionic conductivity within the electrode is low since the ionomer content is small and the PTFE is non-conductive. However the addition of PTFE results in flow pathways being free from water which might help in effective  $\text{CO}_2$  transport from the interior of the catalyst layer to the GDL. Further the lower ionomer content results in greater porosity near the GDL allowing for easy access to reactants and removal of products. The performance in such structures is a delicate balance between the ionic conductivity and material transport.

It has to be pointed out again here that the performance is still lower when compared to conventional PEM direct methanol fuel cells. Such behavior is contrary to the expectation that the performance with alkaline electrodes will be better owing to the enhanced kinetics at higher pH when compared to reactions at lower pH. An explanation for this lower performance might be due to the lower conductivity of the alkaline ionomer that is used in the anode catalyst layer. The conductivity is much lower compared to the conductivity of the PEM ionomer. The mobility of the  $\text{OH}^-$  ion is further slower when compared to that of the  $\text{H}^+$  ions and hence the transport of these to the reaction sites is slower.

Catalyst utilization also plays a role here and it depends on the active surface area of the catalyst and also depends upon the three phase boundary between the catalyst, ionomer and the reactant. Since not all of the catalyst fulfills the three phase boundary criteria the overall performance is low. This again brings to the fore the importance of the ionomer properties and content in the effective utilization of the catalyst. These will be investigated further here.

### **3.2.4 Impact of the Ion Exchange Capacity of the Ionomer**

An ion exchange ionomer is composed of hydrophilic and hydrophobic ion clusters. It is believed that the transport of the ions and methanol mainly occur through the hydrophilic ion cluster domains. A higher IEC therefore would imply a higher density of quaternary ammonium groups which implies a greater conductivity however the negative aspect is the increased water uptake.

A series of experiments were performed with a similar PEM half cell and the only difference is the IEC of the AEM ionomer used for the anode. The ionomer impregnation method is used in the fabrication of the electrodes to observe the effects of the ionomer

IEC. The properties of the different ionomers used in this study are listed below in Table 3.3.

Table 3.3: Properties of the ionomer with different IEC

Ionomer	IEC (meq/g)	Water Uptake % (25 °C)
Ionomer 1-1	1.21	25
Ionomer 1-2	0.92	12
Ionomer 1-3	1.55	39

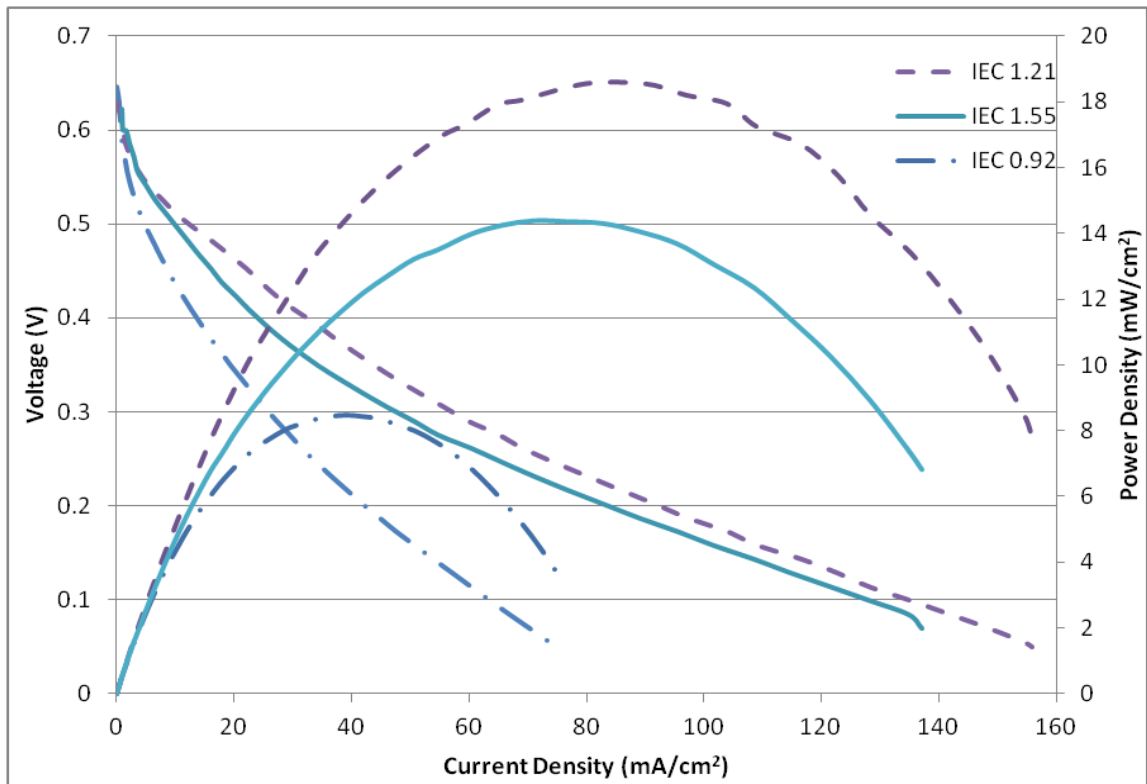


Figure 3.10: Polarization and power density curves of anode hybrid fuel cell operated with different IEC ionomers at the anode: 1.21 (broken lines), 1.55 (lines), 0.92 (dotted lines) meq/g 2M MeOH at 5 ml/min on the anode and 50 sccm O<sub>2</sub> on the cathode at 55 °C

The ion exchange capacity of the ionomer has been shown to explicitly affect the water uptake of the ionomers [57]. Since the water uptake is high then it results in the size of these hydrophilic domains and channels to widen resulting in a faster transport of ions and methanol to the reactant sites [58]. The downside however is the fact that it restricts the transport of the carbon dioxide formed on the anode side resulting in a restricted mass transport and a reduced performance. High water uptake further results in the mechanical degradation of the membrane electrode interface since the electrode tends to peel off from the membrane resulting in poor contact and high ionic resistance. So a balance needs to be achieved between the water uptake and the material transport. This is adjusted by modifying the IEC of the ionomer.

It has been demonstrated here that the higher IEC provides a better performance than the lower IEC ionomers. An IEC in the range of 1.2 to 1.3 meq/g was found to be most appropriate for the fuel cell performance by balancing the conductivity, water uptake and transport properties of reactants and products. Increasing the IEC further beyond this value resulted in a decrease in the overall performance. The increased ionic conductivity is compromised by the reduction in transport of the reaction products and poor interfacial contact as previously explained.

### **3.2.5 Impact of the Ionomer Content**

The distribution of the ionomer within the catalyst layer also plays a crucial role in the overall performance. The ionomer distribution in the catalyst layer is controlled by the quantity of the ionomer added initially to make the catalyst slurry. The ionomer is responsible for the ionic conductivity from within the catalyst layers and the overall catalyst utilization also depends on the ionomer since the catalyst sites without the ionomer cannot contribute to the overall current owing to the lack of ionic conductivity.

In order to find the optimum ionomer content three different values are used. The impact of the different ionomer content in the catalyst layer is illustrated in the Figure 3.11.

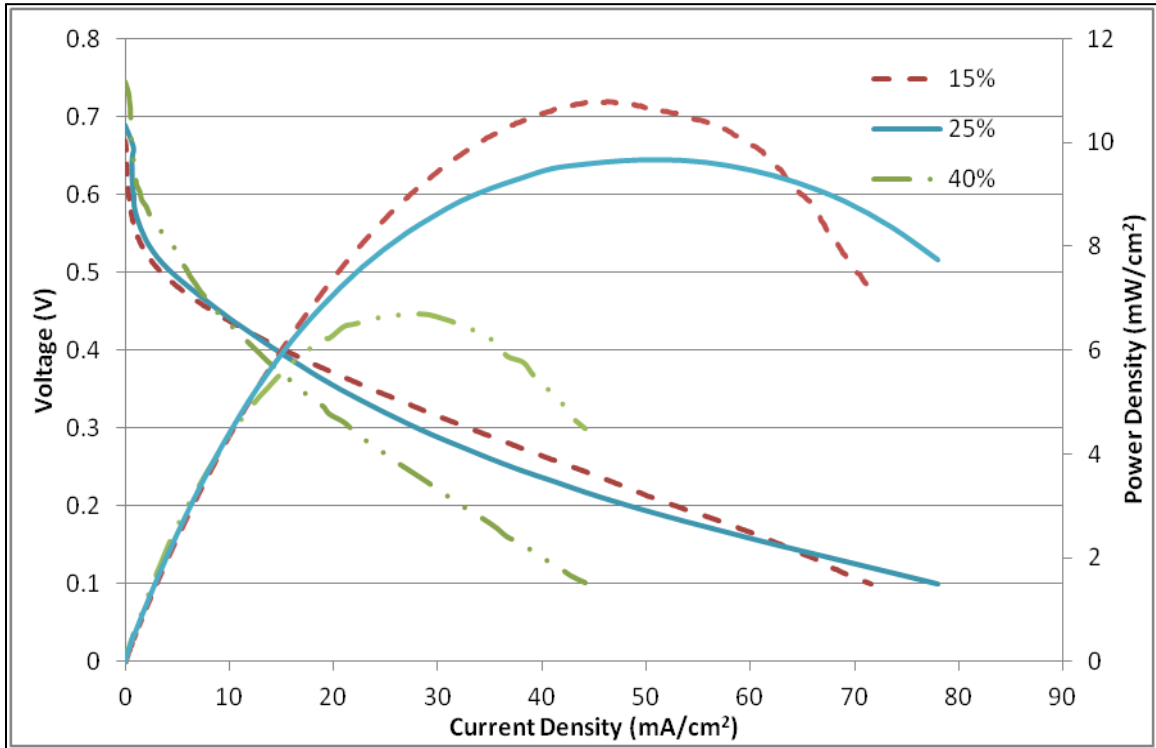


Figure 3.11: Polarization and power density curves of anode hybrid fuel cells with different ionomer contents: 15, 25, 40 % with 2M MeOH at 5 ml/min and 50 sccm O<sub>2</sub> at 55 °C

It can be seen from the fuel cell performance that 15% ionomer content provides for the most ideal ionomer distribution within the catalyst layer. The reasons for the different performance with different ionomer contents can be explained as follows. This is also illustrated in the Figure 3.12. Case (a) low ionomer content: This results in poor ionic conductivity with the catalyst layer despite good electronic and material transport resulting in several 'dead' regions and the overall catalyst utilization is low and this reflects on the performance as well. Case (b) the high ionomer content (40%) results in excellent ionic conductivity, however there is insufficient electronic conductivity since

there is little contact between the catalyst particles. Initially the performance is better but at higher current densities the hydrophilic ionomers result in the catalyst layer channels being flooded with the liquid fuel, hence the  $\text{CO}_2$  formed as a product cannot be removed from within the catalyst layer resulting in a transport limitation of the reactants to the catalyst sites. These factors combined together result in the overall decrease in the performance. Case (c) the optimum ionomer content (15%) will ensure that there is a perfect balance between the ionic, and electronic conductivity, and the mass transport. This ensures that most of the catalyst sites are active providing the best performance.

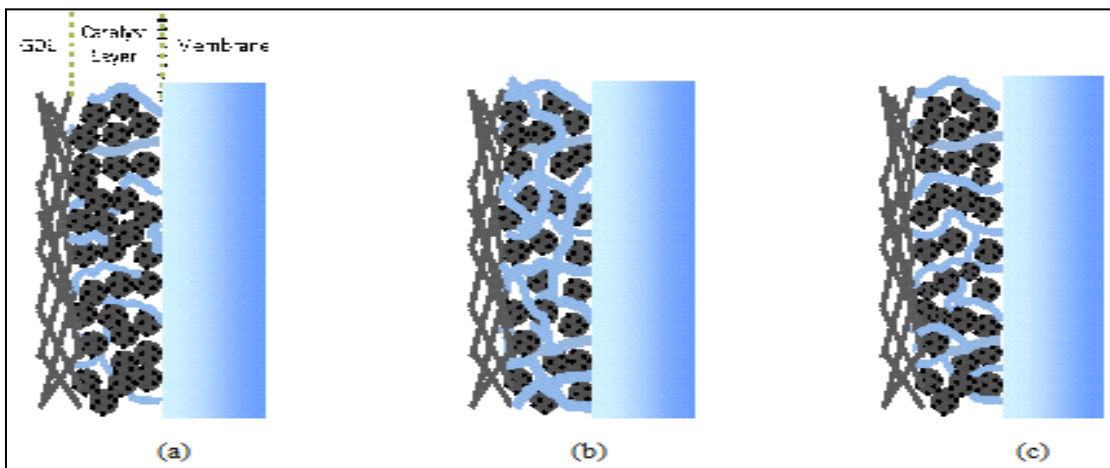


Figure 3.12: Electrode structure of the electrodes with different ionomer distributions in the catalyst layer (a) Low ionomer content (b) High ionomer content (c) Optimum ionomer content

### 3.2.6 Impact of the Different Ionomers

The differences in the ionomer properties were previously studied, now ionomers with the same quaternary ammonium groups with different backbones were studied. The polymer matrix of the ionomers is believed to determine the mechanical, thermal and chemical stability [25]. The variation of the backbone therefore results in modifying all

these properties. The structures of these different ionomers are illustrated in the Figure 2.1, 2.2 and the properties of these ionomers are listed in the Table 3.4. The two different ionomers used in this study had a comparable IEC. Ionomer 1 with partially fluorinated units provided enhanced hydrophobic properties [59]. The additional trifluoromethyl groups on Ionomer II results in greater hydrophobicity compared to that of Ionomer I and hence a lower water uptake, resulting in a lower conductivity for these hydrophobic ionomers. These conductivity values could not be obtained as these ionomers could not produce a free standing membrane. The fuel cell performance with these two different ionomers was demonstrated here.

Table 3.4: Properties of the ionomers with different backbone

Ionomer	IEC (meq/g)	Water Uptake % (25°C)
Ionomer I-1	1.21	25
Ionomer II-1	1.3	--

The Ionomers II despite having greater hydrophobicity and lower conductivity provides a better performance. This might be due to the fact that these ionomers keep a few channels clear of water that allows for the product carbon dioxide gases to escape preventing the buildup of these within the electrode layers preventing material transport to the reaction sites and hence reduced performance. The hydrophobic ionomer further keeps the electrode membrane interface more intact than the hydrophilic ionomer which takes up more water and physically degrades the interface leading to a loss in ionic conductivity and performance. In another study based on modeling it was found the when less water was available within the polymer, the OH<sup>-</sup> ions are not well solvated and

therefore are more reactive [60]. The hydrophobic ionomers have reduced water content and therefore probably result in greater reactivity owing to reduced solvation of OH<sup>-</sup> ions. Ionomer II was favored for further studies.

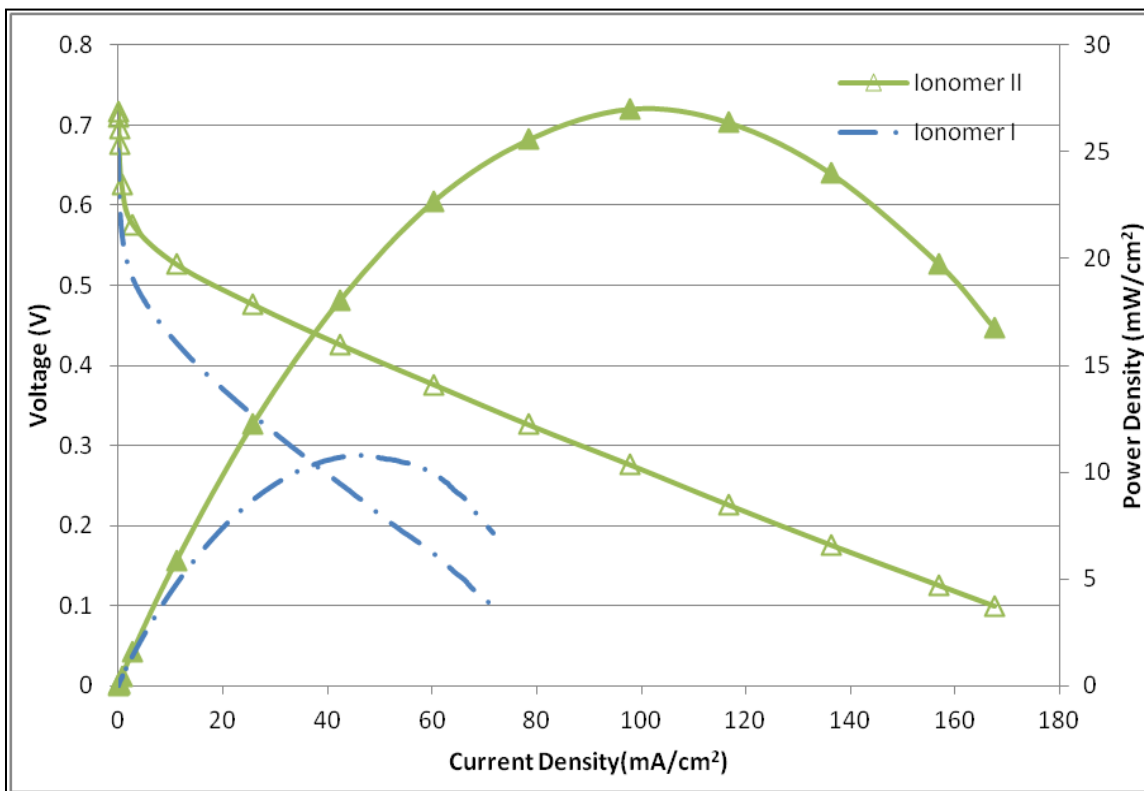


Figure 3.13: Polarization and power density curves of anode hybrid fuel cell operated with different ionomers at the anode with 2M MeOH at 5 ml/min on the anode and 50 sccm O<sub>2</sub> on the cathode at 55°C

### 3.2.7 Impact of the Ionomer Molecular Weight

In studies regarding the ionomers properties the impact of the molecular weight has not been widely studied. Ionomers with the same backbone but with increasing molecular weights from the lowest to the highest (11 k to 40 k) were utilized and the performance of these has been observed in these hybrid fuel cells. The properties of these ionomers have been tabulated in the Table 3.5.

The lower molecular weight ionomers seem to provide a better performance when compared to the higher molecular weight ionomers consistently. This is probably due to the assembly of the ionomer within the catalyst layer, the lower molecular weight ionomers are unable to form continuous film like structures and therefore providing for greater material transport allowing for greater catalyst utilization. The lower molecular ionomers have greater porosity resulting in better material transport.

Table 3.5: Properties of Ionomer II with different molecular weights

Ionomer	MW	PDI	IEC (meq/g)
(a) Ionomer II-1	11.2 k	2.67	1.3
(b) Ionomer II-2	11.8 k	2.27	1.3
(c) Ionomer II-4	40.5 k	5.08	1.3

The chain mobility of polymers is important since the movement of material through the polymers involve a cooperative motion of the polymer chains [61]. In a study with polystyrene films the increase in the molecular weight was associated with a decrease in the chain mobility of the polymer [62]. The greater chain mobility of lower molecular weight ionomers allows for the easier movement of the polymer strands, these two factors combined assists in the material and ionic transport to the reaction sites. Even a slight change in the ionomer molecular weight from 11.2 k to 11.8 k shows a considerable change in the overall fuel cell performance. Therefore it is believed here that the molecular weight of the ionomer plays a role in controlling the transport properties and hence plays a significant role in controlling fuel cell performance.

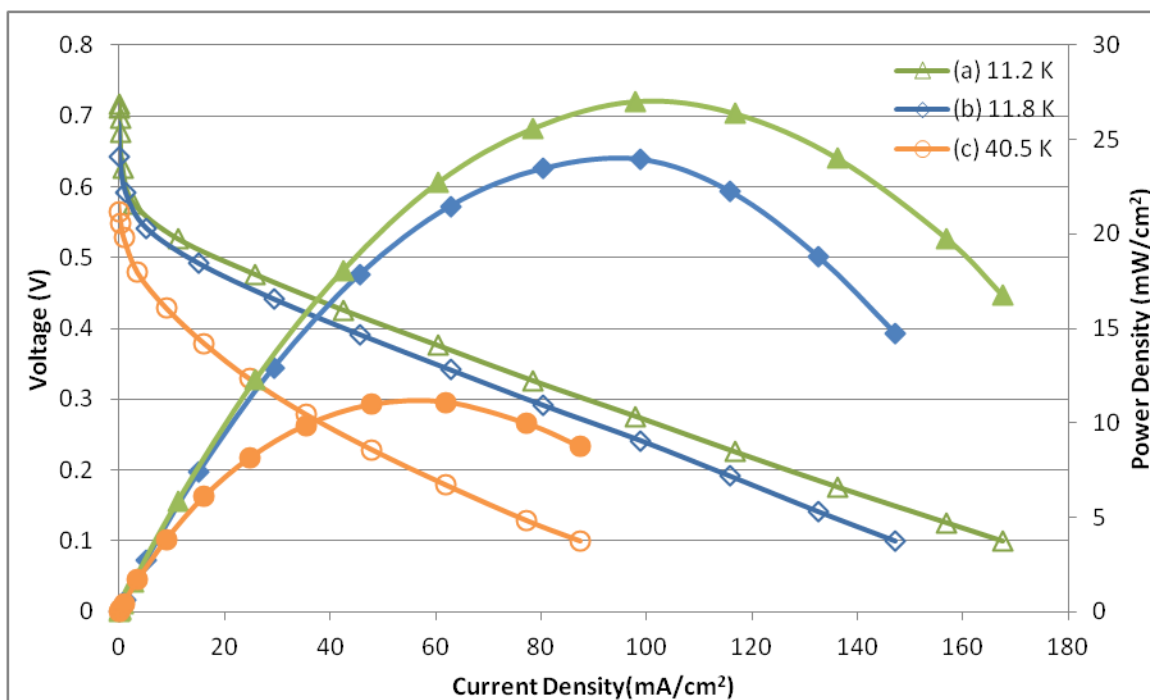


Figure 3.14: Polarization (open symbols) and power density (solid symbols) for the anode hybrid fuel cell with different molecular weight ionomers: 11.2 k, 11.8 k, 40.5 k operated with 2M MeOH at a flow rate of 5 ml/min and oxygen flow rate 50 sccm

### 3.3 Initial Voltage Drop

Alkaline anion exchange membrane fuel cells have recently been receiving a lot of attention; especially methanol based fuel cells owing to their potential for remedying the drawbacks associated with PEM based fuel cells and for powering low power devices. The AEM alcohol based cells have been plagued with low performance when operated without hydroxide solution. An intriguing effect is the initial rapid drop in the voltage in alkaline fuel cells has been observed at low overpotentials. This is especially specific to alcohol based fuel cells operating with the ammonium cations as the exchange group. An important consideration in the performance of such fuel cell performance is related to the double layer structure formed at the electrode-ionomer interface. A brief description of

the double layer structure is provided first and then how this influences the methanol oxidation reaction at the anode is explained.

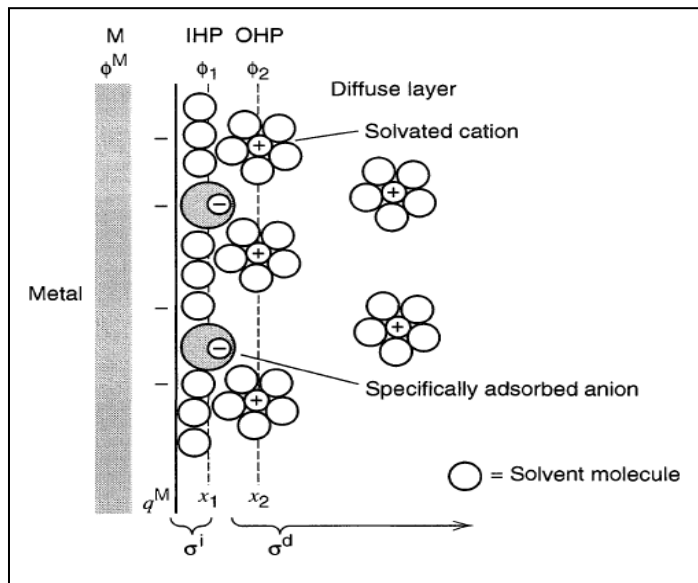


Figure 3.15: Proposed double layer structure for negatively charged electrode with specifically adsorbed anion

The electrical double layer is formed by the separation of the charges at the electrode electrolyte interface. The theoretical structure of the double layer on the solution side is believed to consist of three regions. The region closest to the electrode that consists of solvent molecules and other species (ions and molecules) that are specifically adsorbed on to the electrode surface, the locus of the center of the specifically adsorbed ionic species is called the inner Helmholtz plane (IHP). The plane adjacent to the IHP, which is the plane of the closest approach of the solvated ionic species which are not specifically adsorbed onto the electrode, is termed as the outer Helmholtz plane (OHP). The diffuse region extends from the OHP to the bulk of the solution. The diffuse layer consists of these non specifically adsorbed species dispersed in three dimensional space that are attracted by electrostatic interactions with the electrode surface.

In systems with large polarizations or with more concentrated solutions most of the charge is confined in the OHP with little or almost no contribution from the diffuse layer. Similarly in solutions of low concentrations most of the ions are distributed in the diffuse layer and its contribution to maintaining the electrical neutrality of the double layer is critical.

The diffuse double layer contribution to the potential is considered important in cases where the ionic mobility is limited. This is the case in fuel cells systems where the cations are bound to the polymer backbone. The potential driving the electrode reactions is not  $\varphi_m - \varphi_s$ , where  $\varphi_m$  is the electrode potential and  $\varphi_s$  is the solution potential. The reactions are driven by the potential difference between the metal electrode and the electroactive species at the OHP ( $\varphi_2$ ),  $\varphi_m - \varphi_2$  [63]. The  $\varphi_2$  potential greatly seems to influence the overall rate of the reaction; this correlation was obtained from the Frumkin correction whereby the true rate constant is related to the apparent rate as given below:

$$k_t^o = k^o e^{\left[ \frac{-(\alpha-z)F \varphi_2}{RT} \right]}$$

Where  $k_t^o$  is the true rate constant,  $k^o$  is the apparent rate constant, F is the Faradays constant, R is the universal gas constant, T is the temperature,  $\alpha$  is the symmetry factor, z is the charge.

The value of  $\varphi_2$  potential cannot be predicted in the presence of specific adsorption of ions from the electrolyte. This specific adsorption results in a shift of the  $\varphi_2$  potential positive or negative depending on whether a cation or an anion is adsorbed onto the surface. The  $\varphi_2$  value is therefore very crucial in whether a reaction is accelerated or suppressed. However in concentrated solutions the effect of the blockage of the surface becomes more important and the rate of the reaction is greatly reduced.

This effect is clearly demonstrated by the polarographic reduction of chromate in the presence of the tetra-alkyl ammonium hydroxides. This indicates that when the ammonium hydroxides at low concentrations in the supporting electrolyte are specifically adsorbed, the  $\phi_2$  potential is shifted positive by the cation adsorption therefore accelerating the reaction. However at higher concentrations the surface blockage effects dominate and the performance is significantly reduced. The size of the alkyl group attached to the ammonium hydroxide also plays a significant role in regulating the reduction rate, with larger alkyl groups providing a more significant effect. This effect is illustrated in the Figure 3.16 [64].

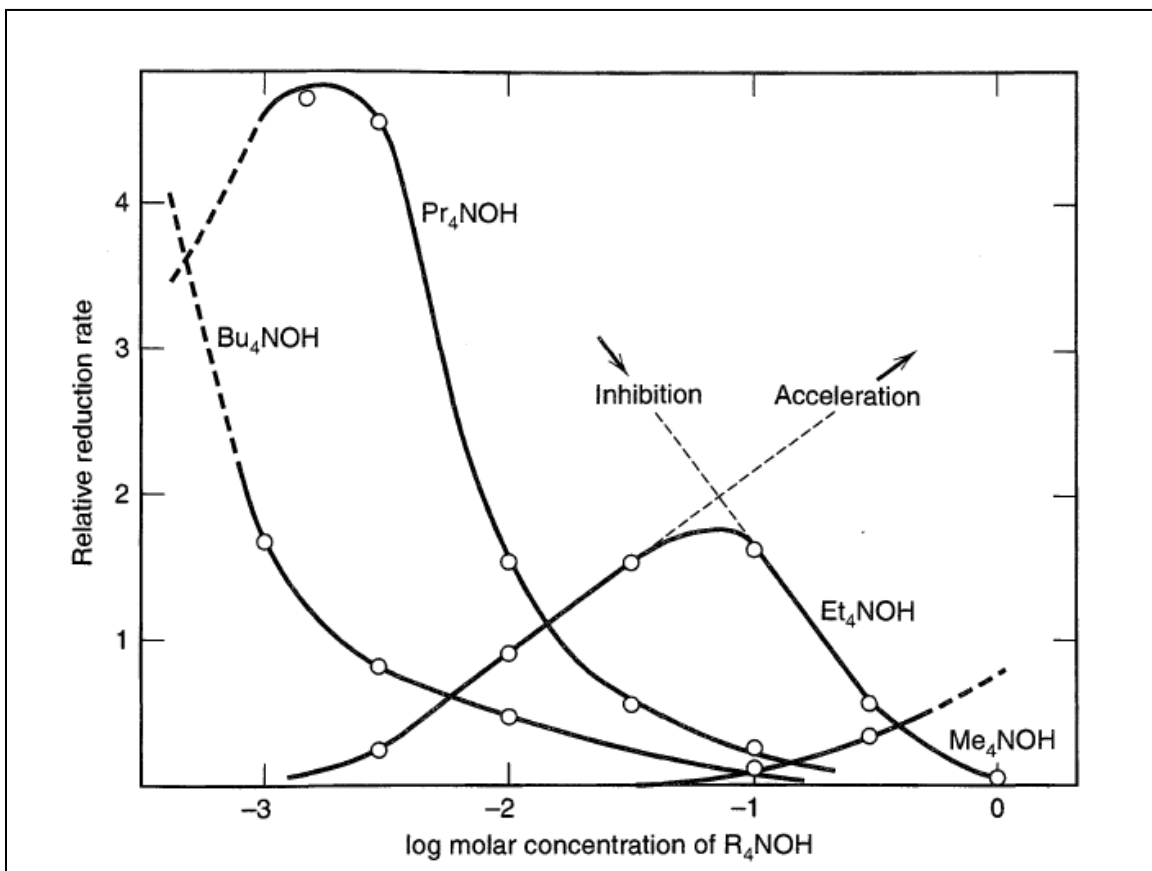


Figure 3.16: Effect of concentration of tetra-alkyl ammonium hydroxide on the rate of reduction of chromate at - 0.75 V vs SCE at 25 °C

These principles that have been discussed up till this point was utilized and an initial study was carried out to understand the effect of the adsorption of different cation onto the surface of Pt from liquid solution in a three electrode cell to rationalize the initial voltage drop for the methanol oxidation. Further, the reasons for the increment in performance with hydroxide solutions are also clarified.

It was explained that the quaternary ammonium ions are weakly solvated and the potential of the electrode being more negative than the potential of zero free charge, the electrostatic attraction of these positively charged ions to the electrode surface was favored. Therefore the specific adsorption of such ions onto the electrode surface might result in a reduction in the active surface area, hence the reduced performance at the electrode surface.

It is further observed that the methanol oxidation reaction proceeds by the Langmuir-Hinshelwood mechanism, which requires the adsorption of the hydroxide ions onto the surface of the electrode. The hydroxide anions have to be transported across the diffuse double layer and specifically adsorbed onto the electrode surface for the methanol oxidation. The oxidation of methanol has been examined with tetramethyl ammonium hydroxide (TMAOH) and poly diallyl dimethyl ammonium hydroxide (PTMAOH).

The double layer structure when the electrode potential was negative of the potential of zero charge is depicted here. The  $\text{TMA}^+$  ions are mobile and they form a compact inner layer since the potential at the electrode is negative compared to that of the solution. This leads to a blockage of the electrode surface, similar to the retardation in case of high concentration electrolytes in Figure 3.17. Despite the fact that the  $\phi_2$  values are much higher than the electrode potential  $\phi_m$ , the blockage of the surface by these ions dominates the performance.

Next the case of the poly electrolyte with the charged group tethered to the backbone (PTMAOH), the mobility of these ions are lower compared to that of the  $\text{TMA}^+$  ions. The tethered cationic group results in the double layer of the solution to be

distributed in the diffuse layer. This results in the  $\phi_2$  potential being closer to the electrode potential, as the  $\phi_2$  potentials are more negative and hence result in repelling away the  $\text{OH}^-$  ions. This results in a reduction of the electrode reaction rate. The potential profile of the double layer interface when the electrode potential is negative of the potential of zero charge is illustrated here in Figure 3.17 for different electrolytes [65].

This further explains the effect of the additional hydroxide in the fuel cell performance; it introduces additional  $\text{OH}^-$  ions which get transported to the electrode reaction sites. Further the introduction of the more mobile  $\text{Na}^+$  ions results in a closely packed double layer and decrease in the thickness of the double layer results in the enhanced fuel cell performance.

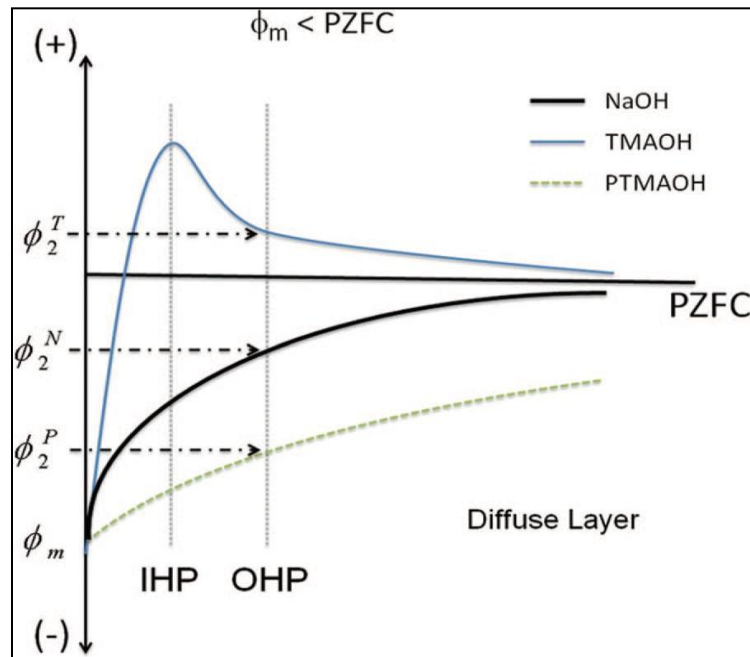


Figure 3.17: Potential profile of double layer interface with different electrolytes for methanol oxidation on platinum electrode at potentials negative of potential of zero charge

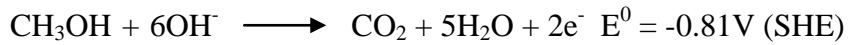
### 3.3.1 Initial Voltage Drop in Anode Hybrid Fuel Cells

The anode hybrid fuel cells are designed with a high pH cathode and a low pH anode. The two electrodes are then assembled onto the PEM Nafion membrane. The performance with such hybrid fuel cells have been demonstrated previously. The polarization curve of the hybrid direct methanol fuel cell is shown in Figure 3.18. The properties of the ionomer used for the MEA fabrication was listed in Table 3.1.

The polarization curves indicate that the performance is similar to complete AEM fuel cells. The low current density regime is of the most interest in these fuel cells. A sharp decline in the open circuit voltage is observed in such fuel cells after which the fuel cell curve is linear indicative of the ohmic polarization regime.

Our concern is the evaluation of this low current density regime. First we note that the quaternary ammonium cations are tethered to the polymer backbone in the ionomer. This greatly restricts the mobility of the cation. The methanol oxidation reaction starts out at potentials negative of the potential of zero charge, resulting the formation of a diffuse double layer at the anode. Hence as the potential at the OHP is negative, transport of the OH<sup>-</sup> ions to the catalyst surface is limited. Hence this steep initial voltage drop is observed.

In order to clarify if the voltage drop does occur at the anode, the anode polarization curve is obtained by purging humidified H<sub>2</sub> at the cathode. The PEM cathode acts like a hydrogen reference electrode and does not contribute to the overpotential. The AEM anode is the working electrode and the polarization curves for such fuel cells were obtained. The polarization currents for the methanol oxidation are shifted positive and included in Figure 3.18. This performance indicated that there was a sharp voltage drop at the low current density region indicative that this performance drop occurred at the anode. The reason for this initial voltage drop at low current density has already been previously explained. The potential for the anode in a conventional AEM anode is given by:



It can be clearly seen in this Figure 3.18 that the potential at the anode is shifted to around .13V vs the internal hydrogen electrode. The cathode does not contribute to the this drop since the only reaction taking place at the cathode is H<sub>2</sub> evolution, methanol oxidation at the cathode is also possible, however since it is occurring under acidic conditions, the potential is close to 0 V, hence the potential is exclusively the anode potential.

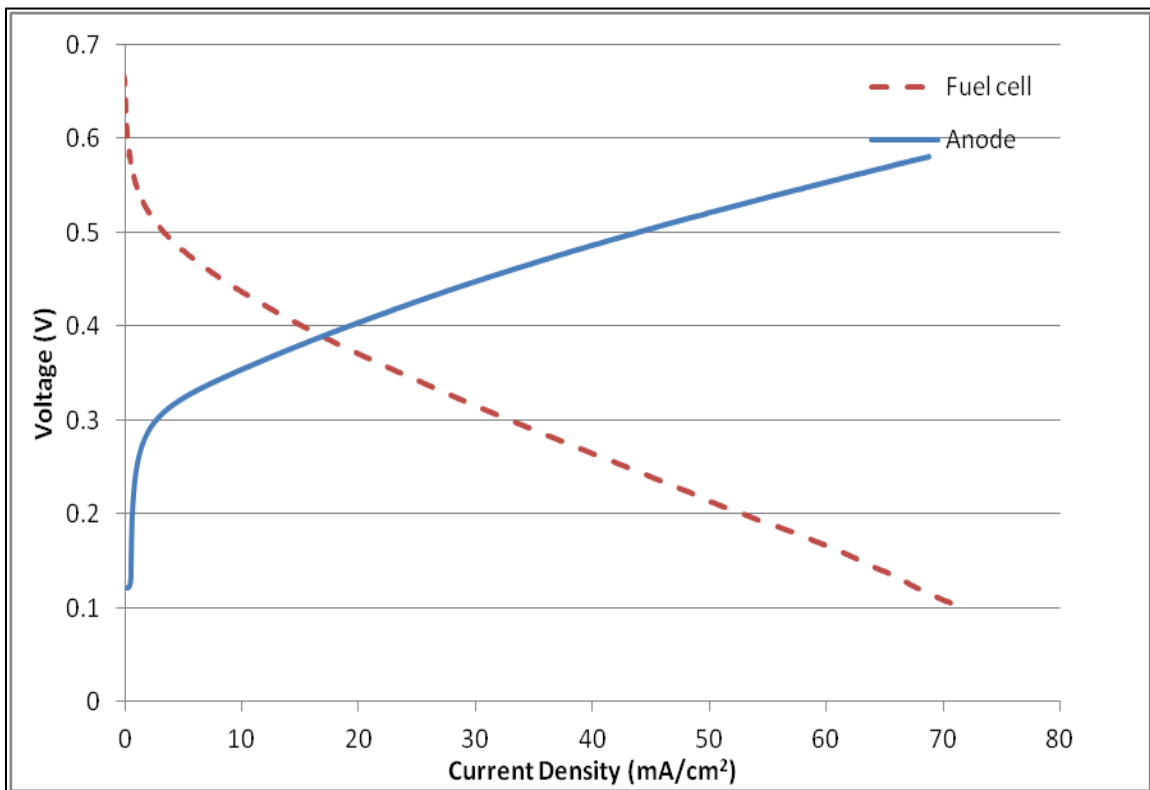
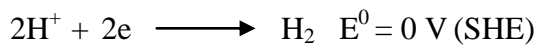


Figure 3.18: Polarization curve of fuel cell (dotted line), anode polarization curve (line) for anode hybrid direct methanol fuel cell operated with 2M MeOH at 5 ml/min on anode and O<sub>2</sub> and H<sub>2</sub> respectively at cathode 50 sccm at 55 °C

This is indicative that the shift in the potential stems from the AEM/PEM junction near the anode where the electric field enhanced dissociation of water contributes to the overall potential. It has been explained that at the junction for unit activity of the  $H^+$  ions and the  $OH^-$  ions the potential difference at the bipolar membrane could be as high as 0.828V.

The anode overpotential in this driven mode is inclusive of this junction potential, similar to that of the entire fuel cell performance. It can be seen clearly that most of the fuel cell overpotential, occurs at the anode. The anode hybrid direct methanol fuel cell provides an excellent diagnostic tool for the separate analysis for the AEM anode working under fuel cell conditions. This further provides definitive proof that the initial potential drop in the AEM fuel cell occurs predominantly at the anode.

The potential drop at the anode needs to be addressed since it results in a significant loss in the fuel cell performance. It can be seen that recovery of even a few mV from this loss at the initial low current density region could significantly impact the performance of alkaline anion exchange membrane fuel cells.

The different approaches to address this include the utilization of a catalyst with a different potential of zero free charge with respect to quaternary ammonium adsorption. This however beyond the scope of current materials, since the replacement for Pt based metals for anodic methanol reduction is currently not available. It was shown in a study with TMAOH that shifting the electrode potential to potentials positive of the potential of zero charge actually enhanced the oxidation current, since at these potentials the electrode charge repelled away the cations on the surface and ensuring better  $OH^-$  transport to the electrode surface. Thus possibly poling the electrodes such that the anode potential is held positive of the potential of zero charge is another approach. This approach however is inconvenient and was tried on the hybrid fuel cell and it led to a very rapid and irreversible decline in the fuel cell performance.

Increasing the ionic conductivity of the ionomer might be another approach, however as things stand the conductivity of alkaline fuel cells are moderate, further the mobility of the OH<sup>-</sup> ions are slower than that of H<sup>+</sup> ions in their acid analogues. Further extensive research might be required in order to develop such ionomers and membranes for alkaline fuel cells.

The most convenient approach at this point would be to develop different cationic groups. The main reason for such an approach would be that since the potential of zero charge is influenced by the type of adsorbate on the electrode surface. Modifying the adsorbate ions could probably result in a shift of the potential of zero charge in a manner that is favorable for electrode kinetics. Further different cationic groups might have different solvation energies, since it has been previously mentioned that quaternary ammonium ions have a weak solvation layer and electrostatic adsorption is favored [65]. Changing the cationic groups from quaternary ammonium ions might have merit. Therefore the approach adopted here to address this initial potential drop was to develop a different cationic group for the ionomer. The cationic group in consideration is quinuclidine. The quinuclidine is attached to the ionomer backbone of Ionomer I.

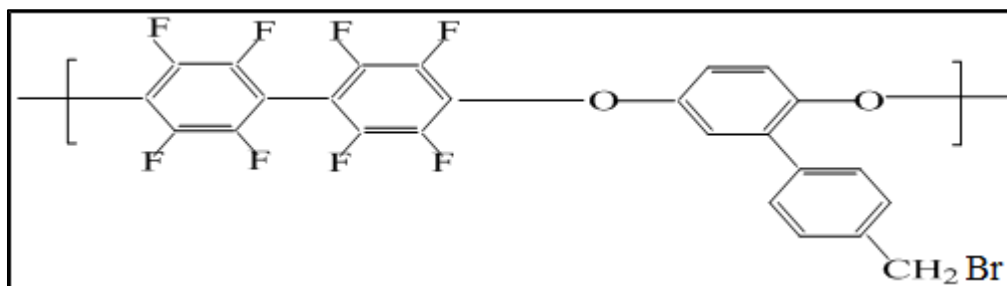
### **3.3.2 Cationic Head Groups for Anode Hybrid Fuel Cells**

The cationic head groups for most AEM ionomers designed till date are based on alkyl ammonium groups as the ion exchange groups. It was desired to compare the performance of such fuel cells with ionomers composed of different cationic groups. The cationic group in consideration was quinuclidine. This is the first such demonstration of a polycyclic amine azo bicyclo (2, 2, 2) octane alkylated as a quaternary ammonium cation, also known as quinuclidine, to be used as ionomer in alkaline electrodes. The properties

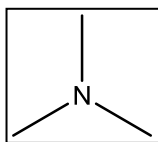
of the ionomer is explained in Table 3.6 and the performance of the fuel cell with the two different cationic group containing ionomers have been demonstrated Figure 3.20.

Table 3.6: Properties of Ionomer I with the ammonium and quinuclidine cationic groups

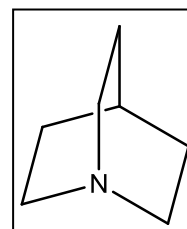
Ionomer	IEC (meq/g)
Ionomer I-4	1.38
Ionomer I-5	1.32



(a)



(b)



(c)

Figure 3.19: Structure of (a) Ionomer I backbone, and the attached cationic groups: (b) Ammonium (c) Quinuclidine

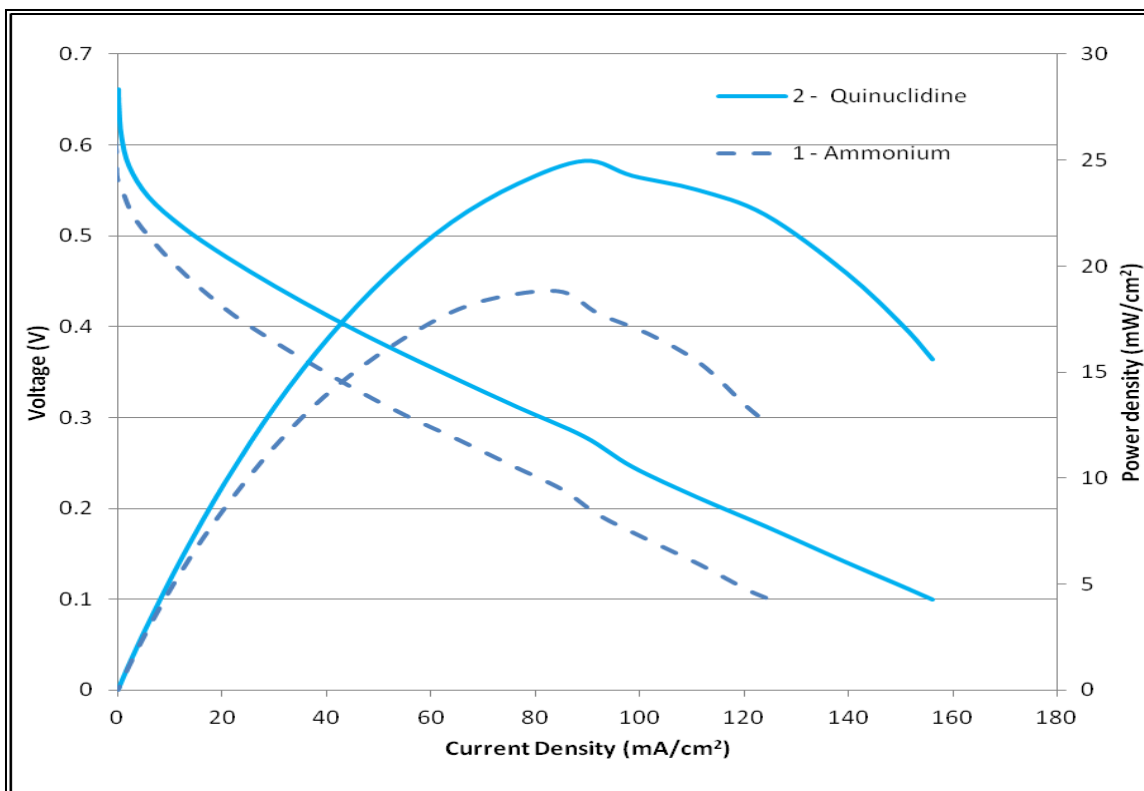


Figure 3.20: Polarization and power density curve of ammonium (dotted lines), quinuclidine (lines) ionomers for anode hybrid direct methanol fuel cell operated with 2M MeOH at 5 ml/min and O<sub>2</sub> at 50 sccm at 55 °C

It can be clearly seen here that there is still a significant initial voltage drop associated with the AEM anode in such hybrid fuel cells are observed in these quinuclidine based ionomers. The reason for this being that the quinuclidine ionomer which is tethered to the polymer backbone has low mobility. This is ascertained from the fact that the rigid cyclic structure of the quinuclidine has very low mobility even in ionic liquids [66]. A diffuse double layer is formed and hence it results in the same effect as that of the ammonium based ionomers.

The size comparison of the quinuclidine and hexyltrimethyl ammonium cations, indicate the Van der Waals volume of quinuclidine being slightly larger [66]. The overall performance with such ionomers are however greater owing to this fact that quinuclidine

is larger compared to the trimethyl ammonium cation providing for greater void volume and hence for better transport properties.

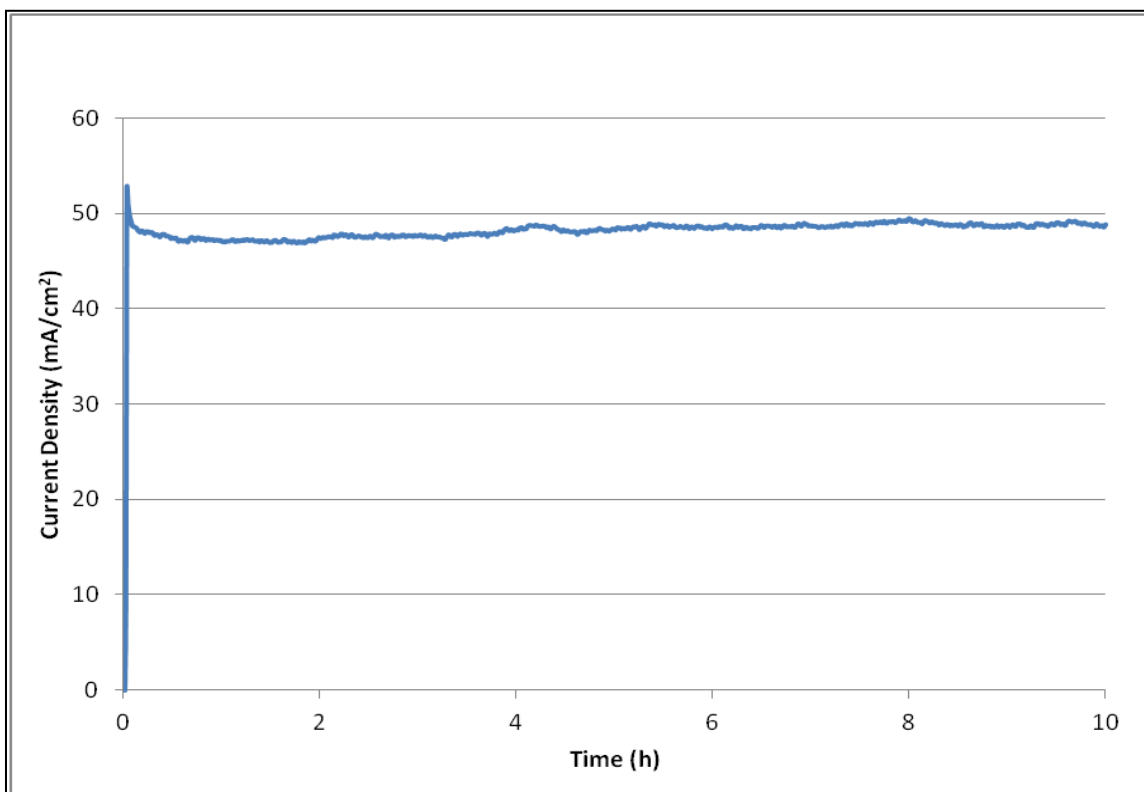


Figure 3.21: Steady state performance of the fuel cell with Ionomer I-5 held at constant potential of 250 mV

The polymer backbones are the same therefore the chain mobility of the ionomers should be almost identical. The only variation in these two materials is the cationic groups and the IEC of the material varies slightly. The steady state performance with this ionomer is also demonstrated here in Figure 3.21. This indicates that the fuel cell with these ionomers can be operated stably for a long time with air as oxidant with no substantial decrease in fuel cell performance.

### 3.4 Summary

The hybrid fuel cell with a high pH AEM anode and a low pH PEM cathode was assembled and the operation of these fuel cells has been demonstrated. This is the first such demonstration of anode hybrid direct methanol fuel cells. The electrode fabrication using ionomer and PTFE as binders was demonstrated. The performance with PTFE bound electrodes providing significant increase in performance compared to using the Ionomer I as the binder. The optimization of the operating conditions with such fuel cells was carried out. The effects of the ionomer content and ion exchange capacity of the ionomer has also been investigated. The optimum ionomer content of 15 wt% with respect to the catalyst and an IEC of 1.3meq/g were chosen as they provided good material transport and ionic conductivity without retaining too much water and impeding the fuel cell performance.

The comparison of the performance with more hydrophobic ionomers (Ionomer II) with the hydrophilic ionomer (Ionomer I) have been made. The hydrophobic ionomer has the best performance in these anode hybrid fuel cells. A comparison of the fuel cell performance with these ionomers with different molecular weights was made. The ionomer with the lowest molecular weight provides the maximum performance with such fuel cells.

A peak power of 27 mW/cm<sup>2</sup> was obtained with the optimized electrode and this is the highest performance obtained using alkaline electrodes in methanol fuel cells without the use of hydroxide solutions.

An initial voltage drop was observed in alkaline anode based systems. The explanation for such a voltage drop in our anode hybrid cell was elucidated. It was further demonstrated that the initial voltage drop originated at the alkaline anode. The anode hybrid cells can be used to diagnose the performance at the AEM anode under direct methanol fuel cell working conditions. The alternative methods to overcome this initial voltage drop were suggested. One of the methods was to use a different cationic group for

OH<sup>-</sup> transport and this was implemented. The new quinculdine based cationic group still had a large initial voltage drop, the performance was still better than the ammonium equivalents with Ionomer I. A peak power performance of 25 mW/cm<sup>2</sup> was achieved. The fuel cell operated stably with air for over 10 hours.

## **CHAPTER 4**

### **CATHODE HYBRID DIRECT METHANOL FUEL CELLS**

#### **4.1 Objective**

Cathode hybrid fuel cells utilized an acidic anode and a basic cathode with a PEM membrane. The principle of operation of these fuel cells has already been elucidated. The use of these fuel cells in the methanol based systems is to be demonstrated here for the first time. The impact of the electrode fabrication protocol was studied. The operating conditions for these fuel cells were optimized. A comparative study of different ionomers was also carried out. The optimum ionomer content in the fuel cell for best performance was determined. The impact of the ionomer properties such as molecular weight, on fuel cells were demonstrated for platinum based electrodes. The main advantage of these fuel cells is the use of a non-platinum catalyst cathode. The non- platinum catalyst cathode based MEA is also demonstrated apart from fuel cells with platinum based electrode. A study of the impact of the different head groups namely ammonium and quinuclidine on the fuel cell performance were also studied here.

## 4.2 Performance of Cathode Hybrid Direct Methanol Fuel Cells

The cathode hybrid fuel cells with the AEM cathode attached to the PEM half cell is characterized. The properties of the ionomer initially used for the characterization is given below.

Table 4.1: Properties of the ionomer used for fabrication of AEM electrode

Ionomer	IEC (meq/ g)	Water Uptake (%) ( 25 °C)
Ionomer I-1	1.21	25

The performance of the fuel cell operating with this ionomer is summarized below.

### 4.2.1 Impact of the Operating Conditions

#### 4.2.1.1 Temperature

Oxygen reduction kinetics was shown to be enhanced by increasing the operating temperature. Testing the cathode hybrid fuel cell at 25 °C, 40 °C and 55 °C seemed to corroborate this. The tests were performed with a 2M methanol solution supplied to the anode at 5ml/min and oxygen supplied to the cathode at 50 sccm. An improvement in the performance in the activation and the ohmic was observed. Increased temperature results in enhanced mass transport and methanol crossover, with the former being more beneficial to the overall performance.

The variation of performance with increase in cell temperature is shown below in Figure 4.1.

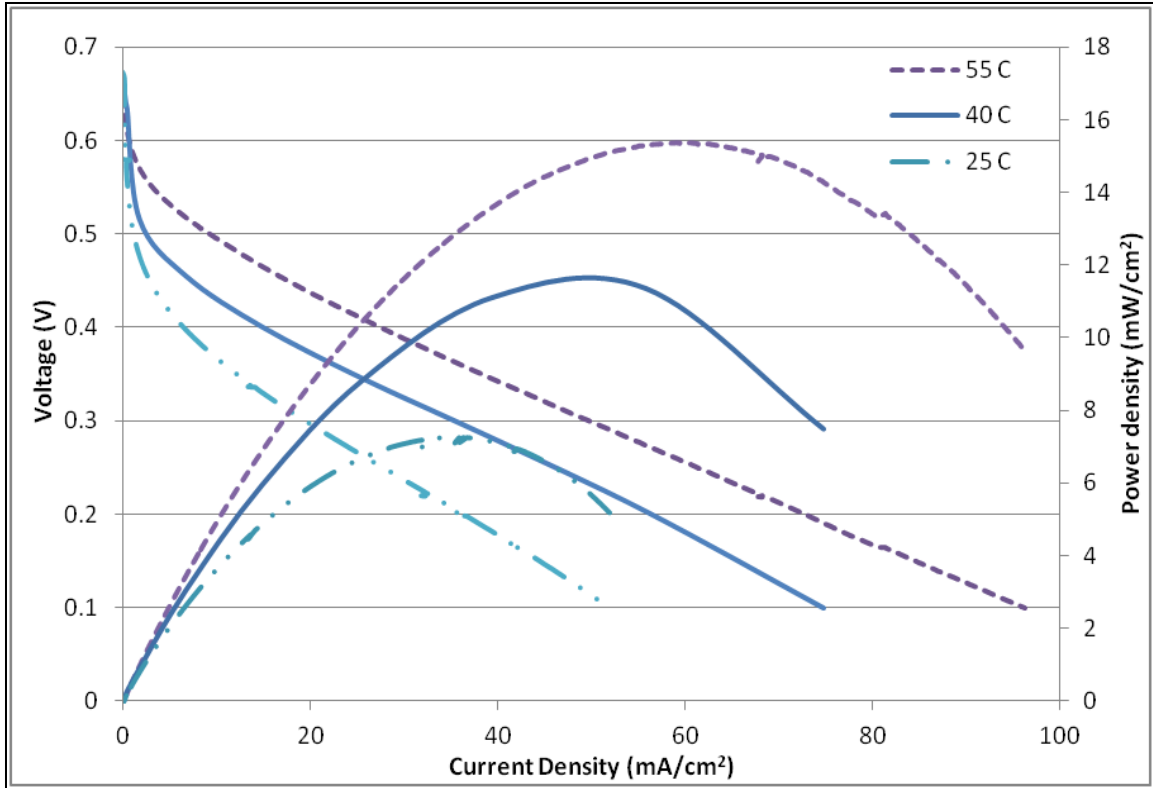


Figure 4.1: Polarization and power density curves of cathode hybrid fuel cell operated at different temperatures: 55 °C (broken lines), 40 °C (lines), 25 °C (double dotted lines), with 2M MeOH at 5 ml/min on the anode and 50 sccm O<sub>2</sub> at the cathode

#### 4.2.1.2 Methanol Concentration

It is interesting to study the impact of the fuel concentration on cathode hybrid fuel cells. Open circuit potentials and fuel cell performances of these fuel cells with different concentrations are shown in Figure 4.2. The highest performance is obtained with 2M MeOH, increasing the concentration further results in a drop in the fuel cell performance. This results from the electro-osmotic drag of methanol along with the H<sup>+</sup> ions similar to the PEM based fuel cells along with methanol diffusion through the membrane is responsible for this large variation in these fuel cells. However the distinct advantage is that these allow the use of non Pt based catalysts and the cross over effects

resulting from the use of high methanol concentrations are insignificant. This is demonstrated later.

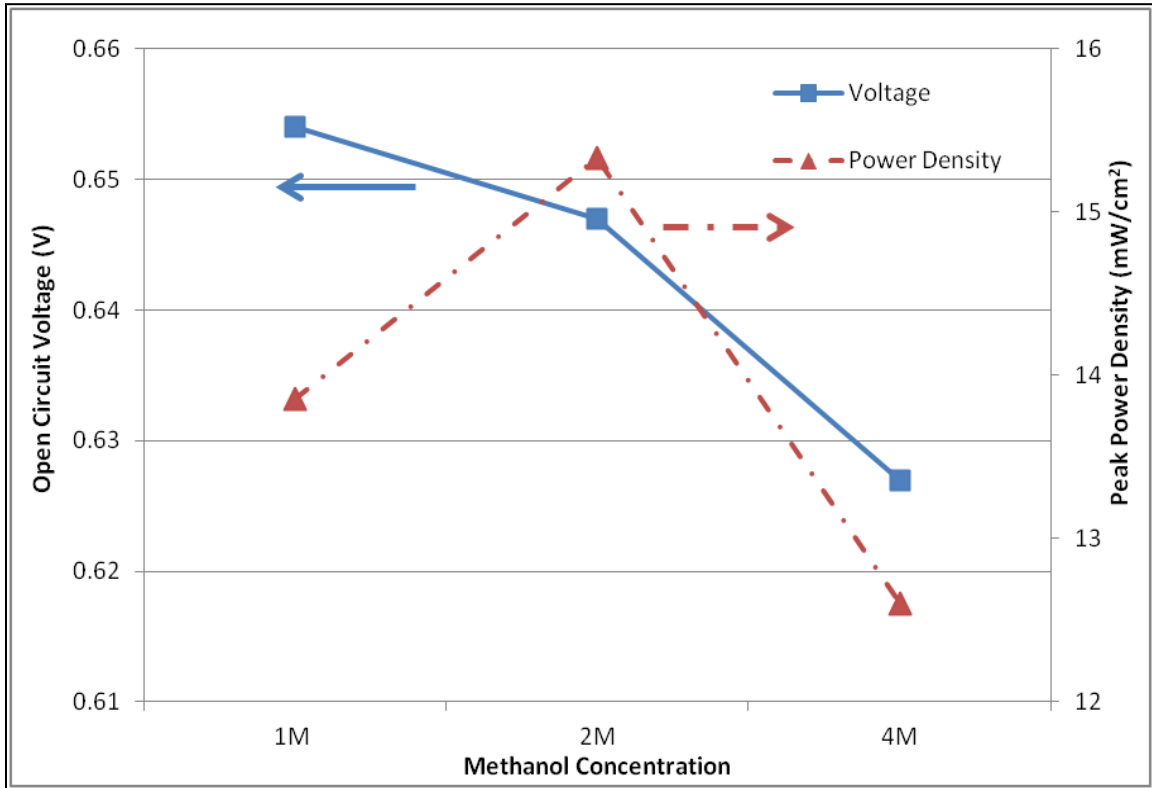


Figure 4.2: Open circuit voltage (squares) and peak power density (triangles) of fuel cell operated with different MeOH concentrations: 1M, 2M, 4M operated with 50 sccm O<sub>2</sub> at the cathode at 55 °C

#### 4.2.1.3 Methanol Flow Rate

A study of the impact of the methanol flow rate shows a behavior similar to the anode hybrid fuel cells. Increasing the flow rate increases the performance up to a certain extent beyond which the flow rate seems to be detrimental to the performance. The peak power was obtained with a flow rate of 5 ml/min. Thus the balance between the transport of methanol to the reaction sites and the crossover of the unreacted methanol is what controls the optimum fuel flow rate.

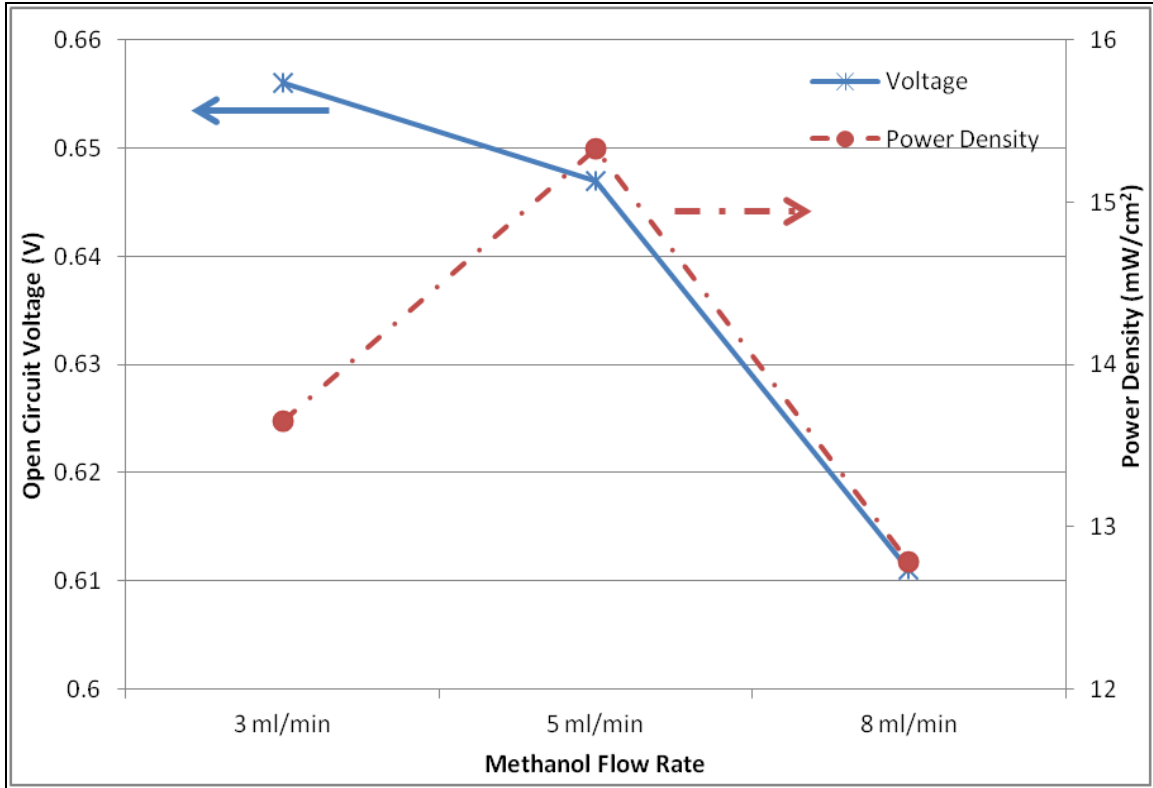


Figure 4.3: Power density (circles) and open circuit voltage (stars) of fuel cell operated with different methanol (2M) flow rates: 3, 5, 8 ml/min operated with 50 sccm O<sub>2</sub> at the cathode at 55 °C

#### 4.2.1.4 Oxygen Flow Rate

It is essential to study the impact of the oxygen flow rate. Varying the oxygen flow rate had a significant impact on the fuel cell performance. Higher flow rates normally favor better performance since it results in higher oxygen transport to the reaction sites and also build up sufficient pressure that lowers methanol cross over and provides physical removal of methanol and the water. However it is important to note that in the cathode hybrid fuel cell water is a reactant and excessive removal could result in dry out of the catalyst layer and poor performance. Therefore the ideal oxygen flow rate is one that maintains this balance. Initially transport and reduction of cross over by increasing the oxygen flow rate seems to dominate, however further increasing the oxygen flow rate beyond 50 sccm does not result in any significant improvement in the

performance since the stoichiometric ratio of the oxygen supplied is very much higher than that required to support such currents. High flow rates however result in higher OCV due to reduced methanol crossover and enhanced methanol removal as previously explained with anode hybrid fuel cells.

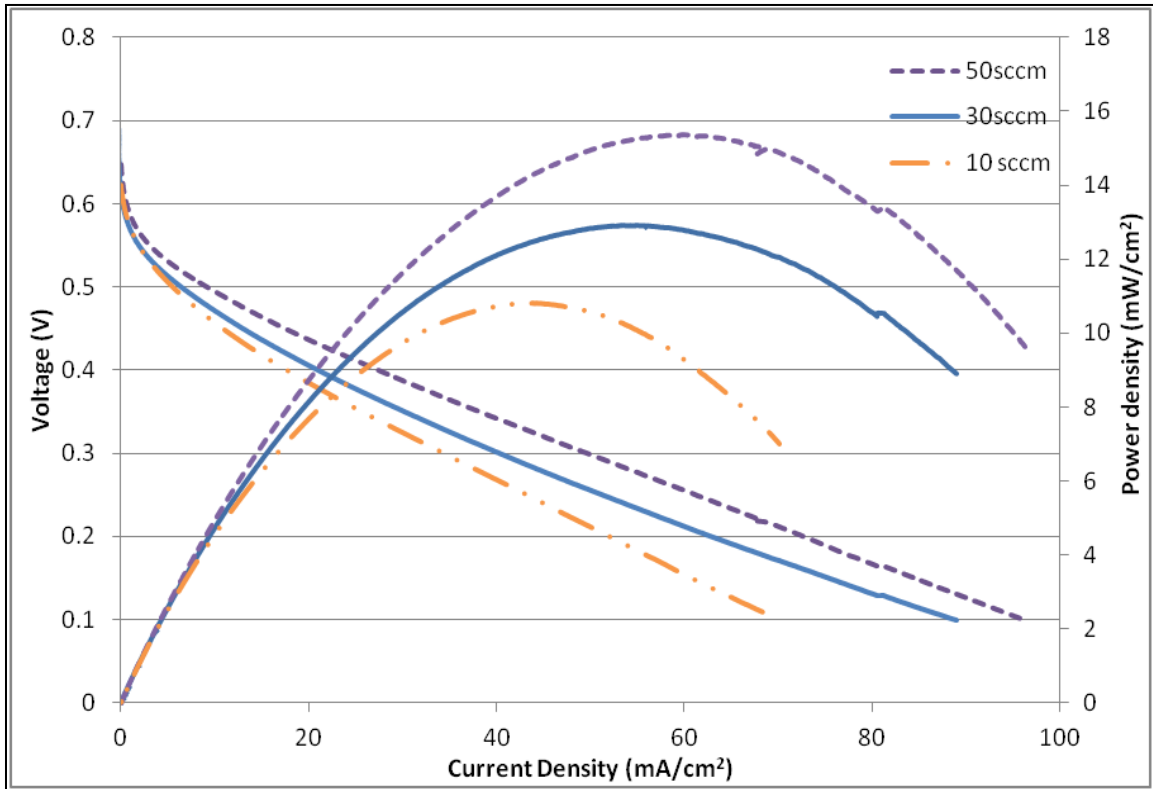


Figure 4.4: Polarization and power density curves of cathode hybrid fuel cell operated with different oxygen flow rates at the cathode: 50 sccm (broken lines), 30 sccm (lines), 10 sccm (double dotted lines), and 2M MeOH at 5 ml/min on the anode at 55 °C.

#### 4.2.1.5 Air Flow Rate

Cathode hybrid fuel cells are tested with air at the cathode and the anode being constantly supplied with 2M MeOH at 5 ml/min. The reduction in performance with air was explained as a result of the reduced oxygen partial pressure. It was observed that

while varying the flow rates with air, changing the air flow rate does not significantly alter the performance. An increase in the OCV and a slight increase in performance are observed owing to the same reasons stated above for increasing the flow rate with oxygen.

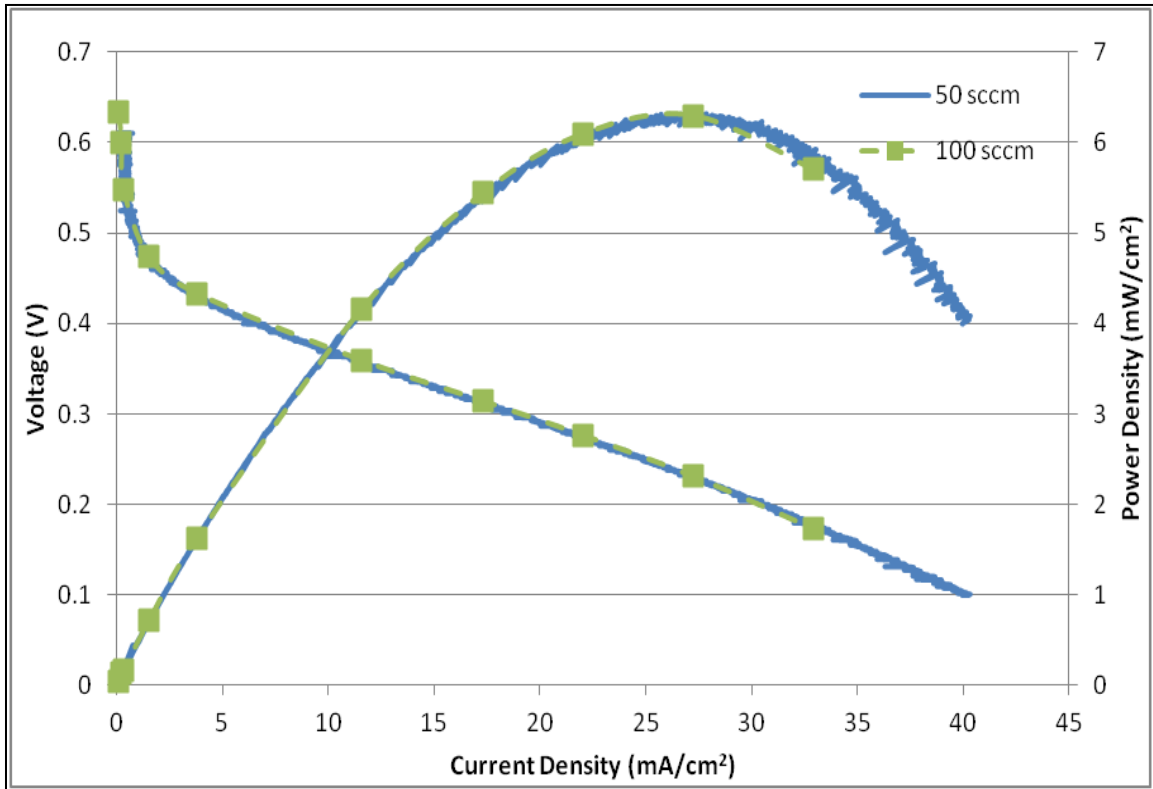


Figure 4.5: Polarization and power density curves of cathode hybrid fuel cell operated with different air flow rates at the cathode: 50 sccm (lines), 100 sccm (squares) and 2M MeOH at 5 ml/min on the anode at 55 °C.

The ideal operating parameters for the cathode hybrid fuel cells are similar to the AEM anode based fuel cells and are summarized in the table below.

Table 4.2: Optimized operating conditions for cathode hybrid fuel cells

Parameter	Operating condition
Temperature	55 °C
Methanol Concentration	2 M
Methanol Flow Rate	5 ml/min
Oxygen Flow Rate	50 sccm
Air Flow Rate	100 sccm

#### 4.2.2 Steady State Operation

The steady state operations of such cells based on alkaline anion exchange ionomers are crucial. The testing of such cells were carried out by operating the cells with 2M MeOH and 50 sccm O<sub>2</sub> at a constant potential of 250 mV and monitoring the current. The fuel cell was operated for 8 h and the current density remained stable over the entire period of time. The fuel cell was continuously tested for 4 days and the performance for one of the 8 hour runs is shown in Figure 4.6.

This is another indication of the stability of the hybrid fuel cells. The slight drop in the current was due to the depletion of the methanol since the cell is operated at high current densities. This could be recovered by again feeding a new methanol solution.

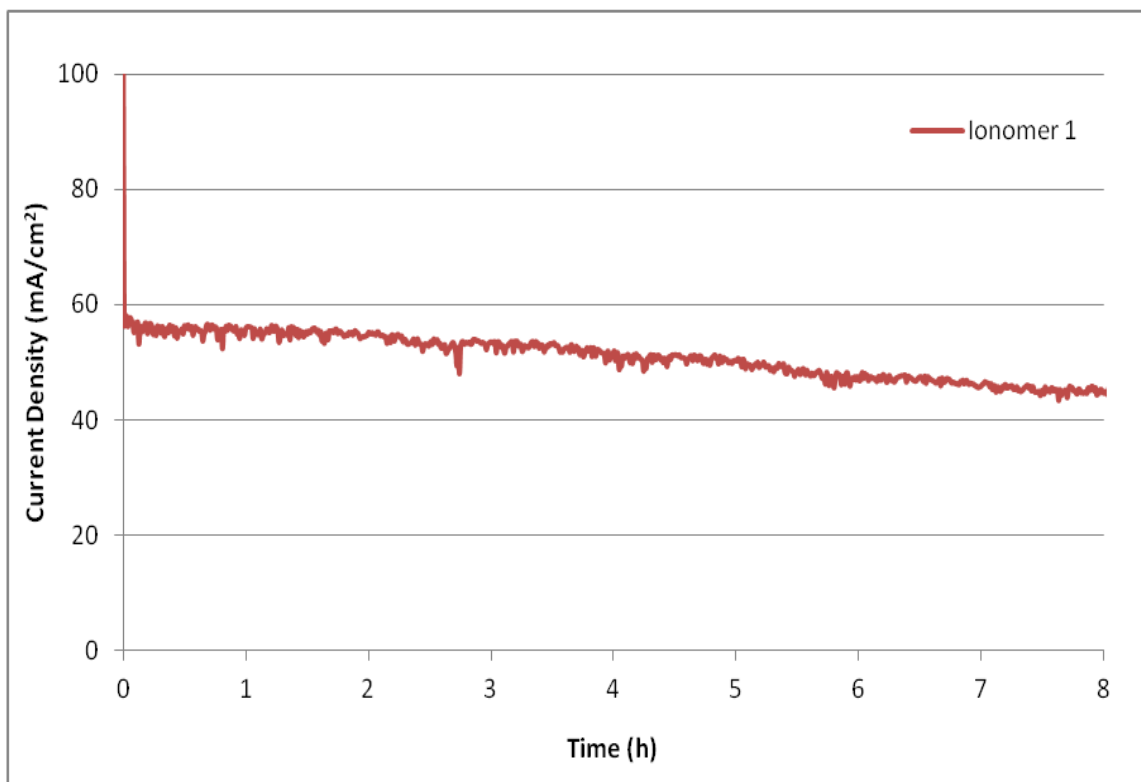


Figure 4.6: Steady state performance of the fuel cell held at constant potential of 250 mV with 2M MeOH, flow rate 5 ml/min and O<sub>2</sub> flow rate 50 sccm supplied at atmospheric pressure at 55 °C

#### 4.2.3 Impact of Fabrication Protocol

It has been previously indicated that the fabrication protocol plays a crucial role for the fuel cell performance with the anode hybrid fuel cells in Chapter 3. Similarly it is crucial for the fuel cell performance with the AEM cathode. Here it is important to note that water is a reactant at the cathode and therefore water distribution within the catalyst layer is critical along with the transport of the oxygen to the reactant sites. Water is supplied to the cathode from the crossover of the H<sup>+</sup> ions through the membrane and also through water production at the PEM membrane/AEM electrode junction. Excessive accumulation of water could result in cathode flooding and excessive removal of water

could lead to poor performance due to non availability of reactants. The fabrication protocol hence plays a crucial role in controlling the performance in fuel cells.

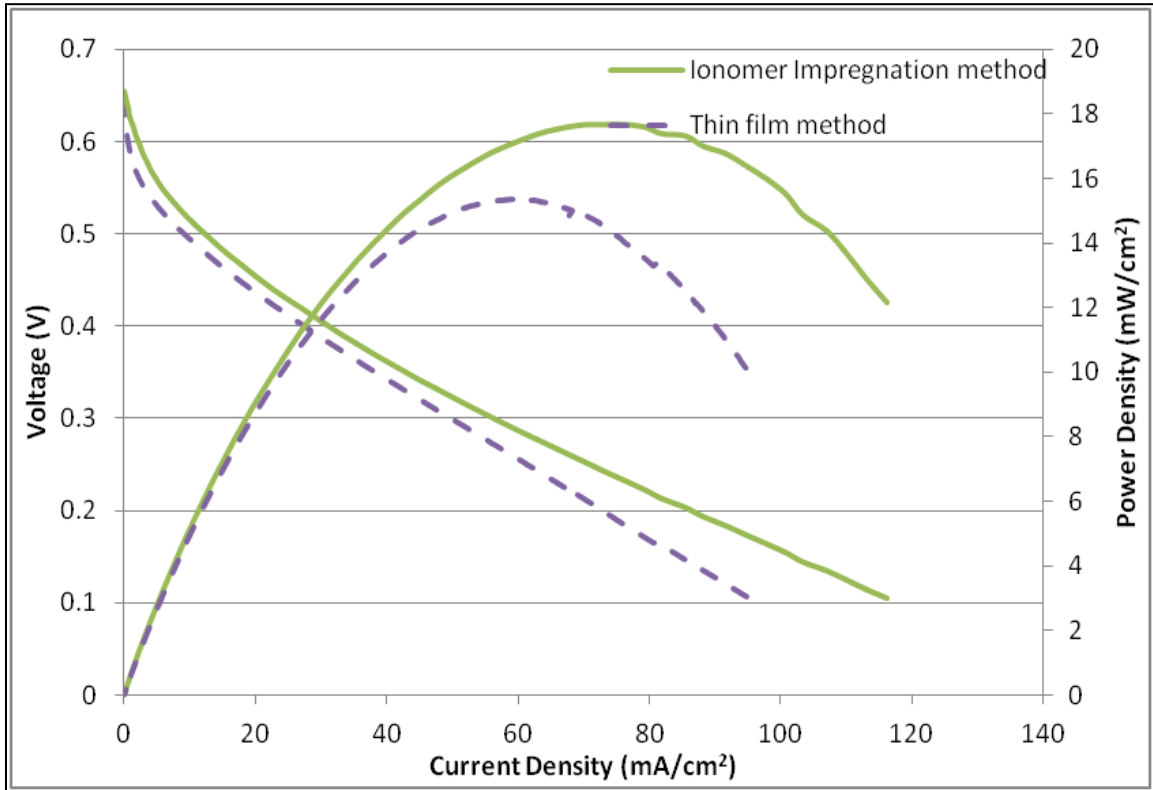


Figure 4.7: Polarization and power density curves for the anode hybrid fuel cell operated with thin film cathode (dotted lines), ionomer impregnated cathode (lines) with 2M MeOH supplied at a flow rate of 5ml/min and O<sub>2</sub> supplied to the cathode at 50 sccm (atmospheric pressure) at 55 °C.

It was desired to ensure fair comparison of the effect of the cathode fabrication protocols, therefore two MEAs were fabricated with identical PEM half cells with the electrodes fabricated by the thin film method. The AEM electrodes were fabricated by the ionomer impregnation and thin film methods described before using the ionomer whose properties were listed in Table 4.1 and performance shown in Figure 4.7.

It has been previously described with the anode hybrid fuel cells how the use of the ionomer which is hydrophilic results in enhanced water retention within the catalyst layer thereby choking the gas transport to the catalyst sites resulting in a lower performance despite the higher conductivity with such ionomers. The utilization of the PTFE as a binder and the ionomer being sprayed from the top results in some of the ionomer penetrating through the catalyst layer, however several channels near the GDL are free from water allowing for gas transport. Catalyst utilization however might be lower since some channels within the catalyst layer are free of water hence does not contribute to the power performance. This tradeoff between catalyst utilization and gas transport is essential for better overall performance.

#### **4.2.4 Impact of the Ionomer Content**

The ionomer content within the catalyst layer controls the ionic conductivity, catalyst utilization and transport properties within the electrodes. Therefore it is again essential to optimize the content of the ionomer within the catalyst layer for the best performance. The ionomer content here is modified by amount added to the slurry while spraying the catalyst onto the GDL layers. Three different ionomer contents were used and their performance is illustrated in the Figure 4.8.

It was previously explained that too little or too much ionomer results in either very low ionic conductivity or losses from electronic conductivity and mass transport respectively. Therefore the 15 wt % seems to be the ionomer content within the catalyst layer providing optimum performance.

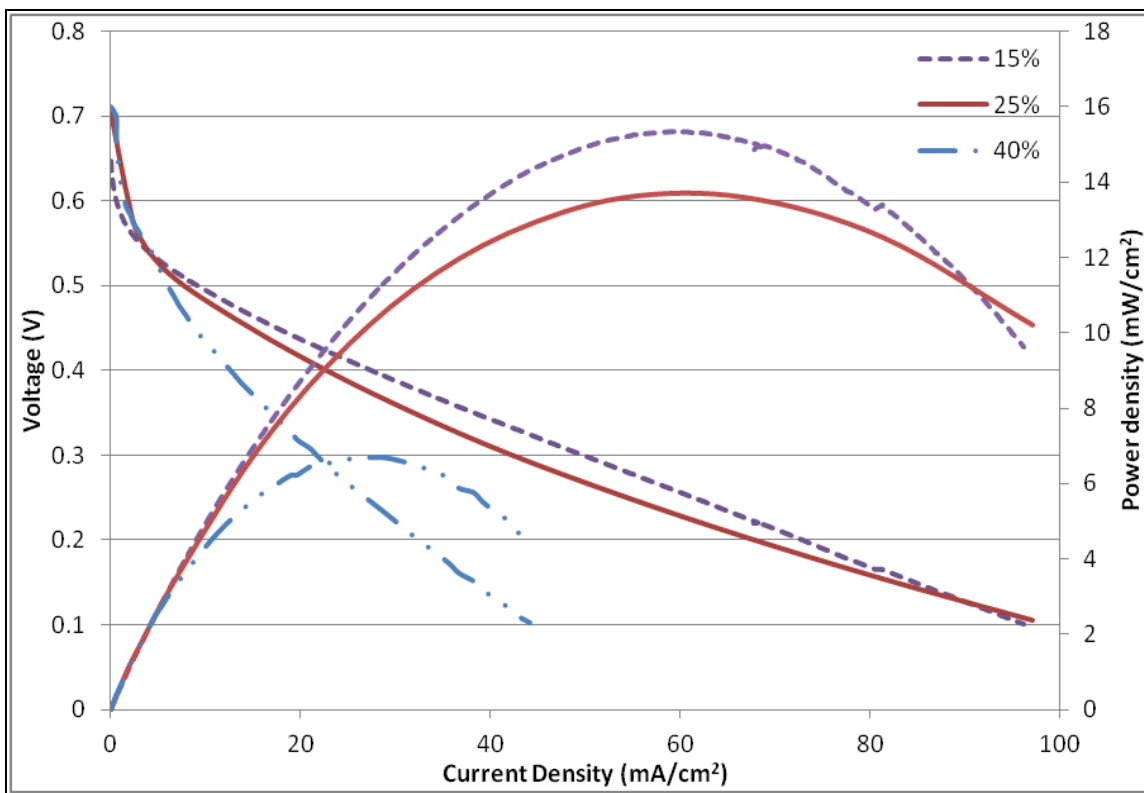


Figure 4.8: Polarization and power density curves of cathode hybrid fuel cells with different ionomer contents: 15, 25, 40 % with 2M MeOH at 5 ml/min and 50 sccm O<sub>2</sub> at 55 °C

#### 4.2.5 Impact of the Different Ionomers

Three different ionomers are used here for making the alkaline cathode and their performance is studied in the cathode hybrid fuel cell. Their structures are shown in chapter 2 and properties of these ionomers have been previously shown in chapter 3. The main differences in the ionomer were based on their hydrophobicity and the resultant reduced water uptake and conductivity. The reduction in the conductivity was however counterbalanced by the improvement in the transport properties and catalyst utilization. The performance of the fuel cells with these ionomers is illustrated in Figure 4.9.

In the cathode hybrid fuel cells water diffuses from across the anode along with the protons transported through the membrane and further produced at the membrane/electrode interface at the cathode. The water however is a reactant in the AEM cathode unlike in the PEM cathode where it is a product. If there is excess water in the cathode channels then oxygen diffusion to the layers might be constricted resulting in a lower performance. The hydrophobic ionomers keeps a few channels clear of water and provides for sufficient gas transport. A similar study with half cells being constructed from Ionomer 1 and a more hydrophilic ionomer showed a similar result [67]. Thus this validates the better performance with the hydrophobic ionomers.

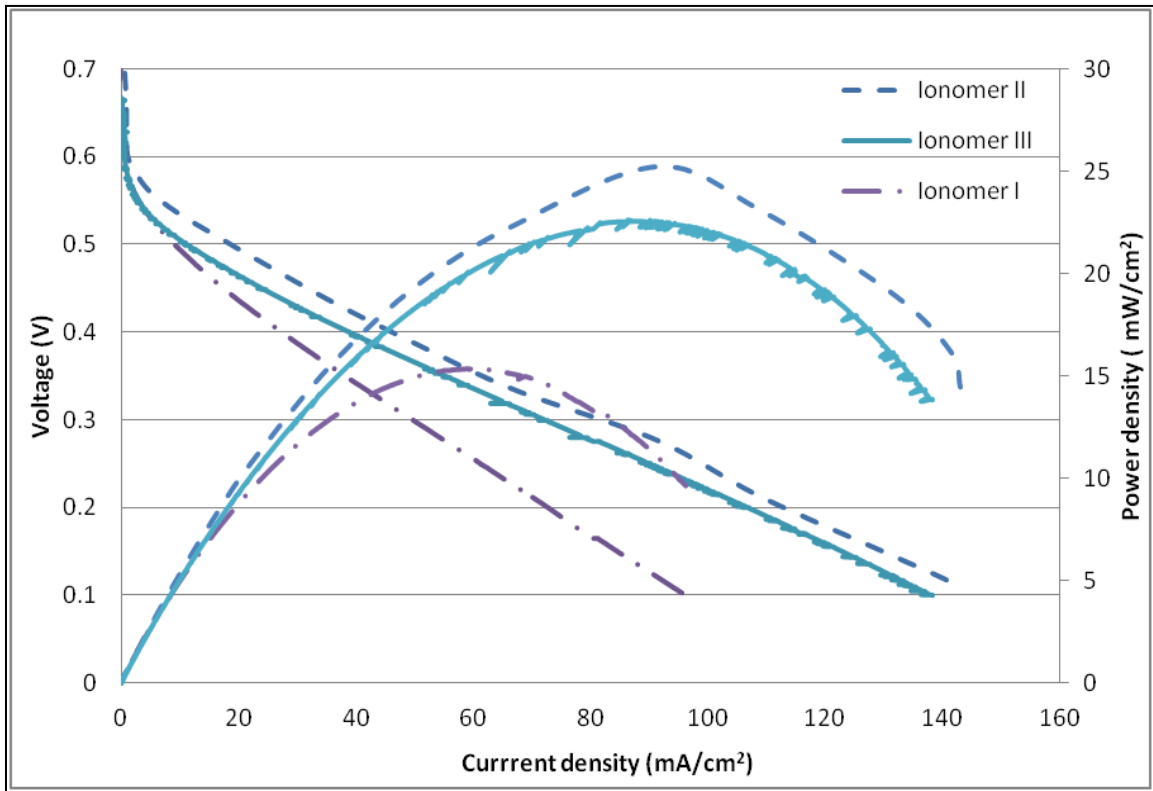


Figure 4.9: Polarization and power density curves of cathode hybrid fuel cell operated with different ionomers: Ionomer I, II, III at the cathode with 2M MeOH at 5 ml/min on the anode and 50 sccm O<sub>2</sub> on the cathode at 55 °C

#### 4.2.6 Impact of the Ionomer Molecular Weight

The molecular weight of the ionomer is again studied for its impact on the oxygen reduction reaction at the cathode. The ionomer molecular weights are again varied from a lower to a higher values (11.2 k to 40.5 k) the electrode fabrication of these ionomers are carried out in the exact same manner as described previously, with the assembly of the AEM cathode onto an identical PEM anode. The properties of the ionomers are summarized again in Table 4.3

Table 4.3: Properties of Ionomer II with different molecular weight

Ionomer	Mn	PDI	IEC (meq/g)
(a) Ionomer II -1	11.1 k	2.67	1.3
(b) Ionomer II -2	11.8 k	2.27	1.3
(c) Ionomer II -3	25.8 k	2.60	1.3
(d) Ionomer II -4	40.5 k	5.08	1.3

Lower molecular weight ionomers again show a significantly better performance than that of higher molecular weight ionomers. It has been previously discussed with the anode hybrid fuel cells that these ionomers provide better assembly onto the catalyst, favorable porosity for enhanced material transport and greater flexibility of the polymer strands for transport to the reaction sites. The lower molecular weight ionomers have more chain ends. This allows for easier access of the gas into the polymer at this discontinuity [68]. This probably accounts for the enhanced performance with such ionomers. The performance with the different molecular weight ionomers is shown in Figure 4.10.

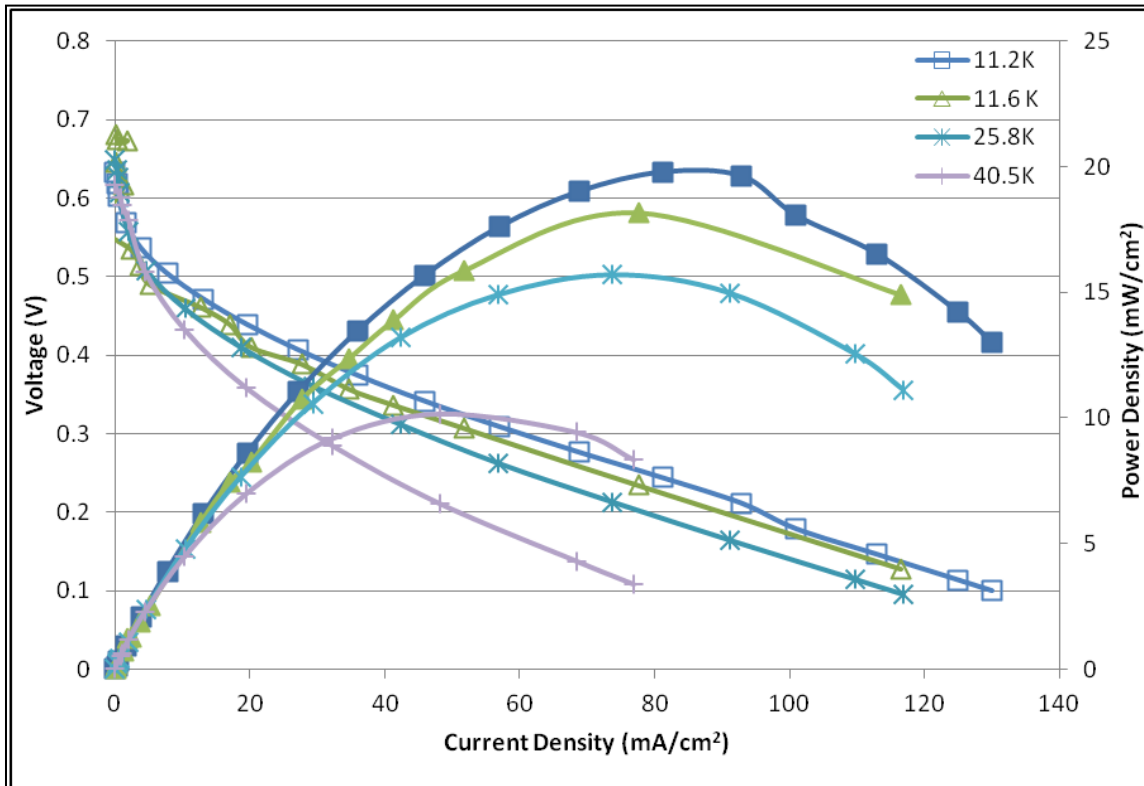
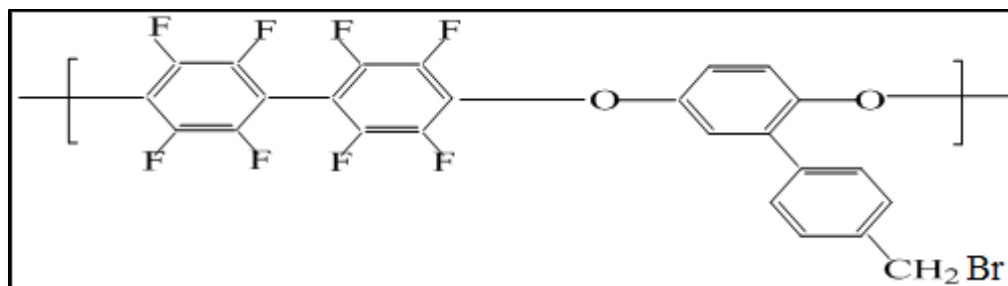


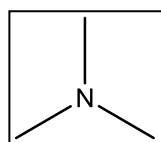
Figure 4.10: Polarization (open symbols) and power density (filled symbols) curves for cathode hybrid fuel cells with different molecular weight ionomers: (a) 11.2 k (b) 11.8 k (c) 25.8 k and (d) 40.5 k operated with 2M MeOH and 50sccm O<sub>2</sub> at 55 °C.

#### 4.2.7 Impact of Different Cationic Groups

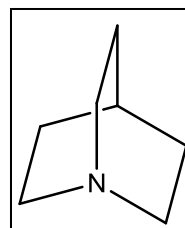
Ionomers used in the study till now have utilized the quaternary ammonium cation as the standard ionic group for OH<sup>-</sup> transport. Several different groups have been suggested in the literature for use as the cationic group in such ionomers. Some of them being phosphonium [33], guanidinium [69], and imidazolium [34,70]. The new ionomer used here was prepared with the same backbone as that of the previously used ammonium ionomers with quinuclidine as the ion exchange group. The backbone and the two different cationic groups (ammonium and quinuclidine) are shown in Figure 4.11.



(a)



(b)



(c)

Figure 4.11: Structure of (a) Ionomer backbone, and the attached cationic groups: (b) Ammonium (c) Quinuclidine

The prepared ionomers with similar properties are compared by application as an ionomer and binder in a cathode hybrid fuel cell. The properties of the ionomers and the fuel cell performance of the two ionomers are illustrated Table 3.6 and Figure 4.12 respectively.

The performance of the fuel cell with the quinuclidine based ionomers is higher than that of the ammonium based ionomer. The reason for this was previously explained based on the relative size of quinuclidine and better transport properties. The greater porosity in the ionomer layers with a reasonable water uptake provides for greater oxygen transport to the catalyst layer. This allows for a higher utilization and a greater performance.

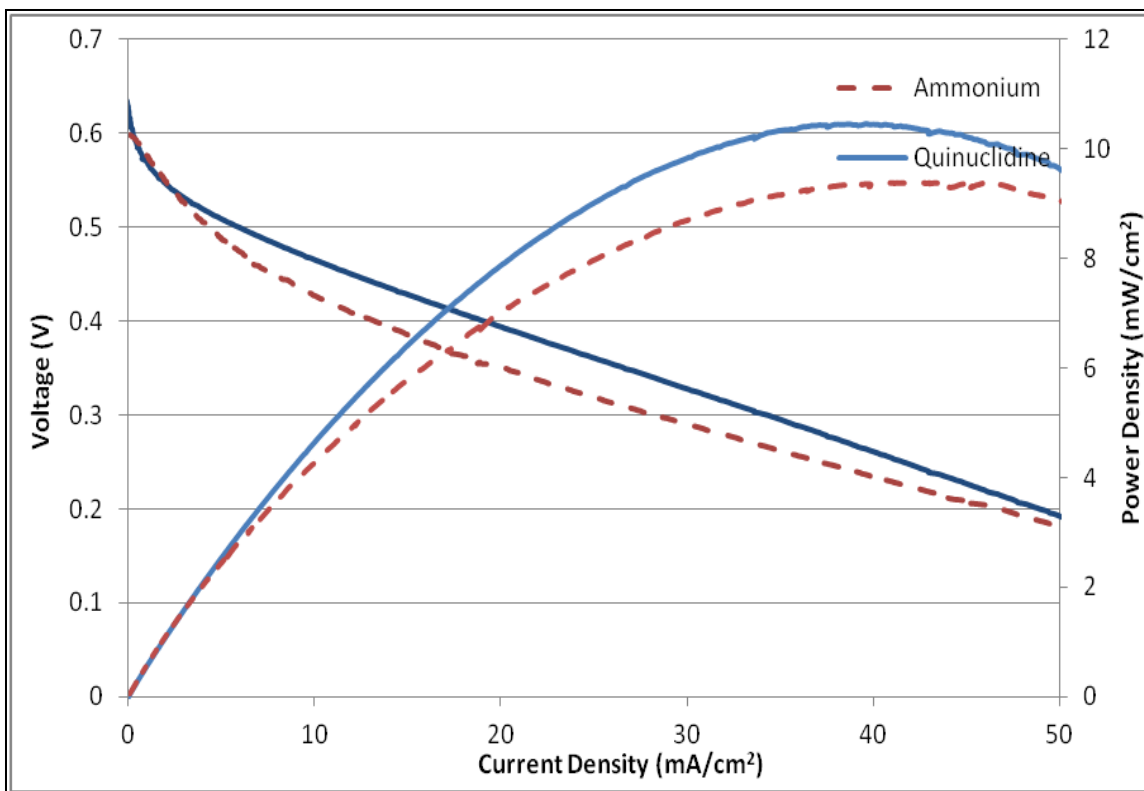


Figure 4.12: Polarization and power density curves for cathode hybrid fuel cells with Ionomer I different cationic groups: quinuclidine (lines), ammonium (dotted lines) operated with 2M MeOH and 50 sccm O<sub>2</sub> at 55 °C.

The catalyst utilized in making these ionomers is slightly different from that used for all other fuel cell performance. Here Pt (66.7wt %) on C was used instead of Pt (40 wt %) on C. The fabrication protocol for the ionomers are still the same, however the electrode has not been optimized for this catalyst and is therefore responsible for the low performance.

#### 4.2.8 Impact of the Non- Platinum Cathode Catalyst

A significant advantage with the use of cathode hybrid fuel cells is the use of a non-platinum catalyst based cathode for the oxygen reduction reaction. The non Pt based

cathode catalysts that have been utilized is Hispec 4020 catalyst from Acta SpA. The electrodes were prefabricated by Acta SpA with Ionomer I and II incorporated into the electrode structure along with PTFE. The PTFE loadings are unknown. The two non Pt cathode electrodes have been fabricated identically with the only difference being the ionomer used. The performance with the use of the non Pt catalyst is shown below in Figure 4.13.

The open circuit voltage of the Acta catalyst is similar to the ones observed with the Pt based catalyst, however the performance is lower. Methanol crossover does not create a mixed potential at the cathode the open circuit voltage is moderate. This low open circuit voltage can be explained owing to the fact that the junction potential at the PEM/AEM interface does not provide a significant contribution to the overall cell voltage. An improper contact between the AEM and the PEM might be responsible for this drop. It was previously mentioned that this interface contributes up to 0.83 V to the cell OCV.

The reason for the lower performance with the Acta catalyst when compared to the Pt based catalyst is that it has a very low metal loading on the carbon (3 wt %) and therefore a very thick layer of the catalyst is required in order to achieve the desired catalyst weight loading, resulting in a mass transport limitation. Further, the diffusion of water within the catalyst layers is also difficult resulting in a very low catalyst utilization and hence a reduced performance. It is also impossible for a continuous network of ionomers to be available for the transport of the ions from near the GDL to the electrode-membrane interface resulting in poor ionic conductivity and hence the overall catalyst utilization is also low.

The performance of the non Pt catalysts with two different ionomers is illustrated here. The performance with the hydrophobic ionomer II is much greater compared to the hydrophilic ionomer I this trend is similar to the one previously observed with Pt based catalyst. The properties of the ionomers used in the study are as follows

Table 4.4: Properties of ionomers used for the non platinum electrode preparation

Ionomer	IEC (meq/g)
Ionomer I-6	0.66
Ionomer II-5	0.53

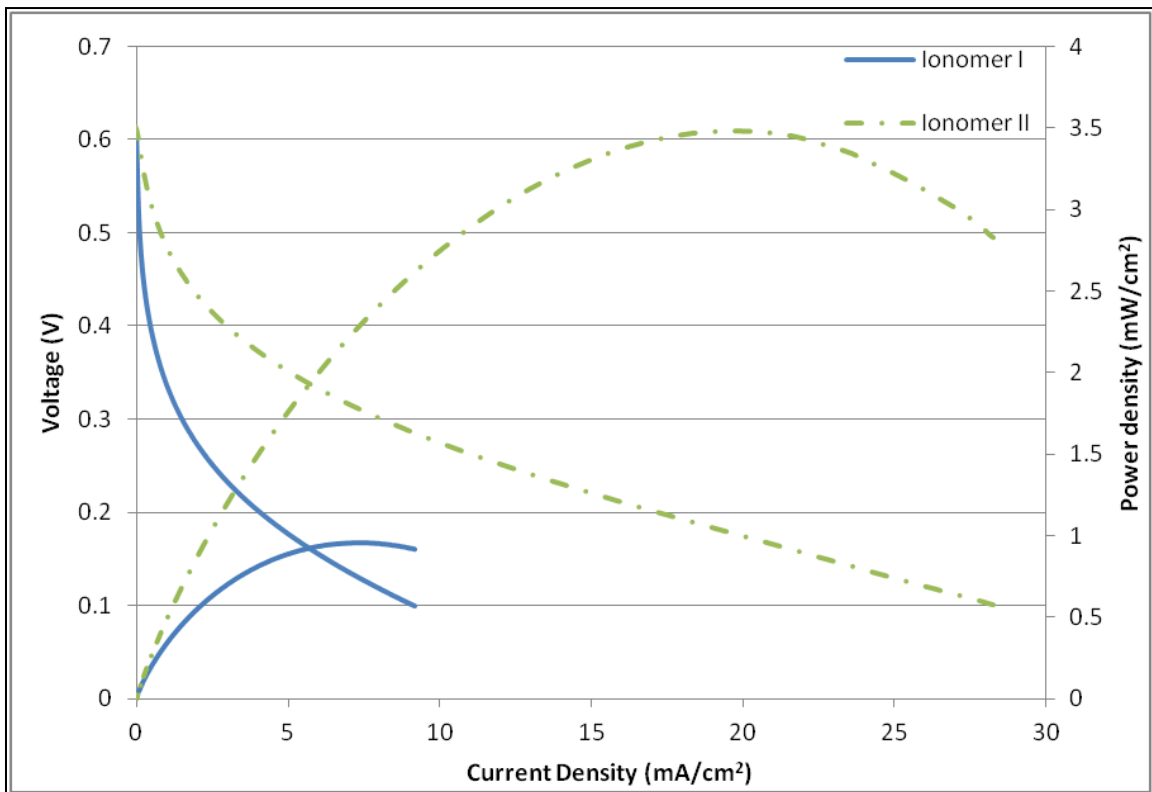


Figure 4.13: Polarization and power density curves of cathode hybrid fuel cells fabricated with Acta non platinum catalyst with two different ionomers Ionomer I (lines), Ionomer II (dotted lines) operated with 2M MeOH and 50 sccm O<sub>2</sub> at 55 °C

The long term operation of the fuel cell is also probed with the fuel cell operated for 4 h at 250 mV. The performance of these fuel cells gradually declined over the 4 h period of operation. Since the fuel cells operate at very low current densities only a fraction of the methanol is consumed, most of the methanol crosses over, there is no mixed potential created at the cathode as the methanol is not oxidized by the non Pt catalyst, however the swelling of the ionomer with the methanol results in a degradation of the electrode ionomer interface that is responsible for the decline in current owing to increased ionic resistance. The performance of the fuel cell operated for 4 h is given in Figure 4.14.

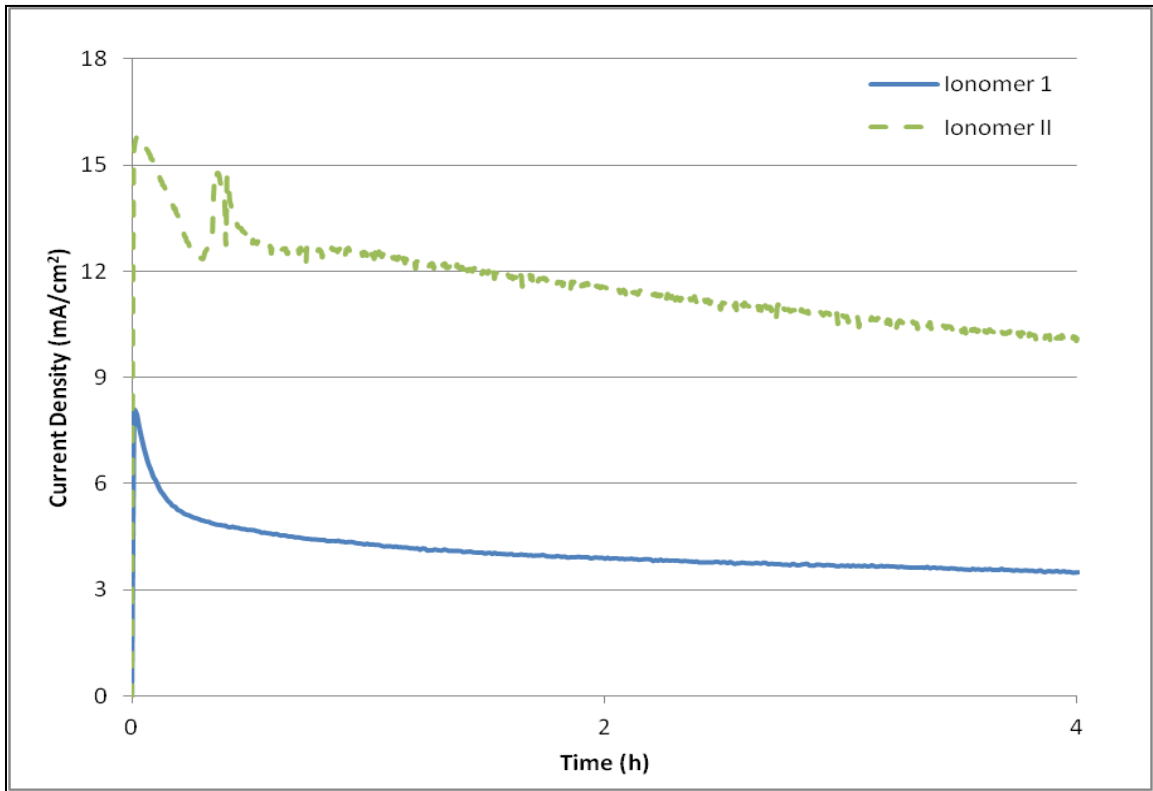


Figure 4.14: Steady state polarization curves with Ionomer I (line) and II (dotted line) for non platinum catalyst based cathode hybrid fuel cell operated with 2M MeOH at 5 ml/min and 50 sccm O<sub>2</sub> at 55 °C

### 4.3 Summary

The cathode hybrid fuel cells operating with methanol has been demonstrated here for the first time. These fuel cells are operated without the use of a hydroxide solution and provide better performance compared to any alkaline based fuel cell reported in literature. Three different ionomers were used in making the electrodes. Initially Ionomer I has been used to demonstrate the fabrication protocol of such fuel cells with PTFE as the binder has been shown to be more advantageous compared to using the ionomer as a binder, resulting from the enhanced water removal and better transport properties. The operating conditions for such fuel cells were narrowed down upon and these conditions were used for all cathode hybrid fuel cell testing. The ionomer content within the catalyst layer for optimum performance with these cathode hybrid fuel cells were also evaluated.

The fuel cell performance of three different ionomers with similar IEC was compared. Ionomer II and Ionomer III had more hydrophobicity compared to Ionomer I. The more hydrophobic Ionomer II showed the highest performance in such fuel cells resulting from the improved transport properties and reduced water retention of such ionomers. The molecular weight properties on the fuel cell performance were studied with Ionomer II and the low molecular weight ionomer provided the best performance owing to the increased chain mobility and enhanced oxygen dissolution properties.

Finally different cationic groups attached to the same ionomer backbone were studied. The use of quinuclidine groups in fuel cells as ionomers for the first time. Quinuclidine provided a better performance when compared to the ammonium cationic group based ionomer and could be used for further studies.

The most significant advantage of these fuel cells is that it offers the possibility of utilizing non platinum cathode. Cathode hybrid fuel cells were operated with non Pt catalyst and this is the first such demonstration for hybrid fuel cells using these electrodes.

## **CHAPTER 5**

### **CONCLUSIONS**

Fuel cell designs that involve the use of a combination of high pH and low pH electrodes with PEM membranes have been investigated. These fuel cells utilize the inherent advantages of the PEM fuel cell and AEM fuel cell technology while countering their disadvantages. Two designs, one with a high pH cathode, and the other with a high pH anode have been demonstrated in direct methanol mode for the first time. The main feature of note in these hybrid fuel cells is that these do not involve the additional hydroxide added to the fuel. The performances obtained are the highest achieved with those of alkaline electrodes without the addition of hydroxide solution to the fuel.

The electrode and ionomer optimization of anode and cathode hybrid designs yielded similar results. Consequently the results have been summarized together. The differences in performance of the two designs have been elucidated later. The optimization of the electrode structure was carried out and PTFE which provided additional hydrophobicity was found to provide better performance when compared to the use of ionomer I as binder. The ideal operating conditions for the fuel cell were optimized. The long term operations with such fuel cells have also been demonstrated, another major advantage of such fuel cells.

The ionomer content within the catalyst layers was optimized and 15 wt % was found to be the optimum value at both the AEM cathode and the AEM anode. IEC values of 1.2 meq/g were determined to be ideal for the best fuel cell performances. The Ionomer II with enhanced hydrophobicity was found to perform the best. The molecular weight of the ionomer II was varied and the performance was enhanced by low molecular weight ionomer in both designs, the greater chain flexibility and porosity was believed to help in material and ionic transport to the catalyst sites. The peak power performance

with the optimized electrode and ionomer in the anode hybrid design was found to be 27 mW/cm<sup>2</sup> with O<sub>2</sub> using ionomer II.

In alkaline fuel cells operated without hydroxide a very steep drop in the voltage was found to occur in the low current density region. In systems operating with hydroxide this does not seem to occur as they behave like a flooded electrolyte system. The anode hybrid design was found to have a similar voltage drop. This was believed to be owing to the specific adsorption of the ammonium cation on to the cathode, and the  $\phi_2$  effects at the double layer at potentials negative of the potential of zero charge. After the potential of zero charge was attained the electrode provided higher current densities. The initial voltage drop has been characterized at the AEM anode using the hybrid design with an internal hydrogen reference electrode. Since the quaternary ammonium groups were found to be responsible, an alternative ionomer with quinuclidine cationic groups were tried in order to mitigate the initial voltage drop. The performance with the quinuclidine was higher than that of the ammonium however the initial voltage drop at the anode still occurred for such ionomers owing to the adsorption and double layer effects.

Cathode hybrid designs have been tested with the ionomers containing the different cationic head groups. Quinuclidine based ionomers provided a better performance compared to the ammonium based ones.

The significant advantage of the cathode hybrid fuel cell was the use of the non Pt cathode. This is the first such demonstration of the hybrid fuel cell with non Pt electrodes. The peak performance of such fuel cell operated with 2M MeOH was 3.5 mW/cm<sup>2</sup>. To improve the performance of non platinum catalyst based electrodes, an ionomer with higher conductivity and increased catalyst loadings were recommended.

## REFERENCES

1. Eg and G. Services, Fuel cell handbook [electronic resource] / EG&G Technical Services, Inc, ed. L. National Energy Technology 2004, Morgantown, WV :: U.S. Dept. of Energy, Office of Fossil Energy, National Energy Technology Laboratory.
2. Bagot'skiĭ, V.S., Fuel cells : problems and solutions. The Electrochemical Society series 2009, Hoboken, N.J. :: John Wiley & Sons.
3. US Department of Energy. Comparison Chart. Energy Efficiency and Fuel Cell Technologies Program .February 2011 [4/15/2011]; Available from: [http://www1.eere.energy.gov/hydrogenandfuelcells/fuelcells/pdfs/fc\\_comparison\\_chart.pdf](http://www1.eere.energy.gov/hydrogenandfuelcells/fuelcells/pdfs/fc_comparison_chart.pdf).
4. Varcoe, J.R. and R.C.T. Slade, Prospects for alkaline anion-exchange membranes in low temperature fuel cells. *Fuel Cells*, 2005. 5(2): p. 187-200.
5. Costamagna, P. and S. Srinivasan, Quantum jumps in the PEMFC science and technology from the 1960s to the year 2000 Part I. Fundamental scientific aspects. *Journal of Power Sources*, 2001. 102(1-2): p. 242-252.
6. Larminie, J., Fuel cell systems explained, ed. A. Dicks 2000, Chichester [England] :: Wiley.
7. Carrette, L., K.A. Friedrich, and U. Stimming, Fuel Cells – Fundamentals and Applications. *Fuel Cells*, 2001. 1(1): p. 5-39.
8. Peled, E., et al., 0.5 W/cm<sup>2</sup> direct methanol-air fuel cell. *Electrochemical and Solid State Letters*, 2004. 7(12): p. A507-A510.
9. Aricò, A.S., S. Srinivasan, and V. Antonucci, DMFCs: From Fundamental Aspects to Technology Development. *Fuel Cells*, 2001. 1(2): p. 133-161.
10. Neburchilov, V., et al., A review of polymer electrolyte membranes for direct methanol fuel cells. *Journal of Power Sources*, 2007. 169(2): p. 221-238.
11. Bauer, B., et al., Electrochemical characterisation of sulfonated polyetherketone membranes. *Journal of New Materials for Electrochemical Systems*, 2000. 3(2): p. 93-98.

12. Mikhailenko, S.U.D., et al., Proton conducting membranes based on cross-linked sulfonated poly(ether ether ketone) (SPEEK). *Journal of Membrane Science*, 2004. 233(1-2): p. 93-99.
13. Hasiotis, C., V. Deimede, and C. Kontoyannis, New polymer electrolytes based on blends of sulfonated polysulfones with polybenzimidazole. *Electrochimica Acta*, 2001. 46(15): p. 2401-2406.
14. Jung, G.B., et al., Effect of operating parameters on the DMFC performance. *Journal of Fuel Cell Science and Technology*, 2005. 2(2): p. 81-85.
15. Qi, Z.G. and A. Kaufman, Open circuit voltage and methanol crossover in DMFCs. *Journal of Power Sources*, 2002. 110(1): p. 177-185.
16. Lu, G.Q., F.Q. Liu, and C.-Y. Wang, Water Transport Through Nafion 112 Membrane in DMFCs. *Electrochemical and Solid-State Letters*, 2005. 8(1): p. A1-A4.
17. Peled, E., et al., Novel approach to recycling water and reducing water loss in DMFCs. *Electrochemical and Solid State Letters*, 2003. 6(12): p. A268-A271.
18. Liu, F.Q., G.Q. Lu, and C.Y. Wang, Low crossover of methanol and water through thin membranes in direct methanol fuel cells. *Journal of the Electrochemical Society*, 2006. 153(3): p. A543-A553.
19. Song, K.Y., H.K. Lee, and H.T. Kim, MEA design for low water crossover in air-breathing DMFC. *Electrochimica Acta*, 2007. 53(2): p. 637-643.
20. Pasaogullari, U. and C.Y. Wang, Liquid water transport in gas diffusion layer of polymer electrolyte fuel cells. *Journal of the Electrochemical Society*, 2004. 151(3): p. A399-A406.
21. McLean, G.F., et al., An assessment of alkaline fuel cell technology. *International Journal of Hydrogen Energy*, 2002. 27(5): p. 507-526.
22. Gulzow, E. and M. Schulze, Long-term operation of AFC electrodes with CO<sub>2</sub> containing gases. *Journal of Power Sources*, 2004. 127(1-2): p. 243-251.

23. Switzer, E.E., et al., Novel KOH-free anion-exchange membrane fuel cell: Performance comparison of alternative anion-exchange ionomers in catalyst ink. *Electrochimica Acta*, 2010. 55(9): p. 3404-3408.
24. Koscher, G.A. and K. Kordesch, Alkaline methanol-air system - A historical survey and some new work. *Journal of Solid State Electrochemistry*, 2003. 7(9): p. 632-636.
25. Merle, G., M. Wessling, and K. Nijmeijer, Anion exchange membranes for alkaline fuel cells: A review. *Journal of Membrane Science*, 2011. 377(1-2): p. 1-35.
26. Yu, E.H. and K. Scott, Direct methanol alkaline fuel cells with catalysed anion exchange membrane electrodes. *Journal of Applied Electrochemistry*, 2005. 35(1): p. 91-96.
27. Tripkovic, A.V., et al., Methanol electrooxidation on supported Pt and PtRu catalysts in acid and alkaline solutions. *Electrochimica Acta*, 2002. 47(22-23): p. 3707-3714.
28. Schulze, A. and E. Gulzow, Degradation of nickel anodes in alkaline fuel cells. *Journal of Power Sources*, 2004. 127(1-2): p. 252-263.
29. Matsuoka, K., et al., Alkaline direct alcohol fuel cells using an anion exchange membrane. *Journal of Power Sources*, 2005. 150: p. 27-31.
30. Varcoe, J.R., et al., Steady-state dc and impedance investigations of H<sub>2</sub>/O<sub>2</sub> alkaline membrane fuel cells with commercial Pt/C, Ag/C, and Au/C cathodes. *Journal of Physical Chemistry B*, 2006. 110(42): p. 21041-21049.
31. Li, Y.S., T.S. Zhao, and R. Chen, Cathode flooding behaviour in alkaline direct ethanol fuel cells. *Journal of Power Sources*, 2011. 196(1): p. 133-139.
32. Santasalo-Aarnio, A., et al., In and ex situ characterization of an anion-exchange membrane for alkaline direct methanol fuel cell (ADMFC). *Journal of Power Sources*, 2011. 196(15): p. 6153-6159.

33. Gu, S., et al., Quaternary Phosphonium-Based Polymers as Hydroxide Exchange Membranes. *Chemosuschem*, 2010. 3(5): p. 555-558.
34. Li, W., et al., Novel anion exchange membranes based on polymerizable imidazolium salt for alkaline fuel cell applications. *Journal of Materials Chemistry*, 2011. 21(30): p. 11340-11346.
35. Wang, G., et al., Developing a polysulfone-based alkaline anion exchange membrane for improved ionic conductivity. *Journal of Membrane Science*, 2009. 332(1-2): p. 63-68.
36. Zhou, J.F., et al., Anionic polysulfone ionomers and membranes containing fluorenyl groups for anionic fuel cells. *Journal of Power Sources*, 2009. 190(2): p. 285-292.
37. Hou, H., et al., Alkali doped polybenzimidazole membrane for alkaline direct methanol fuel cell. *International Journal of Hydrogen Energy*, 2008. 33(23): p. 7172-7176.
38. Agel, E., J. Bouet, and J.F. Fauvarque, Characterization and use of anionic membranes for alkaline fuel cells. *Journal of Power Sources*, 2001. 101(2): p. 267-274.
39. Varcoe, J.R. and R.C.T. Slade, An electron-beam-grafted ETFE alkaline anion-exchange membrane in metal-cation-free solid-state alkaline fuel cells. *Electrochemistry Communications*, 2006. 8(5): p. 839-843.
40. Kim, J., T. Momma, and T. Osaka, Cell performance of Pd–Sn catalyst in passive direct methanol alkaline fuel cell using anion exchange membrane. *Journal of Power Sources*, 2009. 189(2): p. 999-1002.
41. Liu, H., et al., Preparation and characterization of radiation-grafted poly (tetrafluoroethylene-co-perfluoropropyl vinyl ether) membranes for alkaline anion-exchange membrane fuel cells. *Journal of Membrane Science*, 2011. 369(1-2): p. 277-283.

42. Kim, J.H., et al., Electrochemical studies of DMFC anodes with different ionomer content. *Electrochimica Acta*, 2004. 50(2-3): p. 801-806.
43. Kim, J.-H., et al., Performance of air-breathing direct methanol fuel cell with anion-exchange membrane. *International Journal of Hydrogen Energy*, 2010. 35(2): p. 768-773.
44. Prakash, G.K.S., et al., Study of operating conditions and cell design on the performance of alkaline anion exchange membrane based direct methanol fuel cells. *Journal of Power Sources*, 2011. 196(19): p. 7967-7972.
45. Unlu, M., J.F. Zhou, and P.A. Kohl, Hybrid Anion and Proton Exchange Membrane Fuel Cells. *Journal of Physical Chemistry C*, 2009. 113(26): p. 11416-11423.
46. Unlu, M., J.F. Zhou, and P.A. Kohl, Study of Alkaline Electrodes for Hybrid Polymer Electrolyte Fuel Cells. *Journal of the Electrochemical Society*, 2010. 157(10): p. B1391-B1396.
47. Mafe, S. and P. Ramirez, Electrochemical characterization of polymer ion-exchange bipolar membranes. *Acta Polymerica*, 1997. 48(7): p. 234-250.
48. Strathmann, H., et al., Theoretical and Practical Aspects of preparing bipolar membranes. *Desalination*, 1993. 90(1-3): p. 303-323.
49. Nagarale, R.K., G.S. Gohil, and V.K. Shahi, Recent developments on ion-exchange membranes and electro-membrane processes. *Advances in Colloid and Interface Science*, 2006. 119(2-3): p. 97-130.
50. Unlu, M., et al., Characterization of Anion Exchange Ionomers in Hybrid Polymer Electrolyte Fuel Cells. *Chemosuschem*, 2010. 3(12): p. 1398-1402.
51. Scott, K., et al., The impact of mass transport and methanol crossover on the direct methanol fuel cell. *Journal of Power Sources*, 1999. 83(1-2): p. 204-216.
52. Unlu, M., et al., Improved gas diffusion electrodes for hybrid polymer electrolyte fuel cells. *Electrochimica Acta*, 2011. 56(12): p. 4439-4444.

53. Lu, G.Q., F.Q. Liu, and C.Y. Wang, Water transport through Nafion 112 membrane in DMFCs. *Electrochemical and Solid State Letters*, 2005. 8(1): p. A1-A4.
54. Ge, J.B. and H.T. Liu, Experimental studies of a direct methanol fuel cell. *Journal of Power Sources*, 2005. 142(1-2): p. 56-69.
55. Litster, S. and G. McLean, PEM fuel cell electrodes. *Journal of Power Sources*, 2004. 130(1-2): p. 61-76.
56. Bidault, F., et al., Review of gas diffusion cathodes for alkaline fuel cells. *Journal of Power Sources*, 2009. 187(1): p. 39-48.
57. Navessin, T., et al., Influence of membrane ion exchange capacity on the catalyst layer performance in an operating PEM fuel cell. *Journal of the Electrochemical Society*, 2005. 152(4): p. A796-A805.
58. Li, L., et al., Transport properties of PFSA membranes with various ion exchange capacities for direct methanol fuel cell application. *Energy & Environmental Science*, 2010. 3(1): p. 114-116.
59. Zhou, J.F., et al., Solvent processible, high-performance partially fluorinated copoly (arylene ether) alkaline ionomers for alkaline electrodes. *Journal of Power Sources*, 2011. 196(19): p. 7924-7930.
60. Chempath, S., et al., Mechanism of tetraalkylammonium headgroup degradation in alkaline fuel cell membranes. *Journal of Physical Chemistry C*, 2008. 112(9): p. 3179-3182.
61. Nistor, C., et al., Composite membranes with cross-linked matrimid selective layer for gas separation. *Environmental Engineering and Management Journal*, 2008. 7(6): p. 653-659.
62. Kerle, T., et al., Mobility of polymers at the air/polymer interface. *Macromolecules*, 2001. 34(10): p. 3484-3492.
63. Bard, A.J. and L.R. Faulkner, *Electrochemical Methods: Fundamentals and Applications* 2001: Wiley.

64. Gierst, L., J. Tondeur, and E. Nicolas, Double couche electrochimique et cinétique des réactions de électrode - élucidation du cations tétraalkylammonium. *Journal of Electroanalytical Chemistry*, 1965. 10(5-6): p. 397-&.
65. Uenlue, M., et al., Analysis of Double Layer and Adsorption Effects at the Alkaline Polymer Electrolyte-Electrode Interface. *Journal of the Electrochemical Society*, 2011. 158(11): p. B1423-B1431.
66. Kazock, J.Y., et al., Ionic liquids based on 1-aza-bicyclo 2,2,2 octane (Quinuclidine) salts: synthesis and physicochemical properties. *Journal of Applied Electrochemistry*, 2009. 39(12): p. 2461-2467.
67. Kim, H., et al., The effect of hydrophobicity in alkaline electrodes for passive DMFC. *Electrochimica Acta*, 2011. 56(8): p. 3085-3090.
68. George, S.C. and S. Thomas, Transport phenomena through polymeric systems. *Progress in Polymer Science*, 2001. 26(6): p. 985-1017.
69. Wang, J., S. Li, and S. Zhang, Novel Hydroxide-Conducting Polyelectrolyte Composed of an Poly(arylene ether sulfone) Containing Pendant Quaternary Guanidinium Groups for Alkaline Fuel Cell Applications. *Macromolecules*, 2010. 43(8): p. 3890-3896.
70. Qiu, B., et al., Alkaline imidazolium- and quaternary ammonium-functionalized anion exchange membranes for alkaline fuel cell applications. *Journal of Materials Chemistry*, 2012. 22(3): p. 1040-1045.